CANADIAN THESES ON MICROFICHE

I.S.B.N.

THESES CANADIENNES SUR MICROFICHE

National Library of Canada
Collections Development Branch

Canadian Theses on
Microfiche Service

Ottawa, Canada
K1A 0N4

Bibliothèque nationale du Canada
Direction du développement des collections

Service des thèses canadiennes
sur microfiche

NOTICE

The quality of this microfiche is heavily dependent upon the quality of the original thesis submitted for microfilming. Every effort has been made to ensure the highest quality of reproduction possible.

If pages are missing, contact the university which granted the degree.

Some pages may have indistinct print especially if the original pages were typed with a poor typewriter ribbon or if the university sent us a poor photocopy.

Previously copyrighted materials (journal articles, published tests, etc.) are not filmed.

Reproduction in full or in part of this film is governed by the Canadian Copyright Act, R.S.C. 1970, c. C-30. Please read the authorization forms which accompany this thesis.

AVIS

La qualité de cette microfiche dépend grandement de la qualité de la thèse soumise au microfilmage. Nous avons tout fait pour assurer une qualité supérieure de reproduction.

S'il manque des pages, veuillez communiquer avec l'université qui a conféré le grade.

La qualité d'impression de certaines pages peut laisser à désirer, surtout si les pages originales ont été dactylographiées à l'aide d'un ruban usé ou si l'université nous a fait parvenir une photocopie de mauvaise qualité.

Les documents qui font déjà l'objet d'un droit d'auteur (articles de revue, examens publiés, etc.) ne sont pas microfilmés.

La reproduction, même partielle, de ce microfilm est soumise à la Loi canadienne sur le droit d'auteur, SRC 1970, c. C-30. Veuillez prendre connaissance des formules d'autorisation qui accompagnent cette thèse.

THIS DISSERTATION
HAS BEEN MICROFILMED
EXACTLY AS RECEIVED

LA THÈSE A ÉTÉ
MICROFILMÉE TELLE QUE
NOUS L'AVONS REÇUE

NL-339 (r. 82/08)

Canada

COMPARISON OF 2-DIMENSIONAL AND 3-DIMENSIONAL TESTING IN BRIDGE AERODYNAMICS

by

TOMMY MAN-CHEUNG KAN

A thesis
presented to University of Ottawa
in partial fulfillment of the
requirements for the degree of
Master of Applied Science
in
Civil Engineering Program

OTTAWA, Ontario, 1983

ABSTRACT

In this study, 2-dimensional and 3-dimensional wind tunnel tests, with three different bridge sections were carried out in smooth flow, homogeneous turbulence and boundary layer flow to investigate their aerodynamic behaviours. Attempts were also made to predict the response of the test models by using available theories.

The overall comparison of two dimensional and three dimensional testing showed that the scale of turbulence in wind flow has significant influence on the representation of 3-dimensional response by 2-dimensional response.

ACKNOWLEDGEMENTS

The author would like to express his gratitude to Dr. H. Tanaka, Associate Professor in Civil Engineering, the University of Ottawa, for his continous guidance and encouragement throughout this study.

Appreciation is extended to Mr. Winston Kan and Mr. John Ivanyi for their contributions and comments in the preperation of this thesis.

Special gratitude is given to Mr. Edward Tsui for his assistance in the laboratory.

Finally, the author gratefully acknowledges his family for their understanding and encouragement in the period of this study.

TABLE OF CONTENTS

LIST OF TABLES

LIST OF FIGURES

LIST OF SYMBOL

a = reduced amplitude of lateral vibration

b = half value of the section width

B = width of model

C_L = lift force coefficient

C_m = pitching moment coefficient

C_{F_z} = lateral force coefficient

e = eccentricity of section about elastic axis

F = lateral force

G = damping force

h = height of section

I_u = turbulence intensity of u-component

I_w = turbulence intensity of w-component

ℓ = span length

L = lift force

L_u = integral length scale of u-component

m = mass per unit length

M = pitching moment

$\bar{R}$ = correlation function

$S(f)$ = spectral density function

t = time

T = time period

V = mean velocity

V = reduced velocity
$V/f_z h$ for flat plate and H-section
$V/f_z B$ for box section

$u(t)$ = time dependent velocity component in y-direction

$v(t)$ = time dependent velocity component in x-direction

$w(t)$ = time dependent velocity component in z-direction

β = ratio of torsional frequency to flexural frequency f_ϕ/f_z

ζ_z = flexural damping

ζ_ϕ = torsional damping

η = reduced vertical displacement z/b

θ = mass moment of inertia per unit length (about the elastic axis)

μ = mass parameter ($\frac{m}{\pi\rho b^2}$)

ν = dimensionless moment of inertia ($\frac{\theta}{\pi\rho b^4}$)

ξ = ratio of frequency to flexural frequency (f/f_z)

ρ = density of air.

ω_z = circular frequency in flexural mode

ω_ϕ = circular frequency in torsional mode

Chapter I

INTRODUCTION

1.1 GENERAL DESCRIPTION

The development of architectural design and construction techniques has brought highlights to the industry of bridge engineering, by which modern bridges of long-spans and aesthetic appearance are built all over the world. Despite the magnificent appearance of the structure, safety and comfort are of the most concern by the public and the engineers. The high flexibility, low damping and light weight of the modern bridge structure decreases its stability in wind flow, wind being the unavoidable enemy of the structure.

Wind environment is one of the most important pieces of information regarding the stability of the structure. The presence of a bridge at a certain site will expose it to a specific wind environment, whose characteristics depend on the geography of the surrounding area.

The relation between the environment and the forces it induces on the structure is another aspect of study. This involves the derivation of forcing functions from the

dynamics of wind flow. The presence of turbulence in wind flow will complicate the problem because of its random characteristics.

The behaviour of the bridge structure under the action of these forces is the main concern of the engineers. Studies have been focused on aerodynamic behaviour of suspension bridges since the disaster of the Tacoma Narrows Bridge in 1940. Both section model tests and full-bridge model tests have been conducted in many research institutions. Comparison of the response of the prototype structure with test results has stressed the significance of wind tunnel testing in predicting the bridge behaviours in wind, at the same time better simulation of both the wind and the structures as well as a good understanding of the general characteristics of the wind-structure interaction problem is required.

In the early 1960's, Davenport pointed out the significance of bridge response in turbulent flow. This brought an attention to the reliability of the wind tunnel test again.

Ideally speaking, reliable prediction of the behaviour of a bridge structure at a certain site can only be done by placing a full-scale bridge model of the prototype in a wind tunnel, and allowing it to experience a wind environment similar to that existing at the site.

1.2 3-DIMENSIONAL TESTING & 2-DIMENSIONAL TESTING

The wind induced responses of an aeroelastic model in the wind tunnel, with flow conditions similar to that of the full-scale bridge, will give a close estimate of the responses of the full scale structure. This is known as the 3-dimensional testing. This technique employs a scaled-down elastic model of the full-scale bridge structure, which possesses the physical and aerodynamic properties of the latter.

Detailed study of wind forces on bridge structures was carried out after the Tay Bridge disaster in 1879. After the turn of the century, wind tunnel tests of static wind load on engineering structures were conducted extensively.

In 1940, the collapse of the Tacoma Narrows suspension bridge brought attention to aerodynamic instability of slender line-like structures due to wind flow. Studies were carried out at the University of Washington by Farquharson, Vincent and Karman, and a little later, similar studies were done at the National Physical Laboratory in England. Full aeroelastic model and sectional model of the Tacoma Narrows bridge were tested in the wind tunnel to investigate the wind-induced behaviour of them. There was a satisfactory agreement in the prediction of critical wind speed between the full-bridge model test and the sectional model test. However the agreement of these results with the full bridge

behaviour was limited only in quality. The measurements were carried out only in smooth flow.

Section model testing is an economical and an easy-to-handle method in wind tunnel testing. It is adapted by many bridge engineers being expected as a reliable tool in predicting the dynamic responses of full-scale bridges for the last thirty years.

This method in smooth uniform flow was introduced by von Karman and Dunn in the 1940's. But the introduction of turbulence effect in it is a relatively recent idea and not really very popular yet.

In this study, 2-dimensional and 3-dimensional models were exposed to both smooth uniform flow and turbulent flow to find out to what extent a 2-dimensional test could estimate the behaviour of the full aeroelastic model behaviour in smooth and turbulent flow.

Chapter II

WIND INDUGED VIBRATION OF LONG SPAN BRIDGE STRUCTURES

2.1 GENERAL DESCRIPTION OF PHENOMENA

Due to the trend of increasing span lengths in the design of suspension bridges and cable stayed bridges, the instability of a bridge structure in wind flow is gaining more concern from the engineers. The slenderness of these bridges implies high flexibility which is an unfavourable condition for aeroelastic stability.

The phenomenon of aeroelastic instability is the state at which oscillatory or divergent motion of the bridge occurs.

1. Limited Amplitude Response

   a) Buffeting

      Buffeting is a kind of random vibration by an excitation over a wide range of excitation frequencies. This is mostly induced by the fluctuating velocity components of the turbulent wind. This is one of the significant vibration mechanism for many structures at any wind speeds.

   b) Vortex-induced oscillations

When an air stream flows across a bluff structure, vortex shedding will be formed alternatively behind the body as a result of flow separation from the upper and lower edges of the bridge deck. At a certain wind speed, when the frequency of shedding comes close to the natural frequency of the system, resonance will occur. This phenomenon has often quite significant consequences at relatively low wind speeds.

2. Diverging Amplitude Response

a) Classical Flutter

The phenomenon of classical flutter is the state when the two degrees of freedom of the bridge section, flexural and torsional, are coupled together in a wind flow. This phenomenon can be most critical for a bridge which has a relatively shallow cross-section of its girder.

b) Galloping and Stall Flutter

These are almost single-degree-of-freedom oscillations which are driven by the negative aerodynamic damping characteristics of the corresponding force components in the mode of oscillation. In the case of galloping, the lift force is the controlling factor, while stall flutter is excited by the pitching moment.

Divergent oscillations will occur when the magnitude of aerodynamic negative damping exceeds the structural damping of the system.

The mechanisms discussed above are self-excited oscillations which introduce the vibration energy through structural displacements and their time derivatives.

2.2 FUNDAMENTAL EQUATIONS

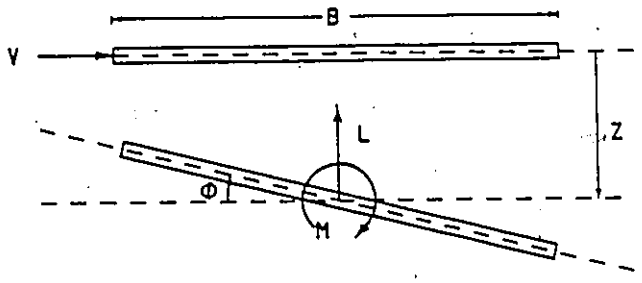

The fundamental equations of motion of a 2-dimensional bridge section in flexural and torsional modes are given as follows :

$$m\left(\ddot{Z} + 2\zeta_z\omega_z\dot{Z} + \omega_z^2 Z\right) = -L \qquad (2.2.1)$$

$$\theta\left(\ddot{\Phi} + 2\zeta_\phi\omega_\phi\dot{\Phi} + \omega_\phi^2\Phi\right) = M$$

in which, m = mass per unit length of bridge girder;

θ = mass moment of inertia per unit length of

bridge girder;

ω_z, ω_ϕ = natural circular frequencies in vertical and torsional modes;

ζ_z, ζ_ϕ = structural damping in vertical and torsional modes as the fraction of critical; and

Z , Φ, L and M are as shown in the figure above.

Equation (2.2.1) can be expressed in terms of reduced responses η and Φ in dimensionless form as follows:

$$\ddot{\eta} + 2\zeta_z\omega_z\dot{\eta} + \omega_z^2\eta = -\frac{L}{mb} \qquad (2.2.2)$$

$$\ddot{\Phi} + 2\zeta_\phi\omega_\phi\dot{\Phi} + \omega_\phi^2\Phi = \frac{M}{\Theta}$$

in which $\eta = \frac{Z}{b}$ and $b = \frac{B}{2}$.

2.3 AERODYNAMIC FORCES

Due to the random nature of wind flow, there are in addition to the mean flow V, three fluctuating velocity components, u,v and w.

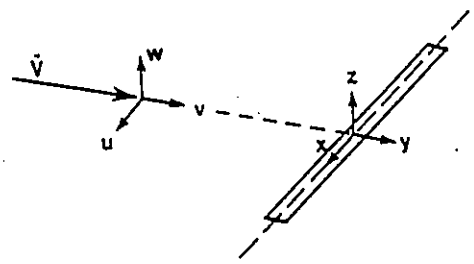

In this study, only the vertical bending vibration and rotation about the x-axis of the bridge deck are considered. Thus the u and v components are considered to have less contribution to these motions, and are ignored in the following computation of the excitation forces responsible for the vibrations.

The applied forces induced by wind flow can then be divided into two components, the force due to the mean flow, which can be characterized by derivatives of the conventional aerodynamic force components, and the force due to the fluctuating velocity component w(t) which is defined as gust loading in this study.

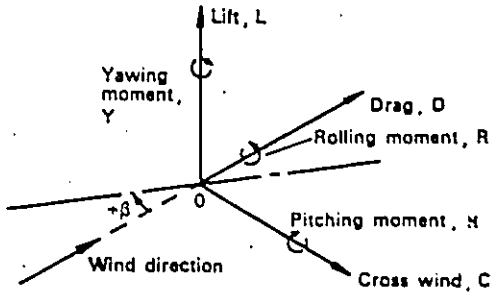

Wind-tunnel axes and notation.
β = model yaw angle : α = model elevation angle.

When a body is submerged in an air stream, it will be subjected to six aerodynamic force components in general, whose magnitudes are decided by the dynamic pressure, the linear dimension of the body and the geometric shape. In bridge structures, normally, we are interested only in the lift force, drag force and pitching moment on the section. For bluff structures such as H-sections and box-sections, separation of air flow from the body makes it very difficult to derive these forces theoretically, thus they can only be determined experimentally, while in the case of the flow over a flat plate, potential flow theory can be applied.

2.3.1 Unsteady Theory

In the absence of turbulence, the aerodynamic forces acting on a bridge section vibrating with a circular frequency of ω in an air stream of mean speed V can be expressed as follows (Ref 3):

$$L^* = -\pi\rho b^3\omega^2 \{ L_z \frac{Z}{b} + L_\phi \phi \}$$

$$M^* = \pi\rho b^4\omega^2 \{ M_z \frac{Z}{b} + M_\phi \phi \} \qquad (2.3.1.1)$$

where L_z, L_ϕ, M_z and M_ϕ are the aerodynamic derivatives expressed as complex functions of reduced frequency

$$k = \frac{\omega b}{V} \qquad (2.3.1.2)$$

In the case of potential flow, these derivatives can be expressed in terms of the well-known Theodorsen's function $C(k)=F(k)+iG(k)$ as follows:

$$L_z = -\frac{2i}{k}C(k) \qquad L_\phi = -\frac{2}{k^2}C(k) - \frac{i}{k}[\, 1 + C(k) \,]$$

$$M_z = \frac{i}{k}C(k) \qquad M_\phi = \frac{1}{k^2}C(k) - \frac{i}{2k}[\, 1 - C(k) \,] \qquad (2.3.1.3)$$

2.3.2 Quasi-Steady Theory

In contrast with unsteady theory, quasi-steady theory deals with the instantaneous displacement rather than the past history of the vibrating section.

When a steady air flow of mean speed V attacks a section at an angle of incidence α, the lift force and pitching moment can be expressed as functions of dimensionless coefficients C_L & C_m, as follows;

$$L(\alpha) = \frac{1}{2}\rho B\bar{V}^2 C_L(\alpha)$$

$$M(\alpha) = \frac{1}{2}\rho B^2\bar{V}^2 C_M(\alpha) \qquad (2.3.2.1)$$

When vibration begins, the flow gives an additional incidence on the section at a relative angle given by the arctangent of the sum of the following terms: $\frac{\dot{Z}}{\bar{V}}$ = relative angular displacement due to the vertical deflection of the section, $\frac{eB\dot{\phi}}{\bar{V}}$ = relative angular displacement due to the rate of angular rotation and ϕ = actual angular displacement, in which e is a linear dimension defined for a given for a given cross-section of the body.

When α is small, the derivative of the force coeffifients at zero can represent the slope of C_L and C_m curves with respect to the angle of attack. Thus, the aerodynamic forcing functions of the section can be approximated by the following expressions:

$$L^* = \frac{\rho \bar{V}^2}{2} B \left(\frac{\partial C_l}{\partial \alpha}\right)\left(\Phi + \frac{\dot{Z}}{\bar{V}} + \frac{eB\dot{\Phi}}{\bar{V}} \right)$$

$$M^* = \frac{\rho \bar{V}^2}{2} B^2 \left(\frac{\partial C_m}{\partial \alpha}\right)\left(\Phi + \frac{\dot{Z}}{\bar{V}} + \frac{eB\dot{\Phi}}{\bar{V}} \right) \qquad (2.3.2.2)$$

2.3.3 Gust Loading

The effect of the fluctuating vertical velocity component in conjuction with the mean flow velocity will give rise to a resultant vector which acts at an angle $\frac{w(t)}{\bar{V}}$ to the mean flow direction. Thus, the gust loading can be approximated, by the quasi-steady theory, in the following form:

$$L_f(t) = \frac{\rho \bar{V}^2}{2} B \frac{\partial C_l}{\partial \Phi} \frac{w(t)}{\bar{V}}$$

$$M_f(t) = \frac{\rho \bar{V}^2}{2} B^2 \frac{\partial C_m}{\partial \Phi} \frac{w(t)}{\bar{V}} \qquad (2.3.3.1)$$

The gust loading, which is random in nature, varies in both time and frequency domains. Thus, only statistical analysis can be applied to evaluate the response due to such loading. Statistical analysis such as proposed by Davenport (Refs 1,2) is a useful tool in solving this problem.

The distribution of the total energy in the turbulence with the various turbulent frequencies can be shown by the spectral density function $S(f)$. Actual distribution can be approximated by any appropriate analytical function,

depending on the shape of the measured wind velocity spectrum.

The aerodynamic admittance function $|\chi_w^L|^2$ and $|\chi_w^m|^2$ for lift force and pitching moment are required to modify the corresponding lift and moment spectra because of the decrease in the correlation of the eddies when the wavelength of the eddies approaches the width of the section. Thus,

$$S_L \propto S_w(f)|\chi_w^L|^2|J_f|^2$$

$$S_M \propto S_w(f)|\chi_w^m|^2|J_f|^2 \qquad (2.3.3.2)$$

The space correlation of the force component along the span length of the structure can be expressed by the joint acceptance function $|J_f|^2$. An exponential decaying function is assumed for the correlation of the force at a certain point on the span influenced by the force at another location on the span. The mode shape ψ of the vibrating structure is involved in the derivation of $|J_f|^2$ as follows:

$$|J_r(f)|^2 = \int_0^\ell \int_0^\ell R(x_1,x_2,f)\psi_r(x_1)\psi_r(x_2)dx_1 dx_2/\ell^2 \qquad (2.3.3.3)$$

where

$$R(x_1,x_2,f) = e^{-\frac{cf}{V}|x_1-x_2|} \qquad (2.3.3.4)$$

is widely accepted as a good approximation.

In this study, we assumed that only the first mode is significant in the model response, thus,

for a sinusodial wave form,

$$|J_f|^2 = \frac{\lambda^2}{\lambda^2+\pi^2} + \frac{2\pi^2(1+e^{-\lambda})}{(\lambda^2+\pi^2)^2} \qquad (2.3.3.5)$$

for a rigid body,

$$|J_f|^2 = \frac{2}{\lambda}[1 + \frac{1}{\lambda}(e^{-\lambda} - 1)] \qquad (2.3.3.6)$$

where

$$\lambda = \frac{cf\ell}{V}$$

2.4 SOLUTION FOR THE EQUATIONS

2.4.1 Linear Theory

1. Buffeting

In a natural wind flow condition, with aerodynamic forces discussed in section 2.3, the equation of motion becomes (Ref 6),

$$m(\ddot{Z} + 2\zeta_z\omega_z\dot{Z} + \omega_z^2 Z) = -L^* - L_f(t)$$

$$\theta(\ddot{\Phi} + 2\zeta_\phi\omega_\phi\dot{\Phi} + \omega_\phi^2\Phi) = M^* + M_f(t) \qquad (2.4.1.1)$$

The aerodynamic forces L^* and M^*, due to uniform velocity V, are complex functions, in which the real part is proportional to the displacement, and the imaginary part is in phase with the velocity of the oscillating section. Thus

$$-L^* = (L^*_{zR} + iL^*_{zI})Z + (L^*_{\phi R} + iL^*_{\phi I})\phi$$

$$M^* = (M^*_{zR} + iM^*_{zI})Z + (M^*_{\phi R} + iM^*_{\phi I})\phi \qquad (2.4.1.2)$$

Equation (2.4.1.1) becomes

$$m(\ddot{Z} + 2\zeta_z\omega_z\dot{Z} + \omega_z^2 Z) = (L^*_{zR} + iL^*_{zI})Z + (L^*_{\phi R} + iL^*_{\phi I})\phi - L_f(t)$$

$$\theta(\ddot{\phi} + 2\zeta_\phi\omega_\phi\dot{\phi} + \omega_\phi^2\phi) = (M^*_{zR} + iM^*_{zI})Z + (M^*_{\phi R} + iM^*_{\phi I})\phi + M_f(t) \qquad (2.4.1.3)$$

For a certain excitation frequency ω, the displacements of the structure are assumed to be simple harmonic motion with frequency ω, that is, $Z = \bar{Z}\, e^{i\omega t}$ and $\phi = \bar{\phi}\, e^{i\omega t}$, then equation (2.4.1.3) can be expressed as

$$\begin{vmatrix} [m(\omega_z^2-\omega^2)-L^*_{zR}]+[2m\omega\omega_z\zeta_z-L^*_{zI}]i & -[L^*_{\phi R}+iL^*_{\phi I}] \\ -[M^*_{zR}+iM^*_{zI}] & [\theta(\omega_\phi^2-\omega^2)-M^*_{\phi R}]+[2\theta\omega\omega_\phi\zeta_\phi-M^*_{\phi I}]i \end{vmatrix} \begin{vmatrix} Z \\ \phi \end{vmatrix} = \begin{vmatrix} -L_f(t) \\ M_f(t) \end{vmatrix} \qquad (2.4.1.4)$$

Equation (2.4.1.4) is written in a simple form as follows

$$\begin{bmatrix} A_1 & A_2 \\ A_3 & A_4 \end{bmatrix} \begin{bmatrix} \eta \\ \phi \end{bmatrix} = \begin{bmatrix} L \\ M \end{bmatrix} \qquad (2.4.1.5)$$

The flexural and torsional motion can be found by solving equation (2.4.1.5) as

$$\eta = \frac{1}{\Delta}(A_4 L - A_2 M) = X_{zz} L - X_{z\phi} M$$
$$\Phi = \frac{1}{\Delta}(A_1 M - A_3 L) = X_{\phi\phi} M - X_{\phi z} L \qquad (2.4.1.6)$$

where

$$\begin{vmatrix} A_1 & A_2 \\ A_3 & A_4 \end{vmatrix} = \Delta \qquad (2.4.1.7)$$

and X_{zz}, $X_{z\phi}$, $X_{\phi z}$ and $X_{\phi\phi}$ are the frequency response functions.

Equation (2.4.1.6) will give the instantaneous response of the structure due to wind loading at a certain excitation frequency.

Assuming that the cross-spectrum terms do not have significant effect in the response spectra,

$$S_\eta = (S_L |X_{zz}|^2 + S_M |X_{z\phi}|^2) |J_f|^2$$
$$S_\phi = (S_L |X_{\phi z}|^2 + S_M |X_{\phi\phi}|^2) |J_f|^2 \qquad (2.4.1.8)$$

By integrating the spectra of η and Φ, root-mean-square values of the respective displacement can be found:

$$\sigma_\eta^2 = \int_0^\infty S_\eta(f)\,df$$
$$\sigma_\phi^2 = \int_0^\infty S_\phi(f)\,df \qquad (2.4.1.9)$$

2. Classical Flutter

In uniform smooth flow there is no excitation due to turbulence and only the steady aerodynamic forces are involved. Considering the equation of motion, in order to have non-trivial solution of η and Φ, we must have (Ref 6)

$$\begin{vmatrix} \mu(1-\xi^2+i2\zeta_z\xi)-\xi^2L_z & -\xi^2L_\phi \\ -\xi^2M_z & \nu(\beta^2-\xi^2+i2\zeta_\phi\beta\xi)-\xi^2M_\phi \end{vmatrix} = 0 \qquad (2.4.1.10)$$

The determinant is a complex function of two variables, frequency and velocity. The real and immaginary components of the determinant must vanish at the same time to satisfy the condition. Thus,

$$\Delta_R = 0$$
$$\Delta_I = 0 \qquad (2.4.1.11)$$

The solutions of the two equations will yeild the critical velocity and the critical frequency of the system at which classical flutter will occur.

2.4.2 Non-linear Theory

1. Galloping

The theory of galloping motion of a

prismatic section subjected to a uniform two dimensional flow suggested by Novak is well-known (Ref 4).

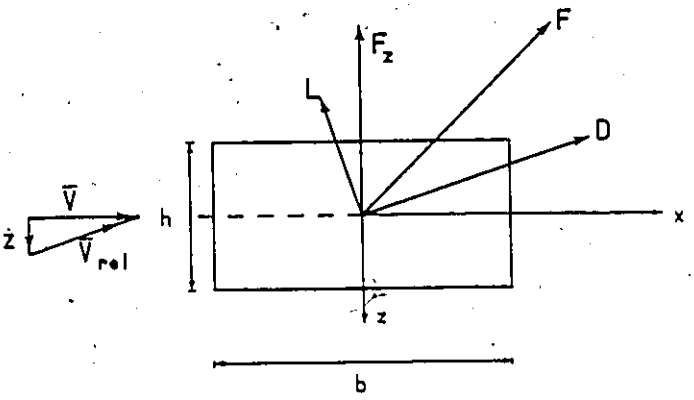

The force coefficient C_{F_z} is given by,

$$F_z = \frac{1}{2}\rho h \bar{V}^2 C_{F_z} \qquad (2.4.2.1)$$

Here, C_{F_z} is assumed to be expandable into a power polynomial of $\tan(\frac{\dot{Z}}{V})$,

Thus,

$$C_{F_z} = \sum_{i=1}^{m} A_i (\frac{\dot{z}}{\bar{V}})^i + \sum_{j=2}^{k} A_j (\frac{\dot{z}}{\bar{V}})^j \frac{\dot{z}}{|\dot{z}|} \qquad (2.4.2.2)$$

The value of C_{F_z} can be determined experimentally by the measurements of the drag and lift force coefficients of the given section.

Introducing dimensionless parameters $n = \frac{\rho h^2 \ell}{4m}$, $a = \frac{z_{max}}{h}$, $U = \frac{V}{\omega h}$ and $Z = \frac{z}{h}$, the equation of motion can be given as

$$\ddot{Z} + \omega^2 Z + G(\dot{Z}) = 0 \qquad (2.4.2.3)$$

in which, the total damping force of the system G(z) is

$$G(\dot{Z}) = 2\zeta\omega\dot{Z} - 2n\left(\sum_{i=1}^{m} A_i \omega^{2-i} \frac{\dot{Z}^i}{U^{i-2}} + \sum_{j=2}^{k} A_j \omega^{2-j} \frac{\dot{Z}^j}{U^{j-2}} \frac{\dot{Z}}{|\dot{Z}|} \right) \qquad (2.4.2.4)$$

When galloping has a steady limit cycle, the total work done by damping terms is required to be zero, and we can therefore conclude that the total energy of the system in a period T should be zero, i.e.

$$W = \int_0^{\ell}\int_0^{T} G(Z)\,dx\,dZ(t) = 0 \qquad (2.4.2.5)$$

Equation (2.4.2.5) will give the relationship between the reduced wind speed and the galloping responses,

$$\frac{1}{\bar{U}} = \sum_{r=1}^{s} A_r B_r C_r \left(\frac{a}{\bar{U}}\right)^{r-1} \qquad (2.4.2.6)$$

where $\bar{U} = \frac{n}{\zeta} U$ and $\bar{a} = \frac{n}{\zeta} a$

The coefficients B_r and C_r were obtained as

$$B_i = 2\,\frac{1\cdot 3\cdot 5\cdot \cdots \cdot i}{2\cdot 4\cdot 6\cdot \cdots \cdot (i+1)} \qquad i = \text{odd}$$

$$B_j = \frac{4}{\pi}\,\frac{2\cdot 4\cdot 6\cdot \cdots \cdot j}{1\cdot 3\cdot 5\cdot \cdots \cdot (j+1)} \qquad j = \text{even} \qquad (2.4.2.7)$$

$$C_r = \frac{\int_0^{\ell} \upsilon^{2-r}(x)\, z(x)^{r+1}\, dx}{\int_0^{\ell} z^2(x)\, dx}$$

where $\upsilon(x)$ is the wind speed distribution along the span.

In uniform flow and two dimensional body, $C_r \equiv 1$. When the vibration mode is a half-sinewave ($z(x)=\sin(\frac{\pi x}{\ell})$) and wind is uniform, then $C_r = B_r$.

2. Stall Flutter

Stall flutter is a kind of self-excited oscillation induced by the negative aerodynamic damping effect.

Assuming that the mean wind velocity is $\bar{V}$ and that the deck width is B, the aerodynamic pitching moment per unit span length can be written as

$$M_\alpha = \frac{1}{2}\rho V^2 B^2 C_m(\alpha) \qquad (2.4.2.9)$$

In general, $C_M(\alpha)$ is a non-linear function of the displacement α. Thus, the non-linear approach similar to the one as described in the case of galloping could also be applied here. The instantaneous angular displacement can be taken as follows

$$\alpha = \Phi + \frac{eB\dot{\Phi}}{\bar{V}}$$

For the definition of these terms, see 2.3.2.

Chapter III

EXPERIMENT

3.1 MODELS

The test models used in this study were designed to investigate the vibration behaviour of 2-dimensional and 3-dimensional structures exposed to various flow conditions.

Classical flutter, stall flutter and galloping are the three main categories of divergent amplitude vibrations which are likely to destroy the structure. Flat plate, H section and box sections, which are known to be unstable in these three vibration mechanisms respectively, were chosen to demonstrate the influence of 2-dimensional and 3-dimensional configurations on each mechanism. The linear dimensions, and dynamic properties of the models are summarized in Table 1 .

TABLE 1

Properties of Test Models

MODEL		FLAT PLATE	TORSIONAL	GALLOPING
MODEL CONFIGURATION		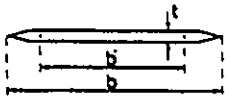	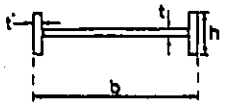	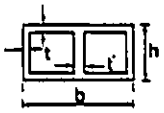
LINEAR DIMENSIONS		b=31.75 mm b=25.40 mm t= 1.28 mm	b=28.56 mm h= 8.92 mm t= 0.82 mm t'= 2.08 mm	b=12.64 mm h= 6.32 mm t= 1.24 mm t'= 2.48 mm
m (kg/m)		0.048	0.057	0.053
Θ (kgm^2/m)		6.15×10^{-6}	7.03×10^{-6}	———
NATURAL FREQUENCY	f_z	12.5 HZ	14.5 HZ	15.7 HZ
	f_α	23.5 HZ	20.0 HZ	———
STRUCTURAL DAMPING	ζ_z	0.90%	0.87%	0.90%
	ζ_α	0.73%	0.44%	———
AERODYNAMIC DERIVATIVES	$\left(\frac{\partial C_l}{\partial \phi}\right)_0$	6.28	-2.86	2.44
	$\left(\frac{\partial C_m}{\partial \phi}\right)_0$	1.57	0.43	———
SUPPORTING MECHANISM		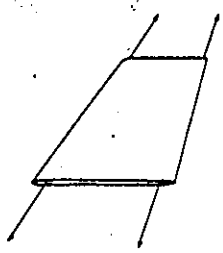	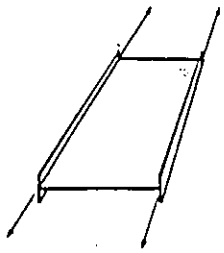	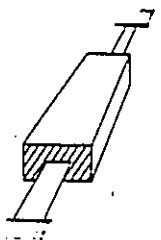

3.2 SET-UP OF THE MODEL

In the testing of flat plate and H-section models, since the vertical as well as torsional displacement were expected to appear, these models were mounted on a pair of piano wires as shown in Figure 1 to allow these vibration modes to the model. The motion of the model in the windflow direction is neglected due to its relatively minor role.

The box-section model was seated on two steel springs which were clamped from two supports outside the wind tunnel as shown in Fig. 2 . This design prevented the rotational displacement which was not desired for the measurement of buffeting and galloping responses in vertical mode for the purpose of this particular study.

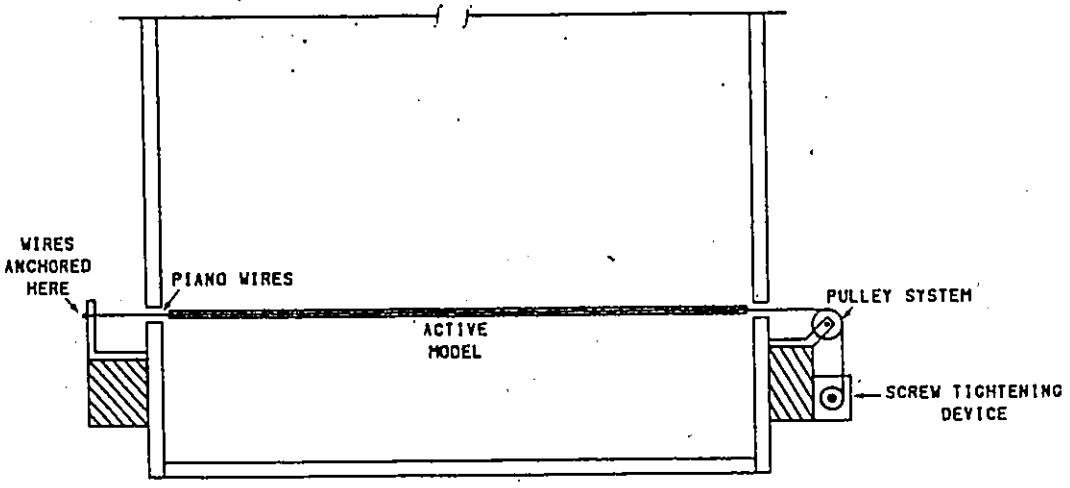

Figure 1: Sketch of 3-D model support mechanism for flat plate and H-section and

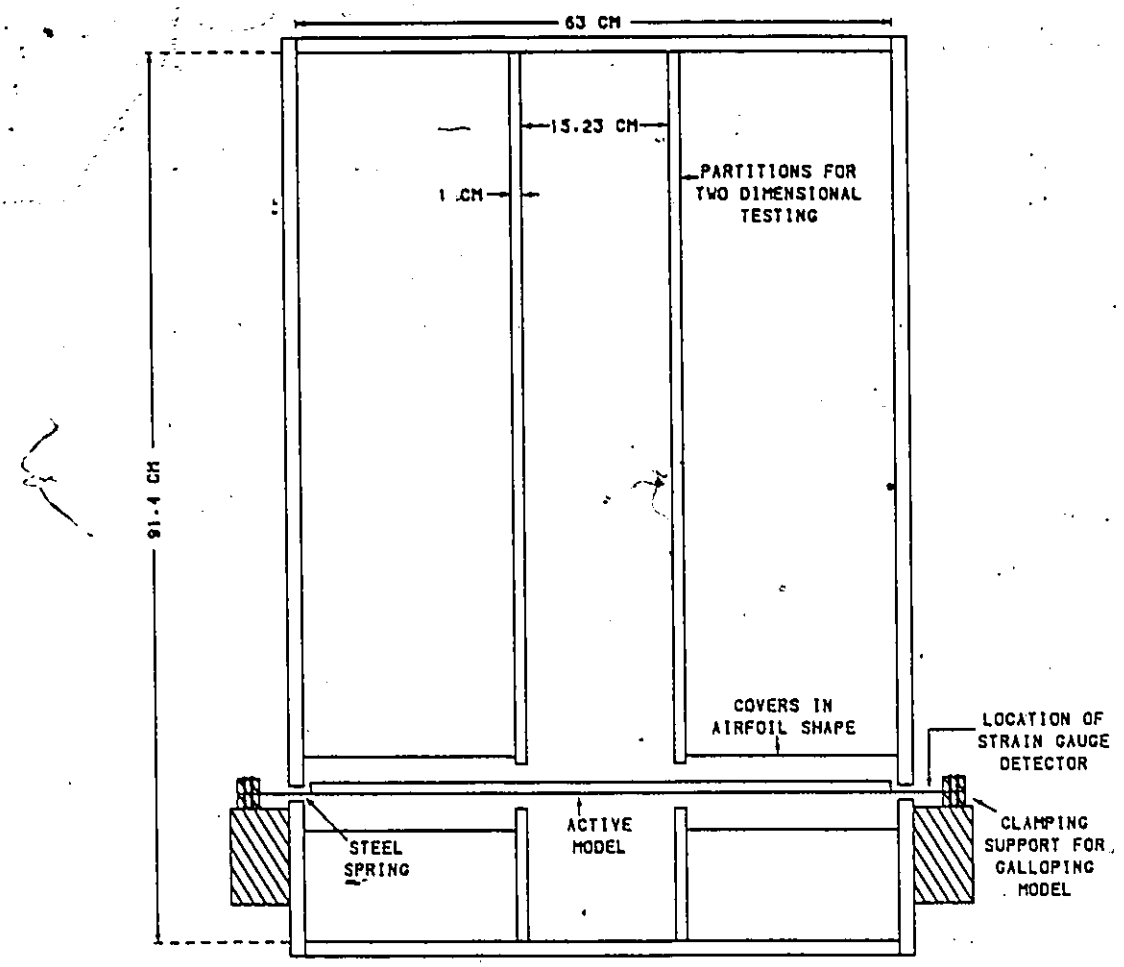

Figure 2: Sketch of 2-D model support mechanism for box-section

3.3 GENERAL PROCEDURES

The model was installed in the test section of the wind tunnel, and tuned to the designed torsional to flexural frequency ratio in the case of flat plate and H-section models. Calibration for the response measurement was done by the method as described in Appendix E. A free vibration test of the model was performed to obtain the structural dampings and natural frequencies of the models.

Four different flow conditions, "smooth" flow, which in reality was a relatively shallow boundary layer flow, homogeneous turbulence induced by a coarse grid and a fine grid and a deep boundary layer flow generated by artificial roughness inside the wind tunnel,were used for the test. The flow conditions are discussed in Section 4.1 in detail. The mean and root-mean-square response of the model were detected through the strain gauge system attached to the model supporting wires immediately outside the tunnel wall. The response of the model was recorded from a voltmeter and the transient vibrations were traced by a paper chart recorder.

The 2-dimensional testing condition consists of simply the isolation of the mid-quarter span of the model by two wooden partitions placed in the wind tunnel along the mean flow as shown in Figure 2 . Each partition was composed of two parts which were assembled in the presence of the model. The sections of the bridge outside of the partitions were enclosed in airfoil shaped coverages. The flow conditions for 2-dimensional models were found to be very similar to those in the 3-dimensional testing.

3.4 MEASUREMENTS

3.4.1 Flow Measurement

The flow condition at the test section is of great importance to the test results. Therefore the measurements were carried out carefully for each flow condition.

Vertical profiles of both mean flow velocity and turbulence intensity of the v-component at the midspan position were obtained with the hot-film anemometer and displayed in calibrated units through integration voltmeters. The velocity spectra of the v-component at certain wind speed were plotted. This analysis was carried out using the Fourier analyser at the Low Speed Aerodynamics Laboratory, NAE/NRCC, from the recorded data in the magnetic tape recorder during the experiment.

3.4.2 Response Measurement

Due to the difference in setup for the test models, two kinds of response detecting devices were applied for the response measurement.

1. DOUBLE GAUGE SYSTEM

In the testing of flat plate and H-section models, the transverse and rotational motions of the models were detected from the vertical deflection of the wires, which extended from the model to the support

outside the wind tunnel wall. This section of the wires were attached to a metal strip fixed at both ends, on which there were two strain gauges attached, as shown in Figure 3 . The dectecting device was mounted on an isolated support to prevent the noises due to the vibration from the wind tunnel.

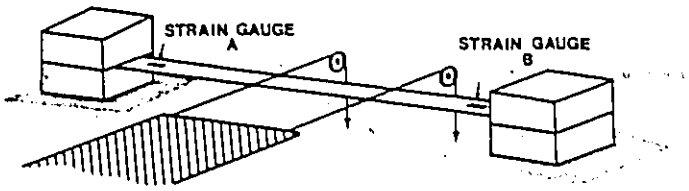

Figure 3: Double Gauge System

Individual vertical motion of the wires will induce bending moment along the metal strip and give corresponding strains at the locations of the gauges. Thus, the mean of two displacement output is proportional to the vertical deflection of e at the centre of the section, while the half of the difference between two signals divided by the distance between the wires gives the torsional displacement of the system. This was done through the sum-and-difference amplifier.

2. SINGLE GAUGE SYSTEM

The rotational stiffness of the model was extremely high in the box-section model and thus only the transverse motion was observed. A strain gauge was attached to the supporting leaf spring which extended from the support to the model. The strain induced by the vertical motion of the model was calibrated to the mid-span deflection.

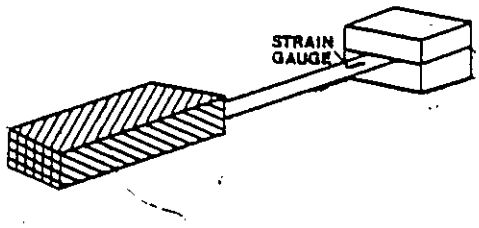

Figure 4: Single Gauge System

Signals from the strain gauges were amplfied as they passed through the strain gauge conditioner. Transient responses of the model were read out from the numerical integrator in the units of voltage display, and recorded by the tape recorder for futher analysis of the response spectra.

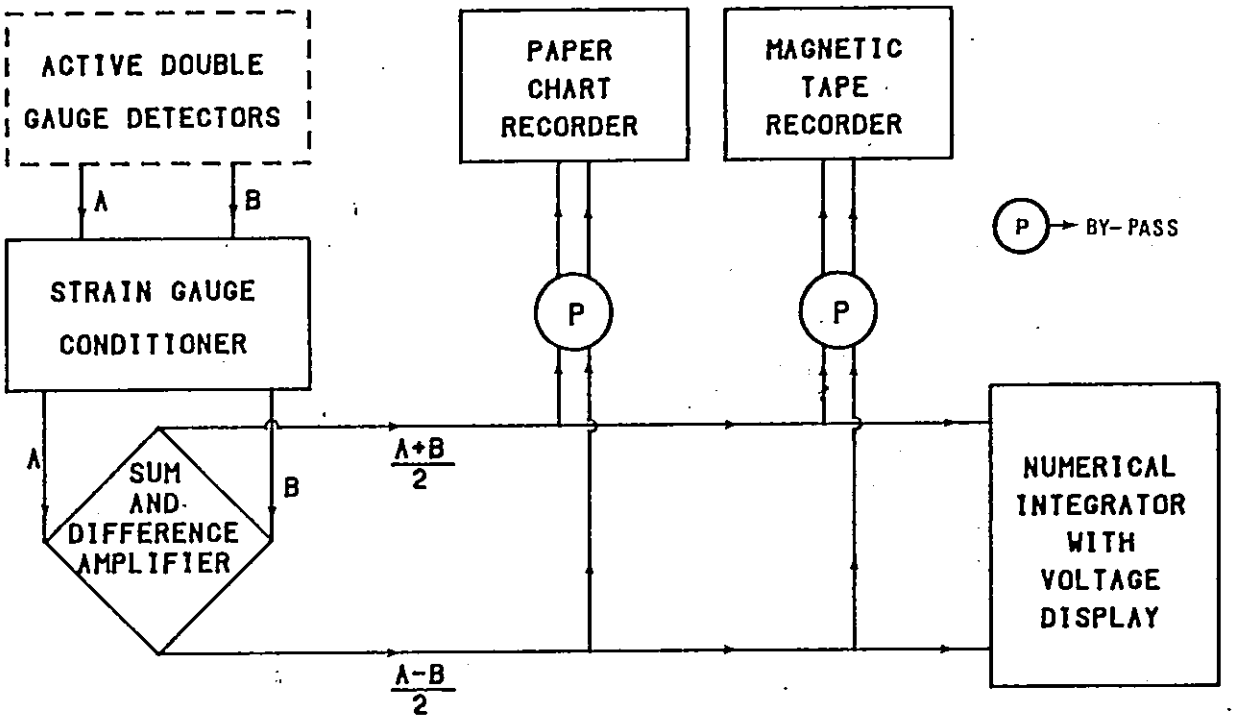

Figure 5: Flow chart of double gauge measuring system

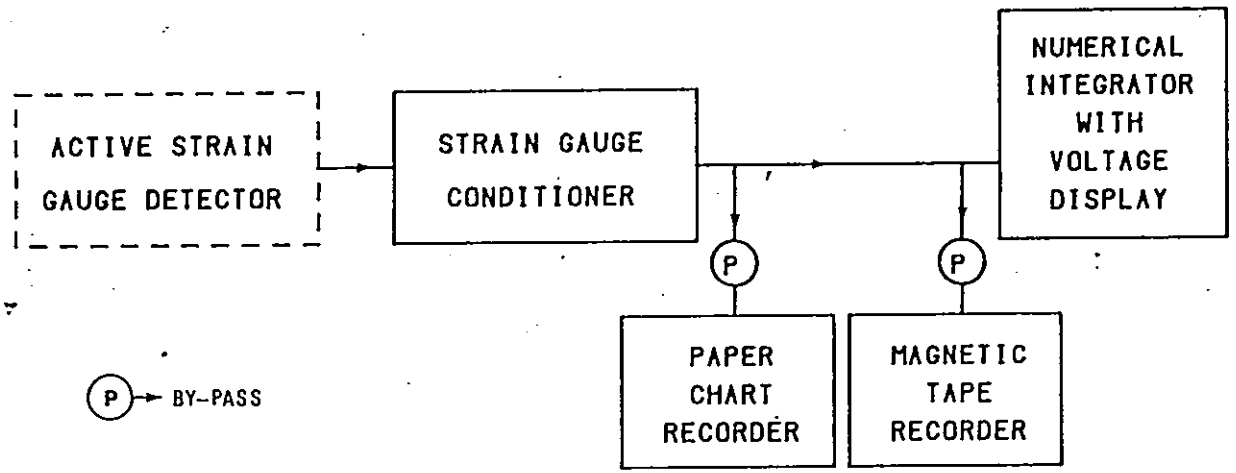

Figure 6: Flow chart of single gauge measuring system

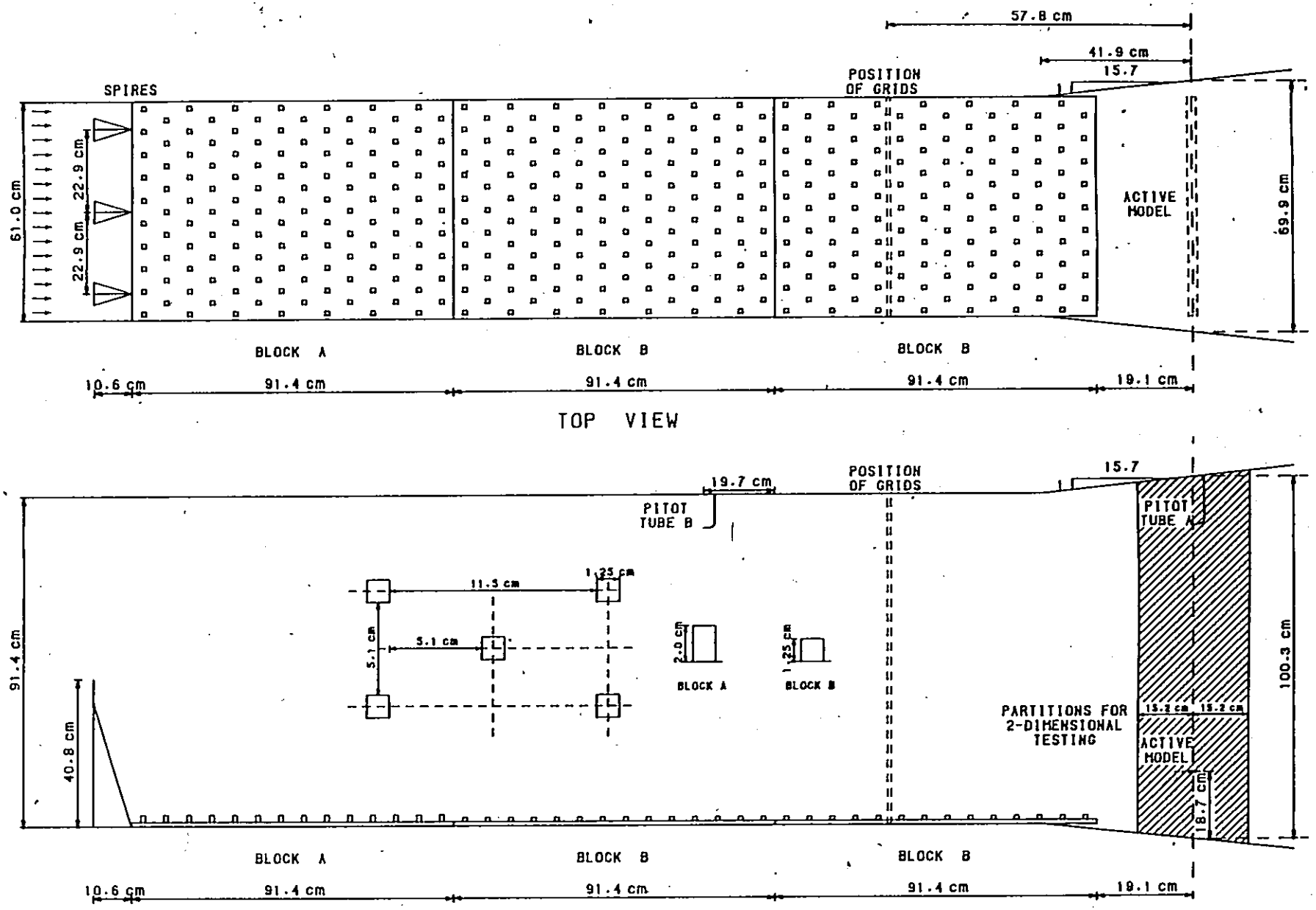

Figure 7: General Layout of The Wind Tunnel and Turbulence Generating Mechanism

Chapter IV

SUMMARY AND DISCUSSION OF EXPERIMENTAL DATA

4.1 DISCUSSION OF ATMOSPHERIC FLOW SIMULATION

Artificial turbulence was generated inside the low speed wind tunnel, to simulate the full-scale atmospheric turbulence in a scale of approximately 1:1000. Homogeneous turbulence was also created by square-mesh grids of two different configurations as shown in Figure 8 .

The artificial turbulence represented the general characteristics of the atmospheric turbulent flow at the elevation of 20 to 80 meters above ground surface, which can be described as a typical turbulence intensity and integral length scale. In the present study the behaviour of bridge structures in shear layer flow is the author's primary concern. The simulated atmospheric boundary layer flow was reproduced by a fetch of 2.7 meter of rough floor which consists of rectangular blocks, arranged in the pattern as shown in Figure 7 . The thickness of the boundary layer flow was augmented by three spires arranged at the entrance of the tunnel.

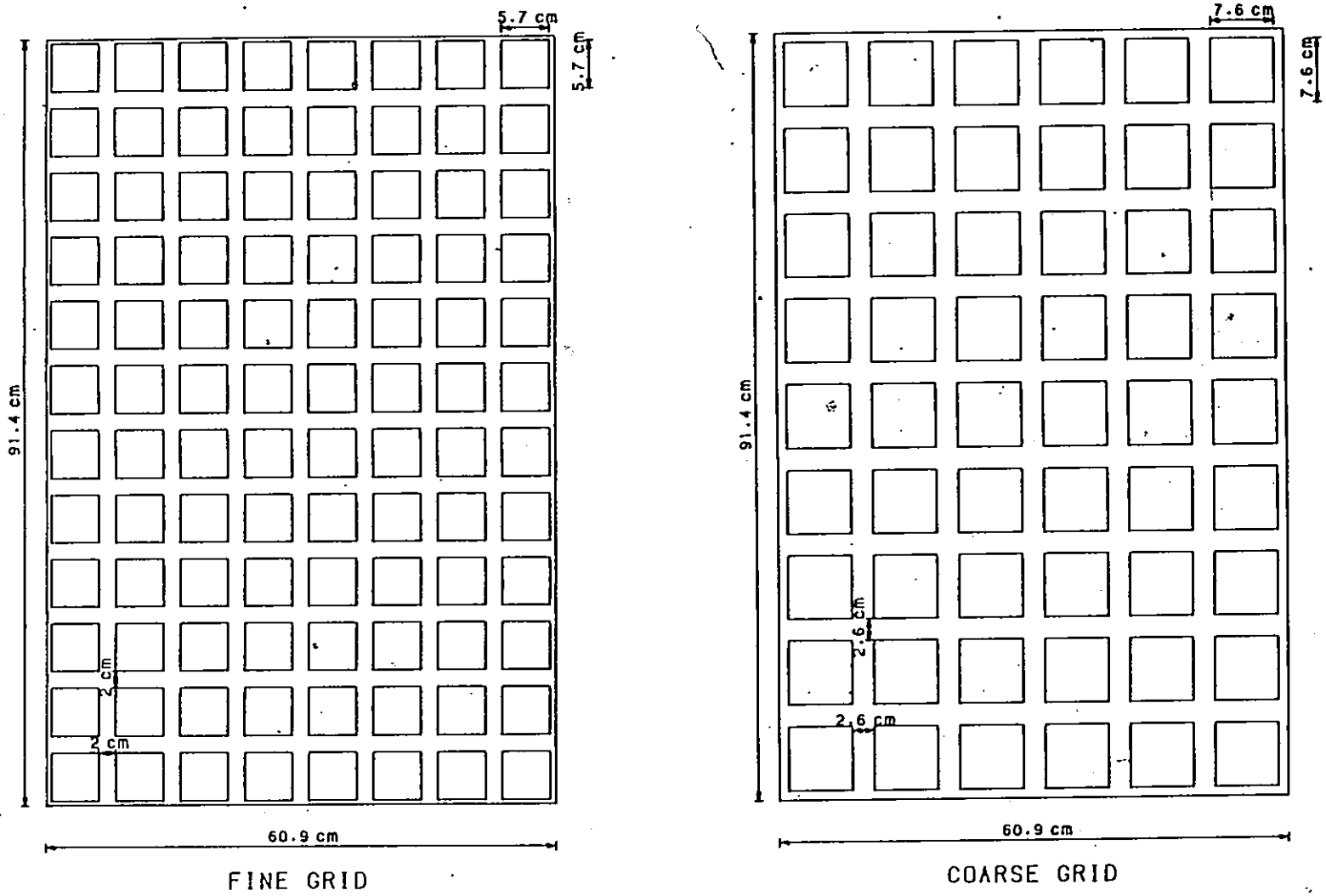

Figure 8: Configuration of Square-mesh Grids

Characteristics of the turbulence produced by the grids and block terrain were measured and analysed as follows:

1. TURBULENCE INTENSITY

The vertical component of turbulence is the most significant source of excitation responsible for buffeting of the bridge models. Its fluctuation σ_w is suggested by Panofsky and McCormick as $\sigma_w = 1.25u_*$ while the standard deviation of the v- component is commonly accepted to be $\sigma_v = 2.5u_*$. Thus, the ratio of I_v to I_w is 2:1, where the turbulence intensities I_v and I_w of the two components are expressed as

$$I_v = \frac{\sigma_u}{\bar{V}}$$

$$I_w = \frac{\sigma_w}{\bar{V}} \qquad (4.1.1)$$

where $\bar{V}$ is the mean flow velocity at the same location.

In this study, flow measurement was carried out only in the longitudinal direction, therefore the intensity of turbulence in the vertical direction was assumed to be closely represented by $I_v = 0.5 * I_w$ as described above.

2. SPECTRA OF TURBULENCE

Normalized spectral density functions for v and w components suggested by von Karman (1948) for

homogenous turbulence were used in this study, because of their generally good agreement with the measured spectra . The functions are expressed as

$$\frac{fS_v(f)}{\sigma_v^2} = \frac{0.637\ \gamma}{(1 + 1.79\gamma^2)^{5/6}}$$

$$\frac{fS_w(f)}{\sigma_w^2} = \frac{\gamma}{\pi}\frac{1 + 4.78\gamma^2}{(1 + 1.79\gamma^2)^{11/6}} \qquad (4.1.2)$$

where

$$\gamma = \frac{2\pi f}{\bar{V}} L_x$$

In boundary layer flow, Panofsky's empirical expression

$$\frac{fS_w(f)}{\sigma_w^2} = \frac{4\ \kappa}{(1 + 4\kappa)^2} \qquad \kappa = \frac{f}{\bar{V}} h_g \qquad (4.1.3)$$

was used.

3. INTEGRAL SCALE OF TURBULENCE

One of the most important parameters in modelling of atmospheric turbulence is the scale of turbulence. The design relation between the scale of turbulence in the wind tunnel and that in the atmosphere is assumed to be 1:1000. From von Karman's spectrum, the peak value of $\frac{2\pi f L_u}{\bar{V}}$ is found to be 0.915; i.e.,

$$\left(\frac{fL_u}{\bar{V}}\right)_{peak} = 0.149 \qquad (4.1.4)$$

The integral length scale of the measured spectrum in the v-direction are calculated from Equation (4.1.4) and listed in Table 2.

4. VERTICAL PROFILE OF MEAN VELOCITY

The vertical distribution of the mean flow velocity in the boundary layer generally follows the power-law. Hence, the mean wind velocity $\bar{V}$ at height z above the ground can be expressed by

$$\frac{\bar{V}}{V_g} = \left(\frac{z}{\delta}\right)^{\alpha} \qquad (4.1.5)$$

where V_g = mean gradient velocity,

z = elevation above ground, and

δ = depth of the boundary layer.

In homogenous turbulence, the mean velocity $\bar{V}$ at any altitude is independent of the height z. Characteristics of the flow conditions inside the wind tunnel were measured and presented in Table 2 .

TABLE 2

Measured Characteristic of Wind Flow

Flow Condition	Turbulence Intensity Iu	Scale of Turbulence Lu	Thickness of Boundary Layer	Power exponent
Smooth Flow (2-D)	4 %			
Fine Grid (2-D)	15 %	25 mm		
Coarse Grid (2-D)	22 %	50 mm		
Boundary Layer (2-D)	14 %	85 mm	39 cm	0.52
Smooth Flow (3-D)	4 %			
Fine Grid (3-D)	15 %	25 mm		
Coarse Grid (3-D)	22 %	50 mm		
Boundary Layer (3-D)	16 %	85 mm	40 cm	0.51

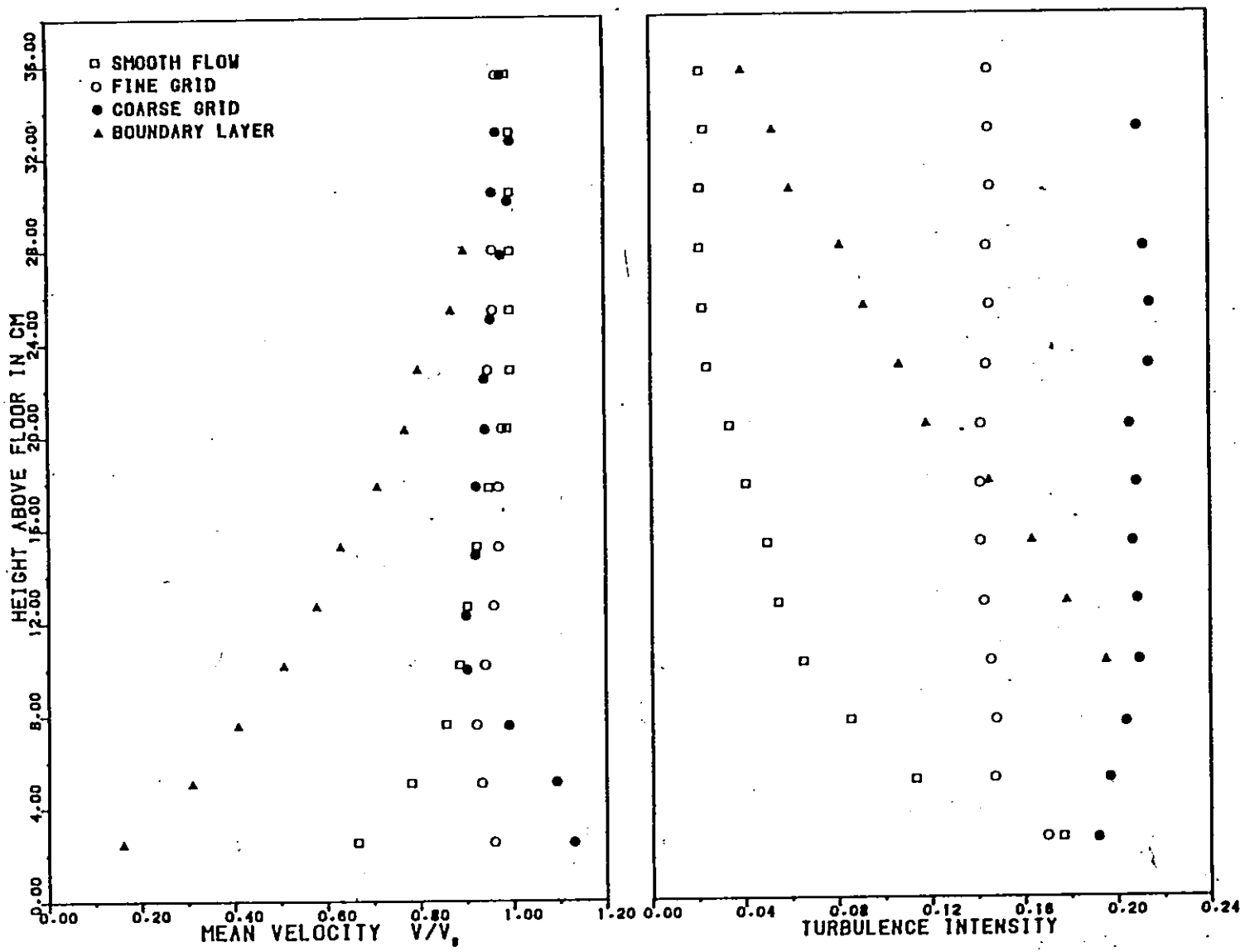

Figure 9: Flow measurements of u-component in 2-D

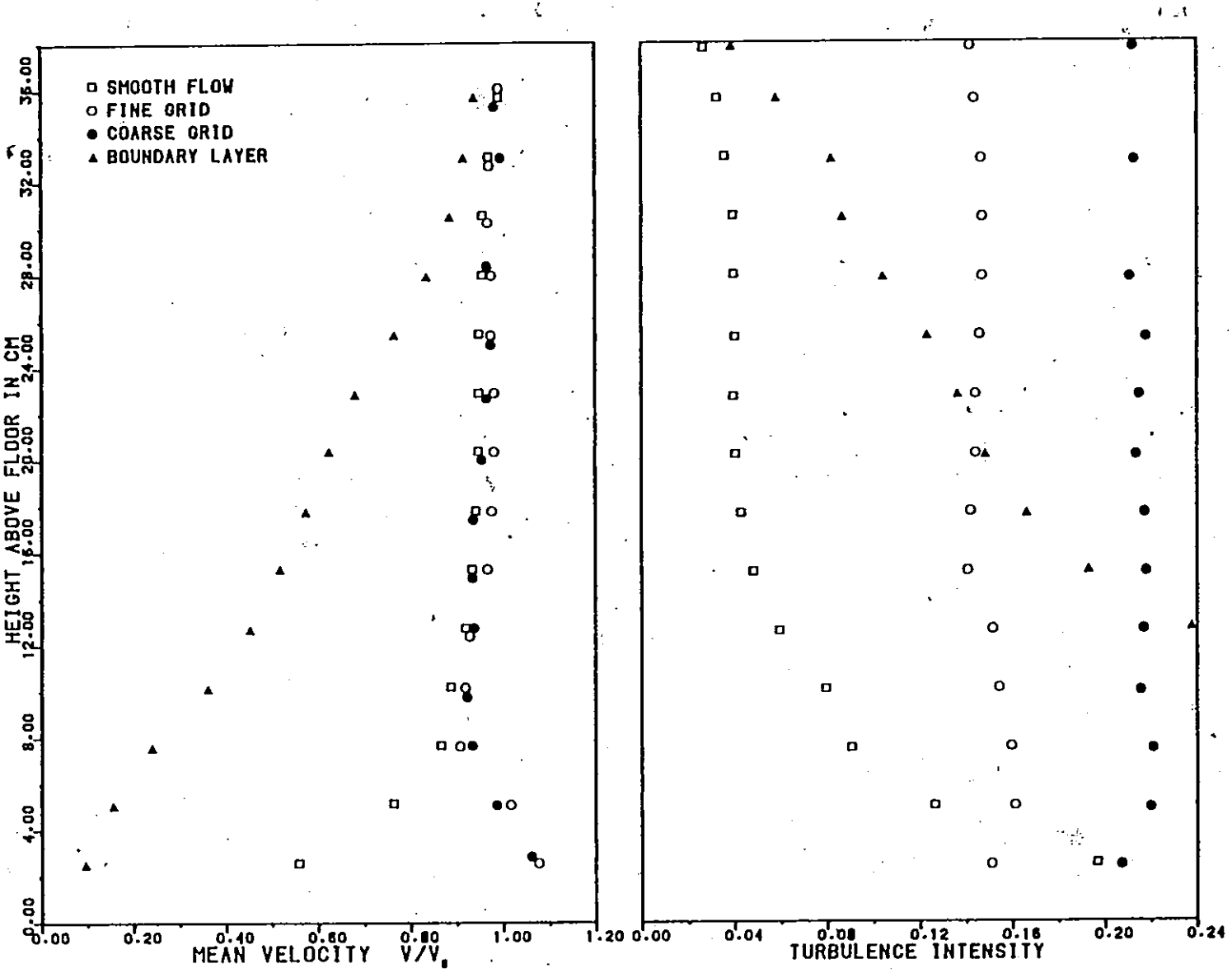

Figure 10: Flow measurements of u-component in 3-D

4.2 APPLICATION OF THEORY TO THE MODELS

The theoretical analyses discussed in Chapter II are applicable to test models with proper boundary conditions and by using the appropriate method.

1. FLAT PLATE

The wind flow around a thin section in small oscillatory amplitude can be considered as potential flow. This is the basic assumption in the treatment of the flat plate problem. The potential flow theory, based on the movement of a streamline body submerged in an incompressible non-viscous fluid, is applied to flutter problem as studied by Theodorsen and Garrick (Ref 15). In uniform steady flow, a flat plate will be subjected to the aerodynamic forces described in section 2.3.1 . Based on its aerodynamic shape, a flat plate can be treated as a typical streamlined body in which potential flow around the section is assumed. Thus the equations (2.4.1.3) become

$$\ddot{\eta} + 2\zeta_z\omega_z\dot{\eta} + \omega_z^2\eta = \frac{\omega^2}{\mu}(L_z\eta + L_\phi) - \frac{L_f(t)}{mb}$$

$$\ddot{\Phi} + 2\zeta_\phi\omega_\phi\dot{\Phi} + \omega_\phi^2\Phi = \frac{\omega^2}{\nu}(M_z\eta + M_\phi\Phi) + \frac{M_f(t)}{\Theta} \qquad (4.2.1)$$

2. BLUFF STRUCTURES

For bluff bodies such as H-sections or box-sections, potential flow theory will no longer be valid due to the separation of flow and vortex shedding behind the section. The quasi-steady theory can be applied only if the aerodynamic derivatives are given.

The equations of motion for this case will become

$$\ddot{\eta} + 2\zeta_z\omega_z\dot{\eta} + \omega_z^2\eta = \frac{\bar{V}^2}{\mu\pi b^2}\left(\frac{\partial C_l}{\partial \alpha}\right)_o\left(\Phi + \frac{b\dot{\eta}}{\bar{V}} + \frac{eB\dot{\Phi}}{\bar{V}}\right) - \frac{L(t)}{mb} \qquad (4.2.2)$$

$$\ddot{\Phi} + 2\zeta_\phi\omega_\phi\dot{\Phi} + \omega_\phi^2\Phi = \frac{2\bar{V}^2}{\nu\pi b^2}\left(\frac{\partial C_m}{\partial \alpha}\right)_o\left(\Phi + \frac{b\dot{\eta}}{\bar{V}} + \frac{eB\dot{\Phi}}{\bar{V}}\right) + \frac{M(t)}{\theta}$$

The box section model tested in this study was designed to study the vertical bending vibration behaviour of this section. Therefore the torsional displacement was neglected. The equation of motion was then expressed as

$$m\left(\ddot{Z} + 2\zeta_z\omega_z\dot{Z} + \omega_z^2 Z\right) = \frac{1}{2}\rho V^2 B\left(\frac{\partial C_l}{\partial \alpha}\right)_o\frac{\dot{Z}}{\bar{V}} - L_f(t) \qquad (4.2.3)$$

4.3 THEORETICAL RESULTS

An attempt was made to theoretically estimate the model responses using available knowledge in flow statistics and vibration theories.

The theoretical responses of the models in various flow conditions were calculated according to the methods described in section 2.4 . In this section, buffeting responses and the instability phenomena, i.e. classical flutter and galloping, of each model are presented.

4.3.1 Buffeting Responses

Random responses of the models were computed by statistical methods (spectral analysis) with the appropriate physical and aerodynamic properties of the models in conjunction with functions which satisfied the corresponding flow conditions. The flow chart of the analysis is given in Table 3, and the computer programs applied are listed in Appendix F . Theoretical response was plotted in the next section for comparison with experimental responses, and tabled in Appendix B for reference.

In the vibration of 3-dimensional bodies, the author tried to apply the 2-dimensional approach with reasonable modifications on the mass and the moment of inertia of the

TABLE 3

Computation of Buffeting responses

FLOW CONDITION	MODEL	$\left(\frac{\partial C_L}{\partial \phi}\right)_0$	$\left(\frac{\partial C_m}{\partial \phi}\right)_0$	AERODYNAMIC ADMITTANCE	JOINT ACCEPTANCE	VELOCITY SPECTRUM
2-D	FLAT PLATE	6.28	1.57	$\lvert\chi_w^L\rvert^2 = \frac{1}{1+2\pi k}$	$\lvert J_f\rvert^2 = \frac{2}{\lambda}\left[1+\frac{1}{\lambda}\left(e^{-\lambda}-1\right)\right]$	HOMOGENOUS TURBULENCE $\frac{fS_u(f)}{\sigma_u^2} = \frac{\gamma}{\pi}\frac{1+4.78\gamma^2}{(1+1.79\gamma^2)^{11/6}}$ $\gamma = \frac{2\pi f}{\bar{V}} L_x$
	TORSIONAL	-2.86	0.43			
	GALLOPING	2.44	—	$\lvert\chi_w^m\rvert^2 = \frac{1}{1+2\pi k}$		
3-D	FLAT PLATE	6.28	1.57	$k = \frac{\omega b}{\bar{V}}$	$\lvert J_f\rvert^2 = \frac{\lambda^2}{\lambda^2+\pi^2} + \frac{2\pi^2(1+e^{-\lambda})}{(\lambda^2+\pi^2)^2}$	BOUNDARY LAYER $\frac{fS_w(f)}{\sigma_w^2} = \frac{6\kappa^2\kappa}{(1+4\kappa)^2}$ $\kappa = \frac{f}{\bar{V}} h_g$
	TORSIONAL	-2.86	0.43			
	GALLOPING	2.44	—			

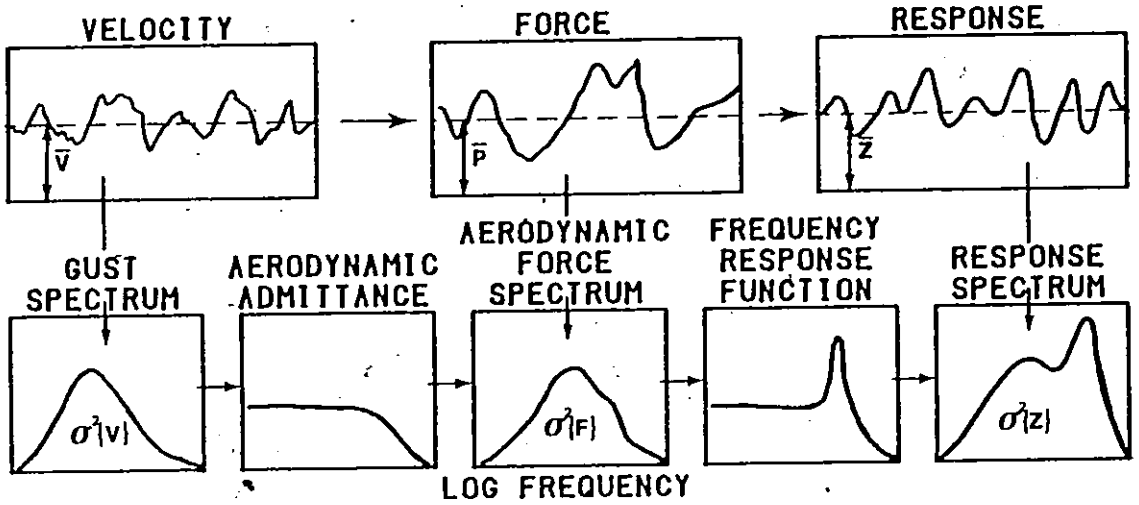

model . Assuming that the model is simply supported at its ends and applying the principle of generalised mass, the model can be assumed to have a uniform mass m^* distributed along its span, where m^* is given by

$$m^* = \frac{m\ell}{2}/\ell = \frac{m}{2}$$

Without loss of generality, the mass moment of inertia of the 3-dimensional model is given by $\theta^* = \frac{\theta}{2}$.

Due to the setup of the testing, the 2-dimensional models employed are actually the 3-dimensional model as a structure but only its mid-quarter span is exposed to the wind flow. This modification is neccessary in the formulations proposed in Chapter II.

In 2-dimensional flow, excitation forces are working on the exposed length of the model, but in fact, the vibration of the entire model is encountered. Assuming a fundamental vibration mode of a half-sine wave, the 2-dimensional model can be approximated as a rigid body at the mid-quarter span with a curvature that is almost neglegible. The generalised mass of the model is therefore assumed to be the generalized mass the whole 3-D span concentrated at the mid-quarter span during vibration of the 2-dimensional model. Thus, mass per unit length m involved in the calcualtion of 2-dimensional model response is substituted by m^{**},

where $$m^{**} = \frac{m\ell}{2}/\frac{\ell}{4} = 2m$$

The same approach was applied to the mass moment of inertia of the 2-dimensional model which yields $\theta^{**} = 2\theta$.

4.3.2 Classical Flutter

The phenomenon of classical flutter had been described in section 2.4 . The expected critical wind speed of classical flutter of the flat plate model was calculated from Equation (2.4.1.10); ie., the vanishing of the determinant

$$\begin{vmatrix} \mu(1-\xi^2+i2\zeta_z\xi)-\xi^2L_z & -\xi^2L_\phi \\ -\xi^2M_z & \nu(\beta^2-\xi^2+i2\zeta_\phi\beta\xi)-\xi^2M_\phi \end{vmatrix} = 0 \qquad (4.3.2.1)$$

The reduced critical wind speeds are found to be as follows:

2-dimensional model $V_r=31.5$ ($V_r=32.5$, in experiment)

3-dimensional model $V_r=16.0$ ($V_r=15.7$, in experiment)

where $V_r = \dfrac{V_{cr}}{f_z B}$

4.3.3 Galloping

The theoretical galloping response of the box section model in both 2-dimensional and 3-dimensional flow was computed by the non-linear analysis described in section

2.4.2 . The calculations were based on the lateral force coefficients C_{F_z} from Novak(1972) on a rectangular prism with side ratio B/h=2/1 in a flow with turbulent intensity equals 5% . The lateral force coefficient was taken from the work by Novak (Ref 4). From Figure 11, the influence of turbulence intensity on the lateral force coefficient is quite significant, and only a turbulence intensity of 5 % is comparable with the flow conditions encountered in this study, therefore, only the coefficient for 5% turbulent intensity, as seen on the graph, is employed in the prediction of galloping response.

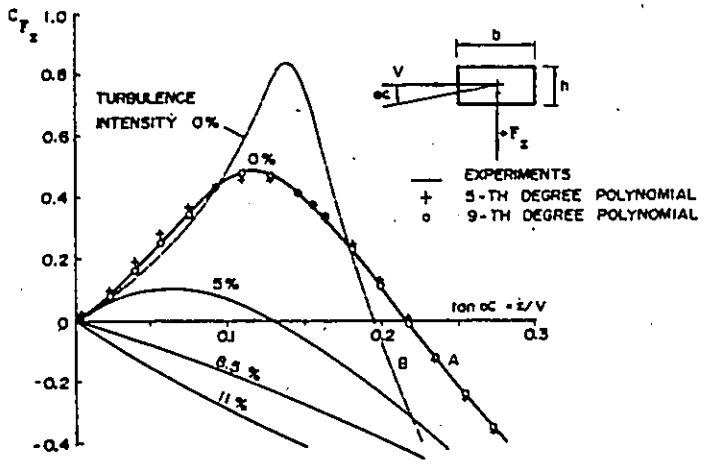

Figure 11: Graph of lateral force coefficient against angle of incidence

The dimensionless velocity $\bar{U}$ and amplitude $\bar{a}$ obtained from the non-linear analysis (Program IV in Appendix F) are functions of the mass parameter and the structural

damping. In the case of the 2-dimensional model, mass per unit length is taken as twice of the actual value because of the apparent mass effect described in the last section, while the mass per unit length in a 3-dimensional model is half of the physical value.

When the response is assumed to be a simple harmonic fluctuation with time, the root-mean-square value of the vibration is equal to $1/\sqrt{2}$ of the absolute amplitude. The root-mean-square galloping responses are plotted against the reduced wind speed $\frac{V}{f_z h}$ in Figure 12 .

4.4 DISCUSSION ON RESULTS OF FLAT PLATE MODEL

Theoretical and experimental responses of the model are plotted in Figure 13 for comparison. In Fig 13 (a) & (c), the measured torsional and flexural responses of the 2-D and 3-D models in homogeneous turbulence show good agreement with the theoretical values, which suggest that the basic assumptions of flow spectra and the apparent mass concept described in section 4.3.1 were believed to be valid.

Classical flutter which occurs at the predicted wind speed, both in the 2-D and 3-D models, stressed that the hypothesis of potential flow theory holds in the flat plate model. The critical wind speed of flutter in the 2-D model was delayed to twice the critical value in the 3-D model. This was due to the doubled mass parameter in the

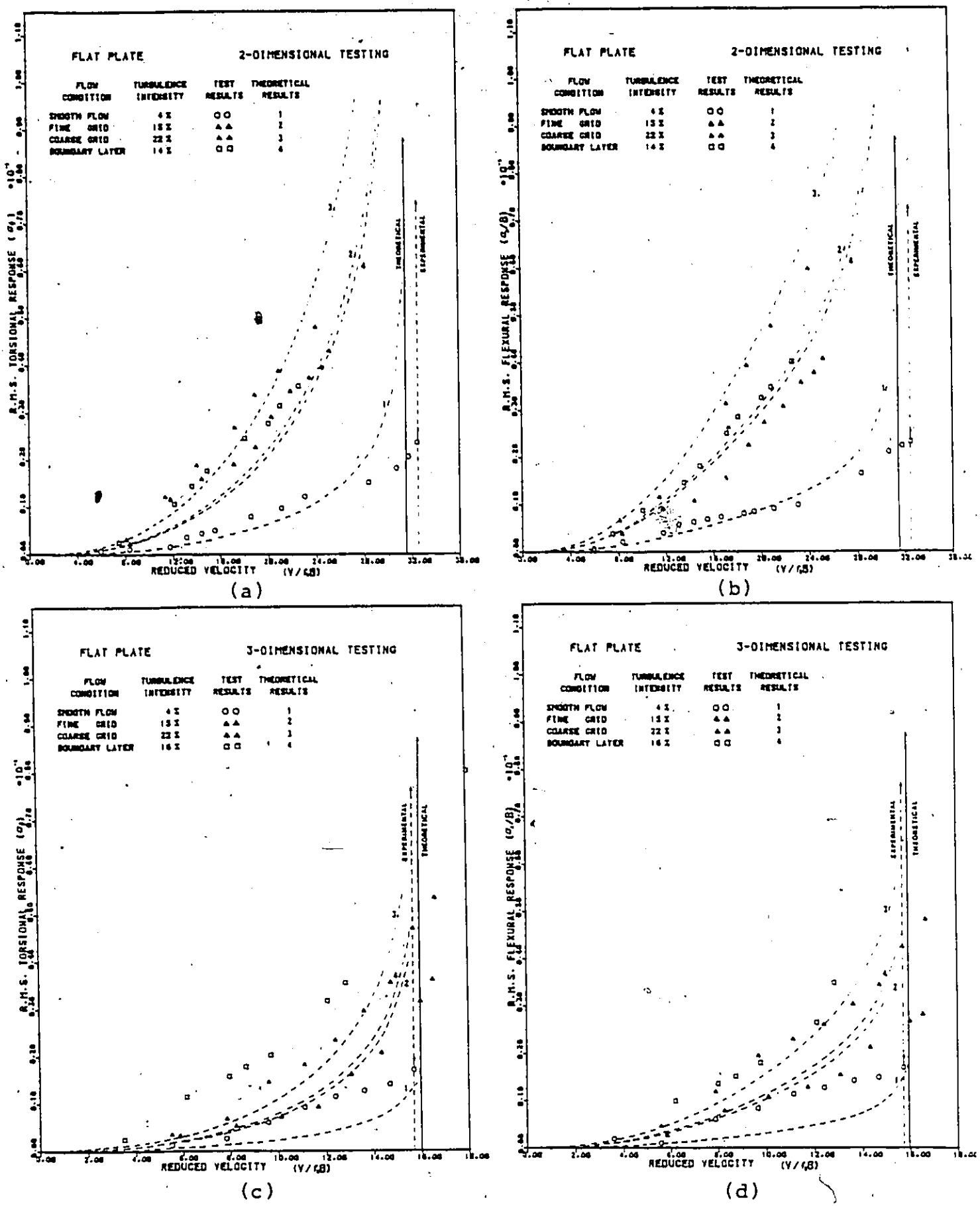

Figure 13: Comparison of response in 2-D & 3-D testing of Flat Plate Model

2-D model as described in section 4.3.1 . The prediction of critical wind speed of 3-D model was based on the assumption that the structure was treated as a rigid body, supported by springs at its ends, which has an apparent mass of half the total mass of the model distributed uniformly along its span. The method successfully predicted the critical wind speed of the 3-D model. Based on the theoretical calculation, the measured responses of the 2-D model in boundary layer flow were underestimated by 30% in torsional mode and 20% in flexural vibration. The agreement was poorer in 3-D testing, where the measured torsional response was twice the theoretical values. This could have been caused by the characteristics of the shear flow. The actual mechanism of this is not immediately explanable.

This poorer agreement in 3-D model was consistently observed in the three different models tested. Possible cause of the behaviour was the three dimensional structure of the turbulence in boundary layer flow.

The above reasoning was further supported by the fact that the measured responses of the 3-D model in boundary layer flows, of turbulence intensity 16%, were higher than the responses in coarse grid turbulence flows with a turbulence intensity of 22%.

4.5 DISCUSSION ON RESULTS OF GALLOPING MODEL

The non-linear galloping response predicted in section 4.3.3 was shown in Figure 14 for comparison with the measured response. The theoretical response was computed only for a turbulence intensity of 5%. The measured response in the 2-D model did not follow the trend of the predicted galloping response, but at a reduced wind speed of 24.0, there was a sudden increase in the response, which may be initiated by a trigger response.

Before galloping occurred, the response was basically buffeting, thus the suggested experimental curve of galloping will take the shape of the curve traced by the dotted line. The galloping response is of the same trend as the theoretical curve, except that the response was overestimated by the theory. This could be due to poor correlation of excitation force along the span which usually happens in 3-D testing but is taken into account by the theoretical calculations.

Generally speaking, galloping responses of the box section in 2-D & 3-D were comparable.

Measured responses are plotted in Figure 15 . As expected, in homogenous turbulent flow, the responses in the 3-D tests were in the order of two times the responses of the 2-D model. Again, as in the flat plate model, the shear

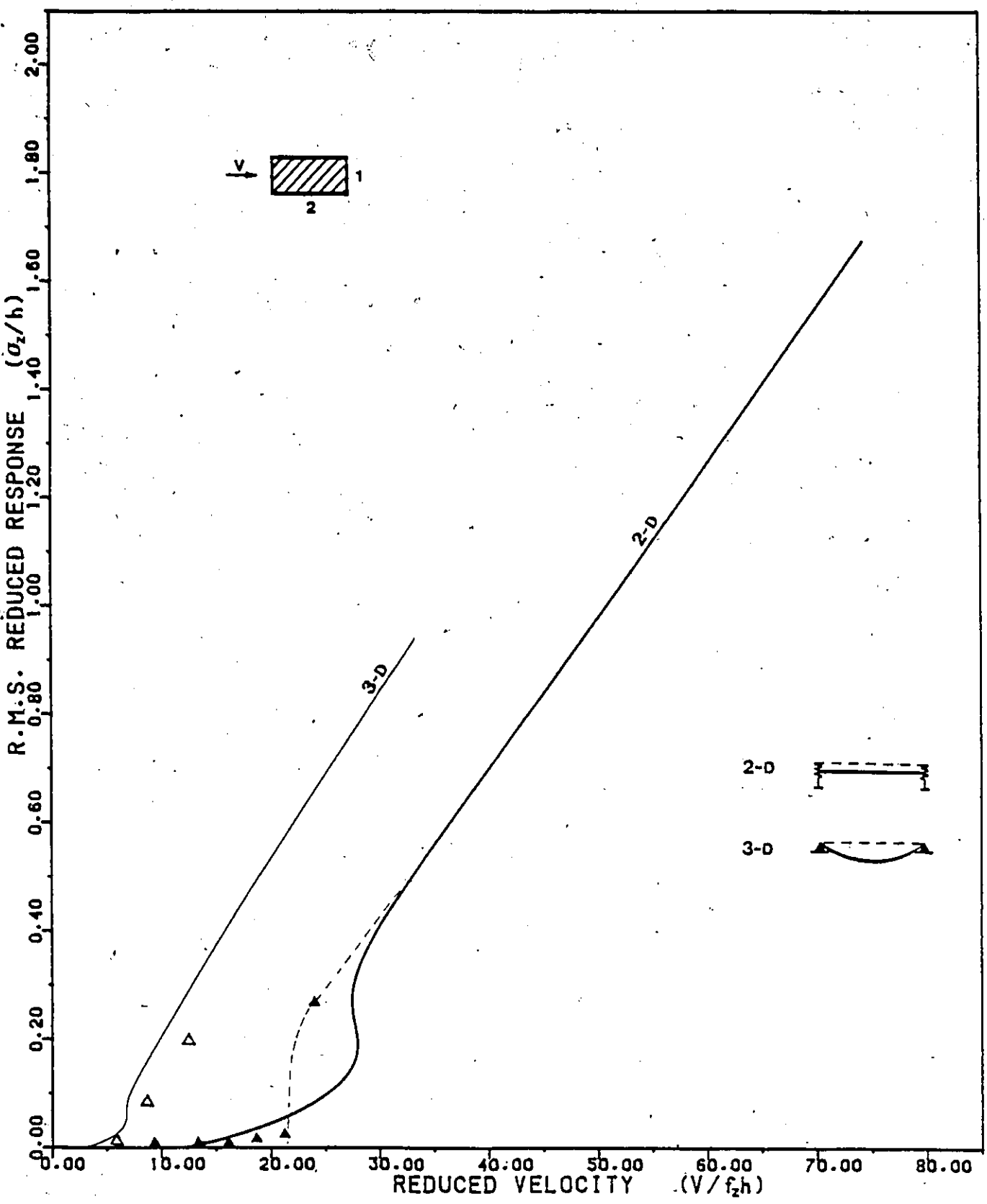

Figure 14: Comparison of galloping response in 2-D & 3-D model at a turbulence intensity of 5 %

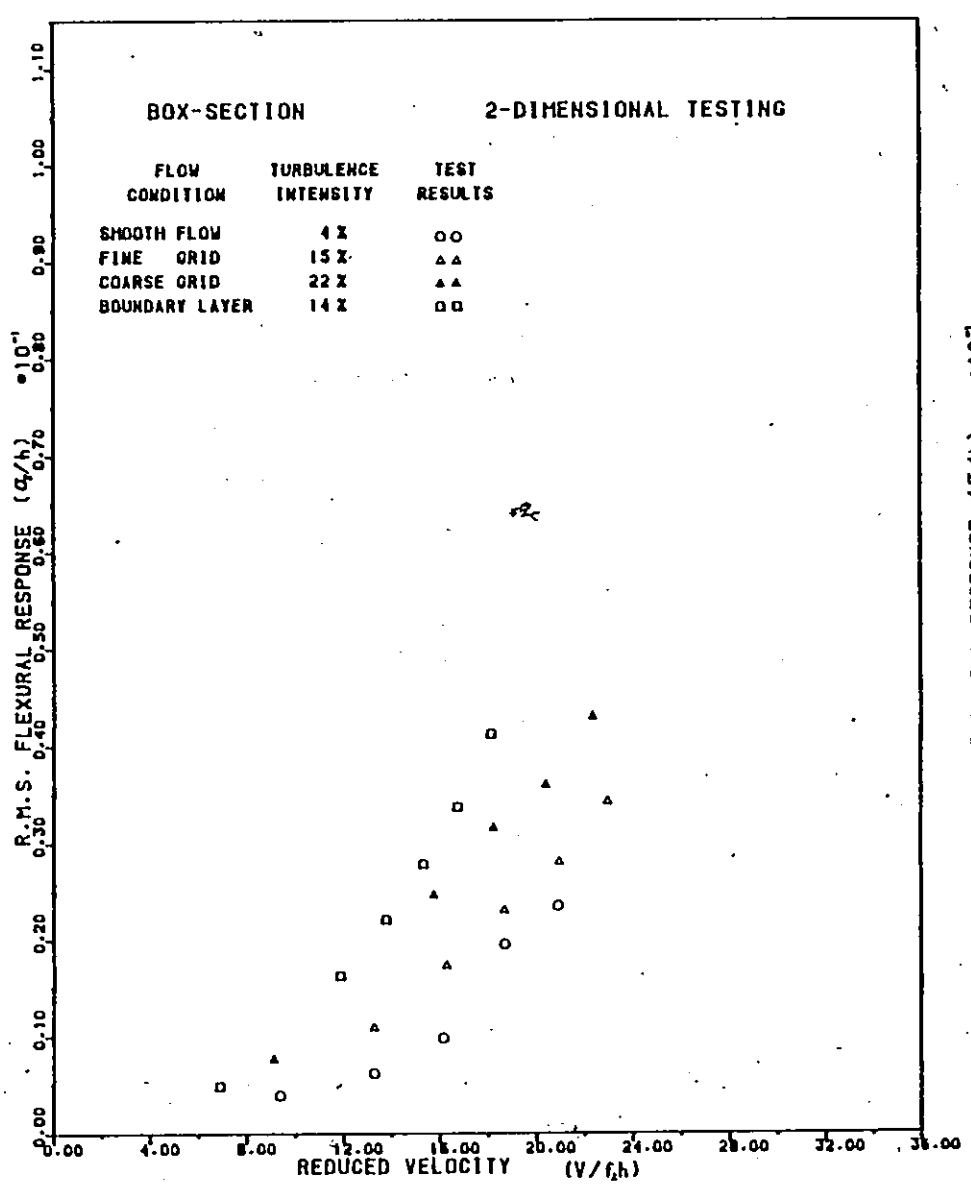

(a)

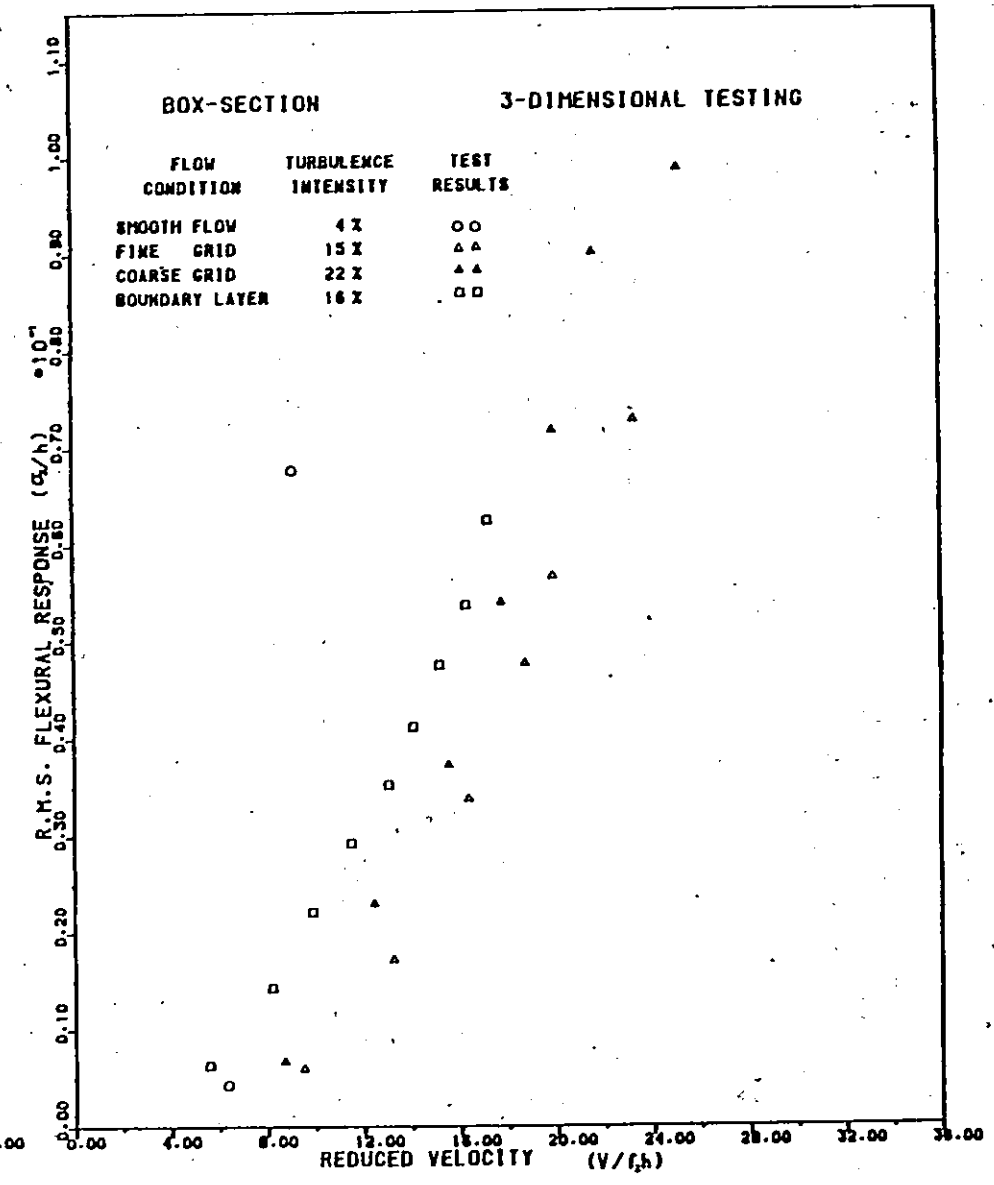

(b)

Figure 15: Comparison of response in 2-D & 3-D testing of Galloping Model

flow has a significant effect on the vibration of the box section, both in the 2-D and the 3-D model. In this case, the shape of the section could be an important factor, because in the 2-D and 3-D model, the responses in boundary layer flow were higher than the responses in the homogenous turbulent flow with a higher turbulence intensity.

4.6 DISCUSSION ON RESULTS OF H-SECTION MODEL

The agreement of experimental data and theoretical prediction of the responses in the H-section model are poor. This could be because of the way the force coefficients used for the response prediction were chosen. Estimated values of the force coefficients were found by interpolation of the measured coefficients for various aspect ratios by Steinman (Ref 13). These coefficients were found to be sensitive to the flow condition. Thus, very careful investigation on the force coefficient is neccessary to predict the response of these sections. Measured responses of the model are presented in Figure 16 (a)&(b).

Stall flutter is generally non-linear response which is similar to galloping. Thus, the similar approach was used to explain the measured response of the H-section. In the low wind speed region, the responses were buffeting responses, and at a range of reduced wind speed 6 to 7, non-linear vibration started to occur. From observation, the

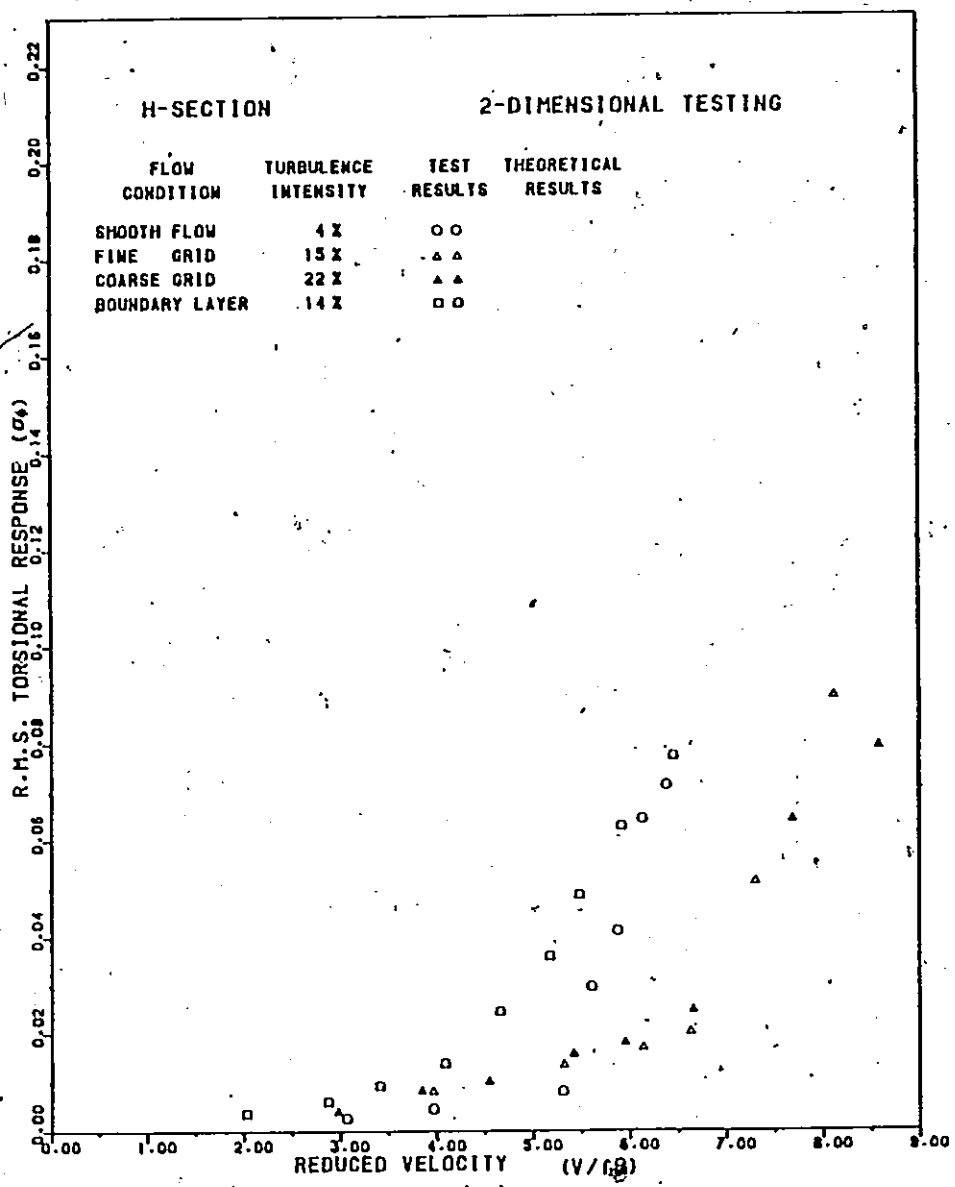

(a)

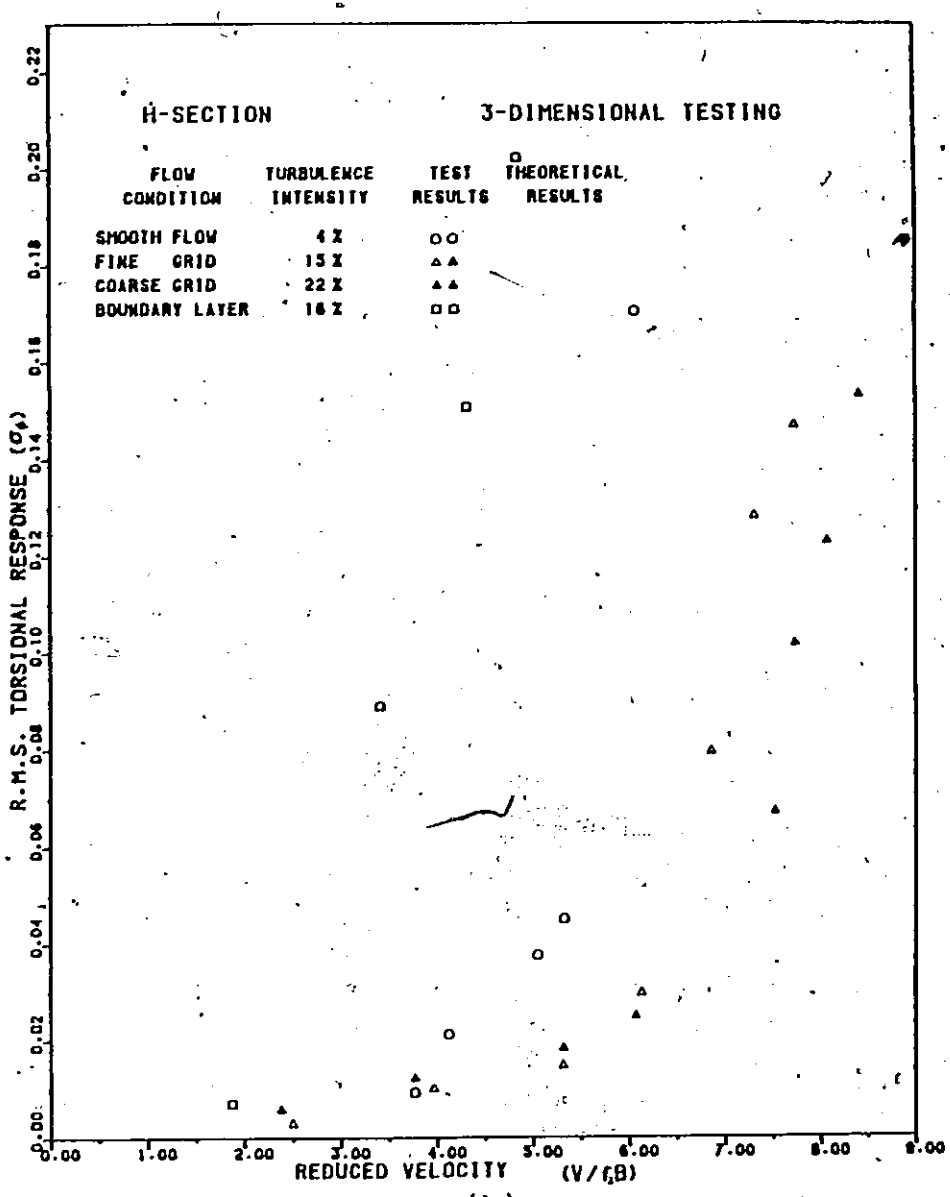

(b)

Figure 16: Comparison of results in 2-D & 3-D testing of Torsional Model

response of the model behind the coarse grid was smaller in magnitude than that in the fine grid turbulence. A possible explanation is the delay in occurrence of stall flutter in the coarse grid turbulence. The non-linear characteristic of the twisting moment are also sensitive to the turbulence intensity of the flow.

4.7 COMPARISON OF 2-DIMENSIONAL & 3-DIMENSIONAL TEST RESPONSES

It appears to be reasonable to assume that the buffeting response is inversely proportional to the mass (Ref 7).

Considering the fact that the generalised mass of the 2-dimensional model is four times that of the 3-dimensional model, comparison can be made between the response of the 3-dimensional model and the quadruple value of the 2-dimensional response.

The comparison shows how accurately 3-dimensional responses can be predicted using 2-dimensional responses. It also clarifies the effect of flow conditions on this prediction.

Examining the ratios between 2-dimensional and 3-dimensional responses as given in Table 4 , the relationship of 2-dimensional and 3-dimensional tests can be summarised as follow:

1. In homogenous turbulence, closer representation of 3-dimensional response by 2-dimensional response was observed behind coarse grid than in the case of fine grid turbulence.
2. The prediction of 3-dimensional response from 2-dimensional response in shear layer flow has higher degree of accuracy over the homogenous turbulence.
3. The smooth flow, as refered in this study, is actually a very shallow boundary layer flow. The 3-dimensional response has closer representation by the 2-dimensional response in this flow regime than that in the deep boundary layer flow.
4. Possible explanation for the above statements is the variation of the scale of turbulence among the four specific flow conditions. Firstly, from Table 2 , the scale of turbulence in fine grid, coarse grid and boundary layer is in increasing order. Secondly, the scale of turbulence in shallow boundary layer flow at the same elevation. Therefore, 3-dimensional response could be well represented by 2-dimensional response, provided that the scale of turbulence is well simulated.

TABLE 4

Comparison of 2-D & 3-D Test Response

	FLOW CONDITION		FLEXURAL RESPONSE		TORSIONAL RESPONSE	
			MEAN	σ	MEAN	σ
FLAT PLATE	SMOOTH	FLOW	1.45	0.06	1.69	0.31
	FINE	GRID	2.28	0.38	3.13	1.23
	COARSE	GRID	2.05	0.34	2.79	0.55
	BOUNDARY	LAYER	1.66	0.05	1.40	0.12
BOX-SECTION	SMOOTH	FLOW	N.A.	N.A.	----	----
	FINE	GRID	2.28	0.42	----	----
	COARSE	GRID	2.55	0.31	----	----
	BOUNDARY	LAYER	1.99	0.21	----	----
H-SECTION	SMOOTH	FLOW	----	----	1.20	0.32
	FINE	GRID	----	----	3.08	1.10
	COARSE	GRID	----	----	1.91	0.56
	BOUNDARY	LAYER	----	----	2.05	0.37

*Note $$\text{MEAN} = \frac{4 * \text{2-D RESPONSE}}{\text{3-D RESPONSE}}$$

The ratios were taken from the regression between 2-D and 3-D results read at the corresponding reduced wind speeds. Comparison was made at the wind speed range in which the buffeting response was predominantly observed.
(cf) Figs. 17(A) and (B)

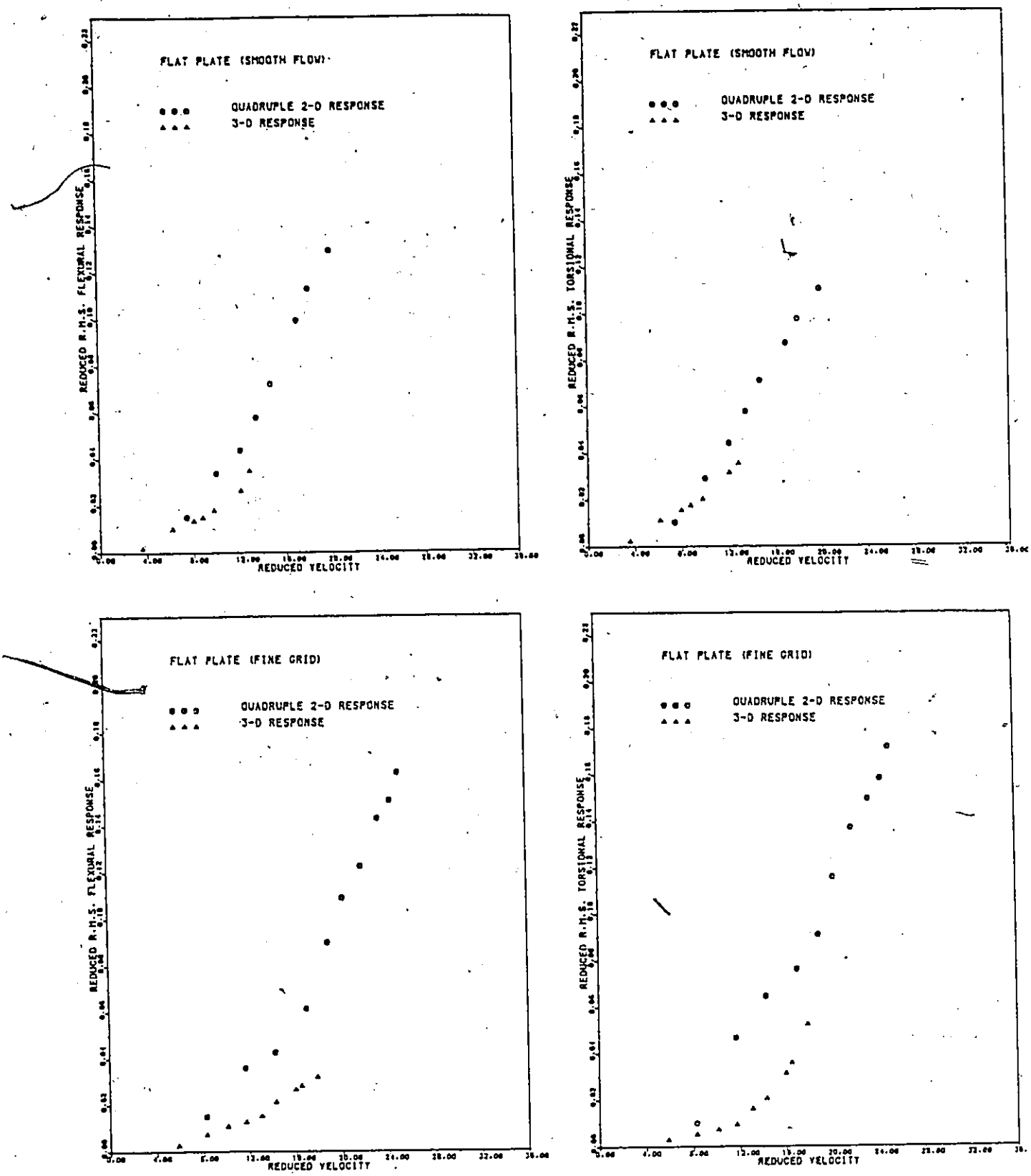

Figure 17: Comparison of 2- D & 3- D response in (a) flat plate

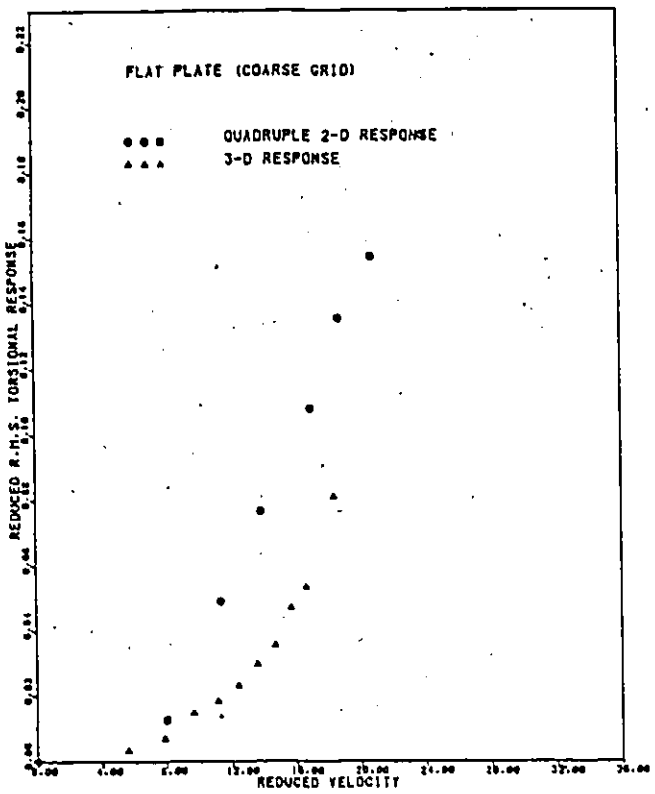

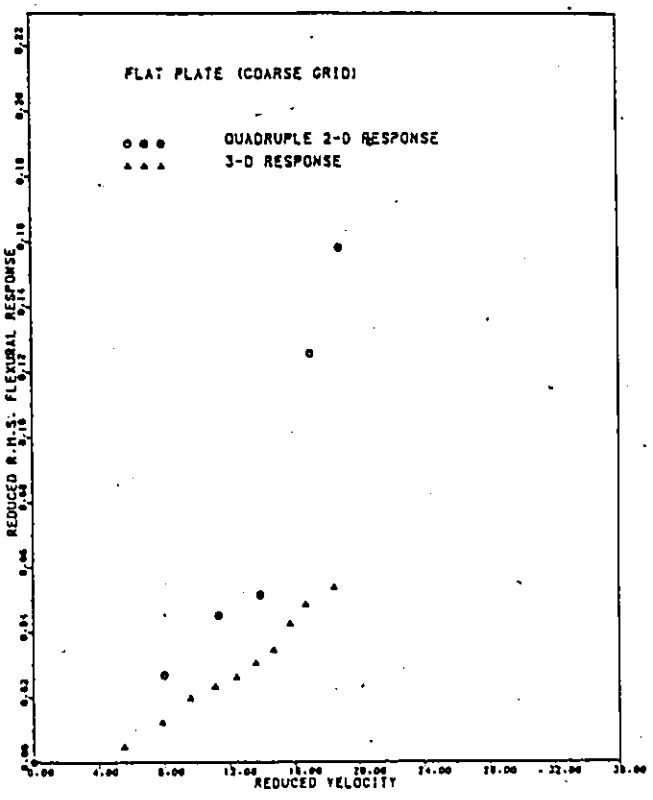

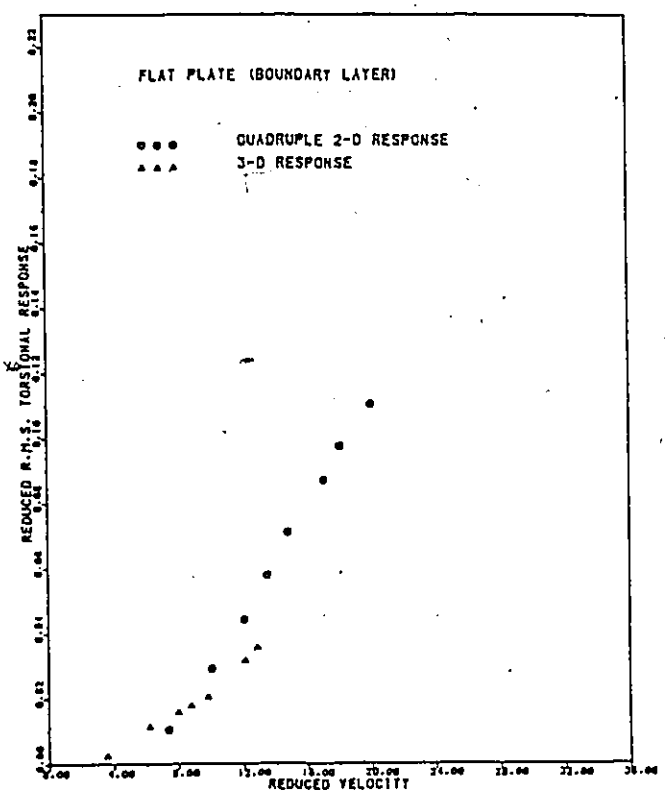

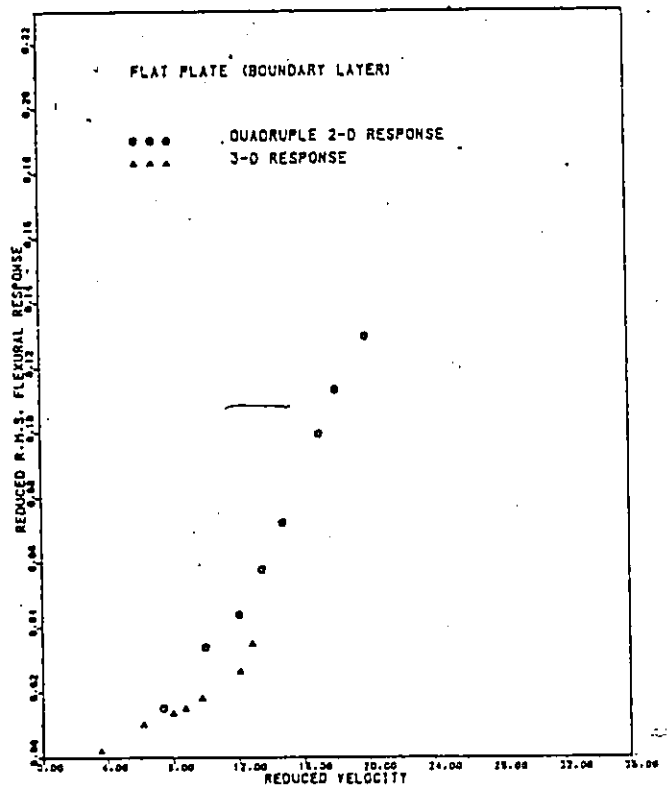

Figure 17: Comparison of 2- D & 3- D response in (b) flat plate

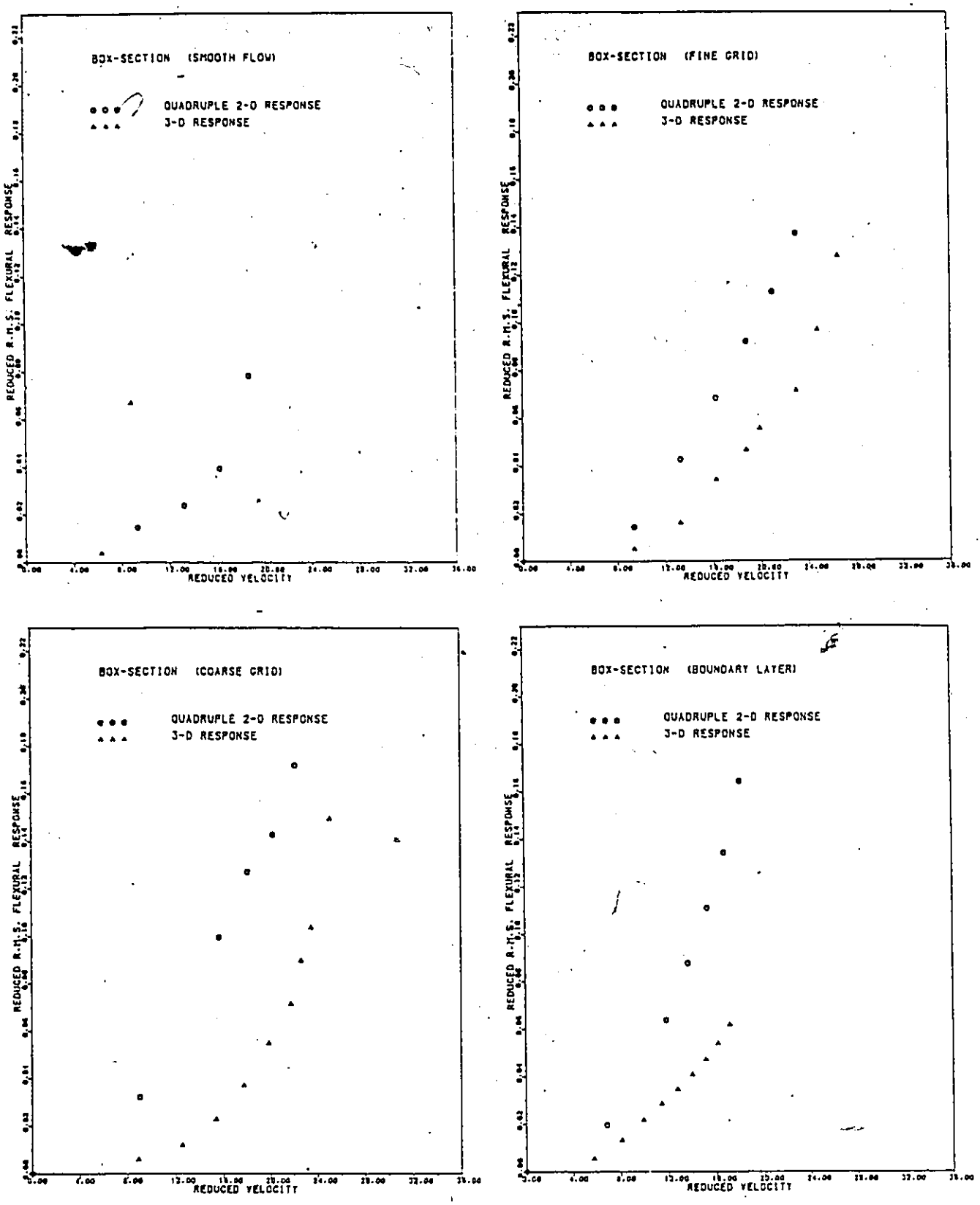

Figure 18: Comparison of 2-D & 3-D response in box-section

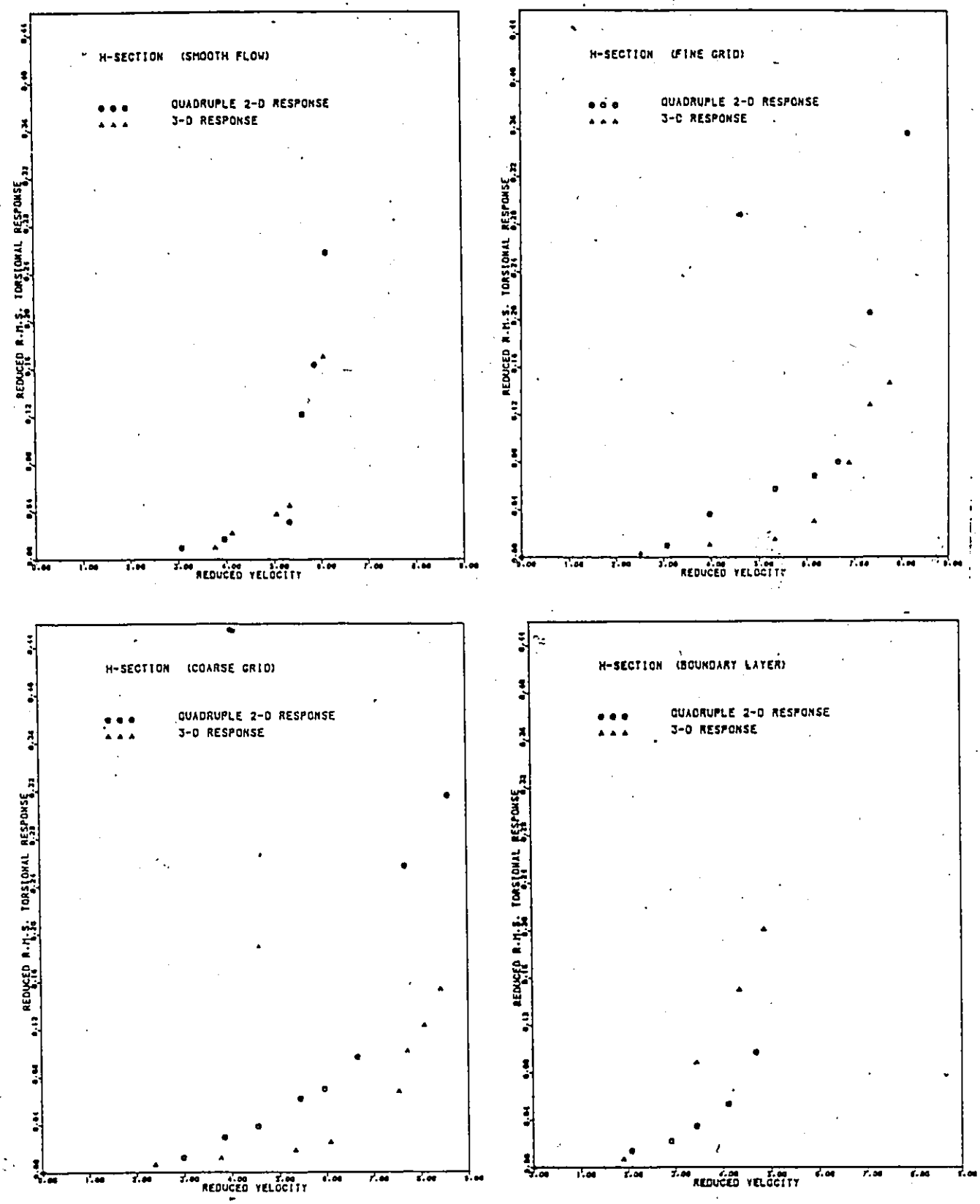

Figure 19: Comparison of 2-D & 3-D response in H-section

Chapter V

CONCLUDING REMARKS

The wind-induced dynamic responses of 2-dimensional and 3-dimensional models were studied. Their behaviour in smooth and scale of turbulent flows are summarized as follows:

1. 2-Dimensional testing is reliable in predicting 3-dimensional response, provided that the simulation of the turbulence is considered.
2. For the flat plate model, buffeting response in homogenous turbulence and the critical wind speed for the flutter instability in smooth flow have good agreement with predictions in both 2-dimensional and 3-dimensional testing. It implies that the section model test is reliable in predicting the response of a bridge structure with a cross section of a flat plate or similar configurations, in which the assumption of potential flow is still applicable.
3. In 3-dimensional testing, the response of flat plat model in shear layer flow showed generally much higher buffeting response than predicted. The apparent onset conditions for flutter were not achieved in this present study, however the response amplitude was found to be high even in the absence of obvious flutter vibrations.

4. Based on the non-linear analysis of galloping, the response of the 3-dimensional model tends to be overestimated. However the agreement of prediction and testing in 2-D is better. The critical wind speed of galloping is higher in 3-D testing. The reason for this could be attributed to the poor space correlation of the excitation force along the span.
5. Presence of turbulence in wind flow tends to postpone the occurrence of instability phenomena, such as galloping or stall flutter. Sometimes the instability may be completely supressed.

BIBLIOGRAPHY

1. Davenport, A.G., The Response of Slender, Line-Like Structures to A Gusty Wind, Proceedings ICE,Vol. 20, Paper No. 6610, 1962, pp. 389-408

2. Davenport, A.G., Buffeting of A Suspension Bridge by Storm Winds, Proceedings of ASCE, ST3, 1962, pp. 233-268

3. Fung, Y.C., An Introduction to The Theory of Aeroelasticity, New York, Dover Publishing, Inc., 1969

4. Novak, M., Galloping Oscillations Of Prismatic Structures, Journal Of Engineering Mechanic Division, EM1, 1972, pp.27-45

5. Steinman, D.B., Simple Model Tests Predict Aerodynamic Characteristics of Bridges, Civil Engineering, vol.17, 1947

6. Tanaka, H., Davenport, A.G., Response of Taut Strip Models to Turrbulent Wind, Journal of the Engineering Mechanics Division, EM1, 1982, pp.33-49

7. Personal correspondance with Mr. E. Tsui, who did the parametric study on buffeting responses, 1983.

BLANK PAGE
PAGE EN BLANC

Appendix A.

TABLES OF EXPERIMENTAL RESPONSE

TABLE 5

Experimental response of flat plate model in 2-dimensional smooth flow

WIND VELOCITY (M/S)	REDUCED VELOCITY (V/fB)	TORSIONAL RESPONSES (ϕ)	FLEXURAL RESPONSES (z/b)
2.316	5.836	0.0007	0.0007
3.275	8.253	0.0011	0.0021
4.632	11.672	0.0015	0.0040
5.179	13.049	0.0039	0.0058
5.673	14.295	0.0048	0.0063
6.128	15.440	0.0052	0.0069
6.551	16.506	0.0077	0.0073
7.324	18.455	0.0082	0.0079
7.682	19.355	0.0090	0.0085
8.351	21.041	0.0099	0.0091
9.119	22.976	0.0122	0.0100
11.228	28.290	0.0149	0.0163
12.146	30.603	0.0181	0.0209
12.580	31.697	0.0205	0.0224
12.896	32.493	0.0235	0.0232

TABLE 6

Experimental response of flat plate model in 2-dimensional fine grid turbulent flow

WIND VELOCITY (M/S)	REDUCED VELOCITY (V/fB)	TORSIONAL RESPONSES (ϕ)	FLEXURAL RESPONSES (z/b)
3.275	8.253	0.0025	0.0038
4.632	11.672	0.0117	0.0090
5.673	14.295	0.0162	0.0107
6.753	17.014	0.0191	0.0154
7.505	18.910	0.0228	0.0225
8.023	20.216	0.0290	0.0273
8.666	21.836	0.0343	0.0307
9.264	23.343	0.0374	0.0358
9.689	24.413	0.0396	0.0377
9.962	25.101	0.0430	0.0407

TABLE 7

Experimental response of flat plate model in 2-dimensional coarse grid turbulent flow

WIND VELOCITY (M/S)	REDUCED VELOCITY (V/fB)	TORSIONAL RESPONSES (Φ)	FLEXURAL RESPONSES (z/b)
3.177	8.006	0.0032	0.0067
4.493	11.322	0.0123	0.0113
5.503	13.866	0.0192	0.0129
6.740	16.982	0.0270	0.0314
7.451	18.775	0.0339	0.0395
8.255	20.799	0.0386	0.0476
9.532	24.017	0.0479	0.0599

TABLE 8

Experimental response of flat plate model in 2-dimensional boundary layer flow

WIND VELOCITY (M/S)	REDUCED VELOCITY (V/fB)	TORSIONAL RESPONSES (ϕ)	FLEXURAL RESPONSES (z/b)
2.928	7.379	0.0026	0.0038
3.965	9.991	0.0073	0.0085
4.782	12.050	0.0111	0.0110
5.347	13.472	0.0145	0.0145
5.857	14.758	0.0178	0.0181
6.763	17.041	0.0218	0.0249
7.173	18.074	0.0244	0.0283
7.930	19.982	0.0276	0.0324
8.283	20.870	0.0315	0.0344
8.947	22.543	0.0357	0.0396

TABLE 9

Experimental response of flat plate model in 3-dimensional smooth flow

WIND VELOCITY (M/S)	REDUCED VELOCITY (V/fB)	TORSIONAL RESPONSES (ϕ)	FLEXURAL RESPONSES (z/b)
2.200	5.544	0.0012	0.0012
3.112	7.840	0.0024	0.0062
3.811	9.603	0.0062	0.0086
4.401	11.088	0.0100	0.0113
4.920	12.397	0.0116	0.0128
5.390	13.580	0.0129	0.0143
5.821	14.668	0.0142	0.0150
6.223	15.681	0.0172	0.0172

TABLE 10

Experimental response of flat plate model in 3-dimensional fine grid turbulence flow

WIND VELOCITY (M/S)	REDUCED VELOCITY (V/fB)	TORSIONAL RESPONSES (ϕ)	FLEXURAL RESPONSES (z/b)
2.316	5.836	0.0029	0.0026
3.275	8.253	0.0052	0.0074
4.012	10.108	0.0072	0.0109
4.632	11.672	0.0093	0.0127
5.179	13.049	0.0161	0.0153
5.673	14.295	0.0207	0.0213
6.343	15.982	0.0315	0.0267
6.551	16.506	0.0360	0.0282
7.101	17.892	0.0526	0.0321

TABLE 11

Experimental response of flat plate model in 3-dimensional coarse grid turbulent flow

WIND VELOCITY (M/S)	REDUCED VELOCITY (V/fB)	TORSIONAL RESPONSES (ϕ)	FLEXURAL RESPONSES (z/b)
2.200	5.544	0.0034	0.0047
3.112	7.840	0.0069	0.0121
3.811	9.603	0.0147	0.0196
4.401	11.088	0.0184	0.0232
4.920	12.397	0.0233	0.0261
5.390	13.580	0.0297	0.0305
5.821	14.668	0.0355	0.0345
6.223	15.681	0.0471	0.0425
6.601	16.632	0.0534	0.0484
7.298	18.388	0.0810	0.0537

TABLE 12

Experimental response of flat plate model in 3-dimensional boundary layer flow

WIND VELOCITY (M/S)	REDUCED VELOCITY (V/fB)	TORSIONAL RESPONSES (ϕ)	FLEXURAL RESPONSES (z/b)
1.413	3.560	0.0023	0.0019
2.447	6.166	0.0113	0.0101
3.159	7.960	0.0157	0.0135
3.461	8.720	0.0177	0.0150
3.869	9.749	0.0204	0.0181
4.791	12.072	0.0317	0.0265
5.094	12.835	0.0356	0.0350

TABLE 13

Experimental response of torsional model in 2-dimensional smooth flow

WIND VELOCITY (M/S)	REDUCED VELOCITY (V/fB)	TORSIONAL RESPONSES (Φ)	FLEXURAL RESPONSES (z/b)
1.269	3.070	0.0025	0.0048
1.638	3.963	0.0043	0.0087
2.197	5.317	0.0079	0.0123
2.316	5.605	0.0306	0.0162
2.429	5.878	0.0410	0.0185
2.537	6.140	0.0645	0.0219
2.641	6.390	0.0713	0.0227

TABLE 14

Experimental response of torsional model in 2-dimensional fine grid turbulent flow

WIND VELOCITY (M/S)	REDUCED VELOCITY (V/fB)	TORSIONAL RESPONSES (Φ)	FLEXURAL RESPONSES (z/b)
1.269	3.070	0.0025	0.0039
1.638	3.963	0.0091	0.0074
2.197	5.317	0.0145	0.0116
2.537	6.140	0.0171	0.0134
2.740	6.631	0.0201	0.0140
3.020	7.308	0.0515	0.0163
3.356	8.122	0.0892	0.0256

TABLE 15

Experimental response of torsional model in 2-dimensional coarse grid turbulent flow

WIND VELOCITY (M/S)	REDUCED VELOCITY (V/fB)	TORSIONAL RESPONSES (ϕ)	FLEXURAL RESPONSES (z/b)
1.231	2.978	0.0031	0.0043
1.589	3.844	0.0074	0.0087
1.880	4.548	0.0097	0.0109
2.247	5.436	0.0155	0.0145
2.461	5.955	0.0175	0.0154
2.752	6.658	0.0242	0.0170
3.177	7.688	0.0643	0.0244
3.552	8.596	0.0790	0.0274

TABLE 16

Experimental response of torsional model in 2-dimensional boundary layer flow

WIND VELOCITY (M/S)	REDUCED VELOCITY (V/fB)	TORSIONAL RESPONSES (Φ)	FLEXURAL RESPONSES (z/b)
0.845	2.046	0.0035	0.0039
1.196	2.893	0.0056	0.0073
1.415	3.423	0.0088	0.0110
1.691	4.091	0.0135	0.0125
1.928	4.665	0.0245	0.0157
2.139	5.175	0.0360	0.0176
2.268	5.489	0.0485	0.0180
2.450	5.929	0.0626	0.0231
2.673	6.469	0.0773	0.0279

TABLE 17

Experimental response of torsional model in 3-dimensional smooth flow

WIND VELOCITY (M/S)	REDUCED VELOCITY (V/fB)	TORSIONAL RESPONSES (ϕ)	FLEXURAL RESPONSES (z/b)
1.556	3.765	0.0100	0.0065
1.704	4.124	0.0222	0.0101
2.087	5.051	0.0381	0.0743
2.200	5.324	0.0454	0.0345
2.509	6.071	0.1705	0.0400

TABLE 18

Experimental response of torsional model in 3-dimensional fine grid turbulent flow

WIND VELOCITY (M/S)	REDUCED VELOCITY (V/fB)	TORSIONAL RESPONSES (ϕ)	FLEXURAL RESPONSES (z/b)
1.036	2.506	0.0030	0.0047
1.638	3.963	0.0105	0.0117
2.197	5.317	0.0153	0.0164
2.537	6.140	0.0300	0.0241
2.837	6.864	0.0796	0.0279
3.020	7.308	0.1284	0.0365
3.193	7.725	0.1468	0.0387

TABLE 19

Experimental response of torsional model in 3-dimensional coarse grid turbulent flow

WIND VELOCITY (M/S)	REDUCED VELOCITY (V/fB)	TORSIONAL RESPONSES (ϕ)	FLEXURAL RESPONSES (z/b)
0.984	2.381	0.0061	0.0049
1.556	3.765	0.0118	0.0114
2.200	5.324	0.0184	0.0162
2.509	6.071	0.0250	0.0202
3.112	7.530	0.0676	0.0286
3.189	7.716	0.1018	0.0326
3.337	8.075	0.1232	0.0355
3.479	8.419	0.1537	0.0413

TABLE 20

Experimental response of torsional model in 3-dimensional boundary layer flow

WIND VELOCITY (M/S)	REDUCED VELOCITY (V/fB)	TORSIONAL RESPONSES (ϕ)	FLEXURAL RESPONSES (z/b)
0.774	1.873	0.0069	0.0069
1.413	3.419	0.0894	0.0251
1.787	4.324	0.1510	0.0431
1.998	4.835	0.2021	0.0613

TABLE 21

Experimental response of galloping model in 2-dimensional smooth flow

WIND VELOCITY (M/S)	REDUCED VELOCITY (V/fB)	FLEXURAL RESPONSES (z/h)
1.864	9.351	0.0037
2.637	13.224	0.0060
3.229	16.196	0.0099
3.729	18.702	0.0196
4.169	20.909	0.0234
4.567	22.905	0.0871

TABLE 22

Experimental response of galloping model in 2-dimensional fine grid turbulent flow

WIND VELOCITY (M/S)	REDUCED VELOCITY (V/fB)	FLEXURAL RESPONSES (z/h)
1.864	9.351	0.0036
2.637	13.224	0.0107
3.229	16.196	0.0171
3.729	18.702	0.0230
4.169	20.909	0.0282
4.567	22.905	0.0343

TABLE 23

Experimental response of galloping model in 2-dimensional coarse grid turbulent flow

WIND VELOCITY (M/S)	REDUCED VELOCITY (V/fB)	FLEXURAL RESPONSES (z/h)
1.809	9.070	0.0081
3.132	15.710	0.0249
3.617	18.141	0.0318
4.044	20.282	0.0357
4.430	22.218	0.0430

TABLE 24

Experimental response of galloping model in 2-dimensional boundary layer flow

WIND VELOCITY (M/S)	REDUCED VELOCITY (V/fB)	FLEXURAL RESPONSES (z/h)
1.361	6.826	0.0049
2.357	11.823	0.0160
2.722	13.652	0.0220
3.043	15.264	0.0278
3.334	16.720	0.0336
3.601	18.060	0.0411

TABLE 25

Experimental response of galloping model in 3-dimensional smooth flow

WIND VELOCITY (M/S)	REDUCED VELOCITY (V/fB)	FLEXURAL RESPONSES (z/h)
1.252	6.281	0.0040
1.771	8.883	0.0672
2.505	12.563	0.3000

TABLE 26

Experimental response of galloping model in 3-dimensional fine grid turbulent flow

WIND VELOCITY (M/S)	REDUCED VELOCITY (V/fB)	FLEXURAL RESPONSES (z/h)
1.864	9.351	0.0052
2.637	13.224	0.0162
3.229	16.196	0.0342
3.729	18.702	0.0466
3.955	19.836	0.0556
4.567	22.905	0.0713
4.933	24.740	0.0968
5.273	26.448	0.1278

TABLE 27

Experimental response of galloping model in 3-dimensional coarse grid turbulent flow

WIND VELOCITY (M/S)	REDUCED VELOCITY (V/fB)	FLEXURAL RESPONSES (z/h)
1.771	8.883	0.0060
2.505	12.563	0.0120
3.068	15.386	0.0230
3.542	17.767	0.0373
3.961	19.864	0.0549
4.339	21.760	0.0716
4.516	22.648	0.0898
4.686	23.503	0.1037
5.010	25.126	0.1494

TABLE 28

Experimental response of galloping model in 3-dimensional boundary layer flow

WIND VELOCITY (M/S)	REDUCED VELOCITY (V/fB)	FLEXURAL RESPONSES (z/h)
1.137	5.704	0.0054
1.608	8.067	0.0132
1.970	9.880	0.0217
2.275	11.408	0.0286
2.543	12.755	0.0347
2.786	13.972	0.0410
3.009	15.091	0.0474
3.217	16.133	0.0542
3.412	17.112	0.0620

Appendix B

TABLES OF THEORETICAL RESPONSES

TABLE 29

Theoretical reponses of flat plate model in 2-dimensional smooth flow

REDUCED VELOCITY (V/fB)	TORSIONAL RESOPNSES (ϕ)	FLEXURAL RESPONSES (z/b)
1.0000	0.00000356	0.00000671
3.0000	0.00005357	0.00011441
5.0000	0.00018177	0.00040898
7.0000	0.00042428	0.00092150
9.0000	0.00082526	0.00165332
11.0000	0.00136006	0.00259207
13.0000	0.00204822	0.00371755
15.0000	0.00297666	0.00500789
17.0000	0.00408765	0.00644748
19.0000	0.00549706	0.00803836
21.0000	0.00725099	0.00981611
23.0000	0.00948172	0.01187945
25.0000	0.01243481	0.01445664
27.0000	0.01664146	0.01808397
29.0000	0.02364065	0.02431222
31.0000	0.04549405	0.04433396
33.0000	0.04672707	0.05732402
35.0000	0.03193592	0.05086020

TABLE 30

Theoretical reponses of flat plate model in 2-dimensional fine grid turbulent flow

REDUCED VELOCITY (V/fB)	TORSIONAL RESOPNSES (Φ)	FLEXURAL RESPONSES (z/b)
1.0000	0.00001239	0.00002333
3.0000	0.00018622	0.00039770
5.0000	0.00063185	0.00142170
7.0000	0.00147488	0.00320332
9.0000	0.00286875	0.00574726
11.0000	0.00472781	0.00901052
13.0000	0.00712000	0.01292292
15.0000	0.01034743	0.01740835
17.0000	0.01420964	0.02241265
19.0000	0.01910879	0.02794327
21.0000	0.02520577	0.03412259
23.0000	0.03296021	0.04129511
25.0000	0.04322571	0.05025396
27.0000	0.05784986	0.06286323
29.0000	0.08217913	0.08451384

TABLE 31

Theoretical reponses of flat plate model in 2-dimensional coarse grid turbulent flow

REDUCED VELOCITY (V/fB)	TORSIONAL RESOPNSES (ϕ)	FLEXURAL RESPONSES (z/b)
1.0000	0.00001841	0.00003468
3.0000	0.00027678	0.00059110
5.0000	0.00093912	0.00211306
7.0000	0.00219212	0.00476110
9.0000	0.00426378	0.00854209
11.0000	0.00702697	0.01339241
13.0000	0.01058250	0.01920740
15.0000	0.01537943	0.02587411
17.0000	0.02111962	0.03331164
19.0000	0.02840158	0.04153177
21.0000	0.03746351	0.05071676
23.0000	0.04898896	0.06137729
25.0000	0.06424558	0.07469279
27.0000	0.08598149	0.09343398

TABLE 32

Theoretical reponses of flat plate model in 2-dimensional boundary layer flow

REDUCED VELOCITY (V/fB)	TORSIONAL RESOPNSES (Φ)	FLEXURAL RESPONSES (z/b)
1.0000	0.00001171	0.00002205
3.0000	0.00017602	0.00037591
5.0000	0.00059723	0.00134380
7.0000	0.00139406	0.00302779
9.0000	0.00271156	0.00543234
11.0000	0.00446875	0.00851678
13.0000	0.00672985	0.01221481
15.0000	0.00978044	0.01645447
17.0000	0.01343102	0.02118455
19.0000	0.01806168	0.02641213
21.0000	0.02382462	0.03225282
23.0000	0.03115415	0.03903231
25.0000	0.04085717	0.04750028
27.0000	0.05467996	0.05941865
29.0000	0.07767612	0.07988286

TABLE 33

Theoretical reponses of flat plate model in 3-dimensional smooth flow

REDUCED VELOCITY (V/fB)	TORSIONAL RESOPNSES (ϕ)	FLEXURAL RESPONSES (z/b)
1.0000	0.00000663	0.00001201
2.0000	0.00004130	0.00007529
3.0000	0.00011198	0.00020439
4.0000	0.00022359	0.00040476
5.0000	0.00038266	0.00067929
6.0000	0.00059541	0.00102927
7.0000	0.00086911	0.00145525
8.0000	0.00121927	0.00195822
9.0000	0.00165806	0.00254126
10.0000	0.00220890	0.00321210
11.0000	0.00290173	0.00398783
12.0000	0.00378916	0.00490333
13.0000	0.00496235	0.00602818
14.0000	0.00663334	0.00751094
15.0000	0.00965318	0.00980754
16.0000	0.04160647	0.02860428

TABLE 34

Theoretical reponses of flat plate model in 3-dimensional fine grid turbulent flow

REDUCED VELOCITY (V/fB)	TORSIONAL RESOPNSES (ϕ)	FLEXURAL RESPONSES (z/b)
1.0000	0.00002165	0.00003923
2.0000	0.00013492	0.00024596
3.0000	0.00036581	0.00066769
4.0000	0.00073040	0.00132222
5.0000	0.00125001	0.00221902
6.0000	0.00194499	0.00336226
7.0000	0.00283910	0.00475379
8.0000	0.00398295	0.00639692
9.0000	0.00541632	0.00830141
10.0000	0.00721572	0.01049284
11.0000	0.00947898	0.01302688
12.0000	0.01237792	0.01601751
13.0000	0.01621034	0.01969203
14.0000	0.02166882	0.02453571
15.0000	0.03153364	0.03203791

TABLE 35

Theoretical reponses of flat plate model in 3-dimensional coarse grid turbulent flow

REDUCED VELOCITY (V/fB)	TORSIONAL RESOPNSES (ϕ)	FLEXURAL RESPONSES (z/b)
1.0000	0.00003255	0.00005898
2.0000	0.00020284	0.00036977
3.0000	0.00054996	0.00100380
4.0000	0.00109807	0.00198782
5.0000	0.00187927	0.00333609
6.0000	0.00292411	0.00505484
7.0000	0.00426826	0.00714688
8.0000	0.00598801	0.00961706
9.0000	0.00814295	0.01248041
10.0000	0.01084816	0.01577502
11.0000	0.01425075	0.01958470
12.0000	0.01860877	0.02408082
13.0000	0.02437077	0.02960508
14.0000	0.03257715	0.03688669
15.0000	0.04740789	0.04816604

TABLE 36

Theoretical reponses of flat plate model in 3-dimensional boundary layer flow

REDUCED VELOCITY (V/fB)	TORSIONAL RESOPNSES (Φ)	FLEXURAL RESPONSES (z/b)
1.0000	0.00002371	0.00004296
2.0000	0.00014777	0.00026938
3.0000	0.00040065	0.00073128
4.0000	0.00079996	0.00144815
5.0000	0.00136906	0.00243035
6.0000	0.00213023	0.00368248
7.0000	0.00310949	0.00520654
8.0000	0.00436228	0.00700615
9.0000	0.00593217	0.00909202
10.0000	0.00790294	0.01149216
11.0000	0.01038174	0.01426755
12.0000	0.01355677	0.01754300
13.0000	0.01775417	0.02156746
14.0000	0.02373254	0.02687246
15.0000	0.03453689	0.03453689

TABLE 37

Theoretical reponses of H-section model in 2-dimensional smooth flow

REDUCED VELOCITY (V/fB)	TORSIONAL RESOPNSES (ϕ)	FLEXURAL RESPONSES (z/b)
1.0000	0.00000099	0.00000204
2.0000	0.00000585	0.00001341
3.0000	0.00001584	0.00004066
4.0000	0.00003228	0.00009032
5.0000	0.00005685	0.00016738
6.0000	0.00009148	0.00027478
7.0000	0.00013852	0.00041364
8.0000	0.00020107	0.00058384
9.0000	0.00028373	0.00078456

TABLE 38

Theoretical reponses of H-section model in 2-dimensional fine grid turbulent flow

REDUCED VELOCITY (V/fB)	TORSIONAL RESOPNSES (Φ)	FLEXURAL RESPONSES (z/b)
1.0000	0.00000344	0.00000708
2.0000	0.00002034	0.00004661
3.0000	0.00005507	0.00014135
4.0000	0.00011222	0.00031396
5.0000	0.00019761	0.00058186
6.0000	0.00031800	0.00095520
7.0000	0.00048154	0.00143790
8.0000	0.00069898	0.00202953
9.0000	0.00098634	0.00272728

TABLE 39

Theoretical reponses of H-section model in 2-dimensional coarse grid turbulent flow

REDUCED VELOCITY (V/fB)	TORSIONAL RESOPNSES (ϕ)	FLEXURAL RESPONSES (z/b)
1.0000	0.00000511	0.00001053
2.0000	0.00003023	0.00006928
3.0000	0.00008185	0.00021008
4.0000	0.00016680	0.00046664
5.0000	0.00029370	0.00086482
6.0000	0.00047265	0.00141972
7.0000	0.00071572	0.00213713
8.0000	0.00103891	0.00301650
9.0000	0.00146606	0.00405357

TABLE 40

Theoretical reponses of H-section model in 2-dimensional boundary layer flow

REDUCED VELOCITY (V/fB)	TORSIONAL RESOPNSES (Φ)	FLEXURAL RESPONSES (z/b)
1.0000	0.00000325	0.00000670
2.0000	0.00001923	0.00004406
3.0000	0.00005205	0.00013360
4.0000	0.00010607	0.00029676
5.0000	0.00018678	0.00054998
6.0000	0.00030058	0.00090286
7.0000	0.00045515	0.00135911
8.0000	0.00066067	0.00191833
9.0000	0.00093230	0.00257784

TABLE 41

Theoretical reponses of H-section model in 3-dimensional smooth flow

REDUCED VELOCITY (V/fB)	TORSIONAL RESOPNSES (Φ)	FLEXURAL RESPONSES (z/b)
1.0000	0.00000181	0.00000362
2.0000	0.00001159	0.00002384
3.0000	0.00003209	0.00006657
4.0000	0.00006557	0.00013467
5.0000	0.00011668	0.00023154
6.0000	0.00019967	0.00036300
7.0000	0.00037220	0.00053998
8.0000	0.00076675	0.00078389
9.0000	0.00079418	0.00113686

TABLE 42

Theoretical reponses of H-section model in 3-dimensional fine grid turbulent flow

REDUCED VELOCITY (V/fB)	TORSIONAL RESOPNSES (ϕ)	FLEXURAL RESPONSES (z/b)
1.0000	0.00000590	0.00001184
2.0000	0.00003785	0.00007788
3.0000	0.00010484	0.00021747
4.0000	0.00021421	0.00043992
5.0000	0.00038115	0.00075636
6.0000	0.00065234	0.00118579
7.0000	0.00121653	0.00176394
8.0000	0.00251046	0.00256071
9.0000	0.00259688	0.00371373

TABLE 43

Theoretical reponses of H-section model in 3-dimensional coarse grid turbulent flow

REDUCED VELOCITY (V/fB)	TORSIONAL RESOPNSES (ϕ)	FLEXURAL RESPONSES (z/b)
1.0000	0.00000887	0.00001780
2.0000	0.00005690	0.00011709
3.0000	0.00015762	0.00032694
4.0000	0.00032205	0.00066138
5.0000	0.00057304	0.00113712
6.0000	0.00098085	0.00178272
7.0000	0.00183031	0.00265190
8.0000	0.00378629	0.00384978
9.0000	0.00390952	0.00558325

TABLE 44

Theoretical reponses of H-section model in 3-dimensional boundary layer flow

REDUCED VELOCITY (V/fB)	TORSIONAL RESOPNSES (Φ)	FLEXURAL RESPONSES (z/b)
1.0000	0.00000646	0.00001297
2.0000	0.00004145	0.00008530
3.0000	0.00011483	0.00023818
4.0000	0.00023461	0.00048182
5.0000	0.00041745	0.00082840
6.0000	-0.00071448	0.00129873
7.0000	-0.00133255	0.00193194
8.0000	0.00275093	0.00280459
9.0000	0.00284483	0.00406742

TABLE 45

Theoretical reponses of box-section model in 2-dimensional smooth flow

REDUCED VELOCITY (V/fB)	FLEXURAL RESPONSES (z/b)
1.0000	0.00000026
2.0000	0.00000187
3.0000	0.00000570
4.0000	0.00001270
5.0000	0.00002406
6.0000	0.00004118
7.0000	0.00006566
8.0000	0.00009922
9.0000	0.00014373
10.0000	0.00020117
11.0000	0.00027367

TABLE 46

Theoretical reponses of box-section model in 2-dimensional fine grid turbulent flow

REDUCED VELOCITY (V/fB)	FLEXURAL RESPONSES (z/b)
1.0000	0.00000068
2.0000	0.00000630
3.0000	0.00002341
4.0000	0.00005919
5.0000	0.00012078
6.0000	0.00021497
7.0000	0.00034794
8.0000	0.00052529
9.0000	0.00075201
10.0000	0.00103264
11.0000	0.00137149

TABLE 47

Theoretical reponses of box-section model in 2-dimensional coarse grid turbulent flow

REDUCED VELOCITY (V/fB)	FLEXURAL RESPONSES (z/b)
1.0000	0.00000085
2.0000	0.00000774
3.0000	0.00002864
4.0000	0.00007290
5.0000	0.00015068
6.0000	0.00027270
7.0000	0.00045013
8.0000	0.00069446
9.0000	0.00101748
10.0000	0.00143130
11.0000	0.00194834

TABLE 48

Theoretical reponses of box-section model in 2-dimensional boundary layer flow

REDUCED VELOCITY (V/fB)	FLEXURAL RESPONSES (z/b)
1.0000	0.00000085
2.0000	0.00000614
3.0000	0.00001874
4.0000	0.00004174
5.0000	0.00007905
6.0000	0.00013531
7.0000	0.00021574
8.0000	0.00032602
9.0000	0.00047226
10.0000	0.00066097
11.0000	0.00089920

TABLE 49

Theoretical reponses of box-section model in 3-dimensional smooth flow

REDUCED VELOCITY (V/fB)	FLEXURAL RESPONSES (z/b)
1.0000	0.00000043
2.0000	0.00000334
3.0000	0.00001084
4.0000	0.00002579
5.0000	0.00005353
6.0000	0.00010414
7.0000	0.00019750
8.0000	0.00037681
9.0000	0.00075543
10.0000	0.00175490
11.0000	0.00737422

TABLE 50

Theoretical reponses of box-section model in 3-dimensional fine grid turbulent flow

REDUCED VELOCITY (V/fB)	FLEXURAL RESPONSES (z/b)
1.0000	0.00000103
2.0000	0.00001031
3.0000	0.00004183
4.0000	0.00011723
5.0000	0.00027019
6.0000	0.00055650
7.0000	0.00107855
8.0000	0.00205246
9.0000	0.00403896
10.0000	0.00911637
11.0000	0.03698513

TABLE 51

Theoretical reponses of box-section model in 3-dimensional coarse grid turbulent flow

REDUCED VELOCITY (V/fB)	FLEXURAL RESPONSES (z/b)
1.0000	0.00000131
2.0000	0.00001280
3.0000	0.00005164
4.0000	0.00014555
5.0000	0.00033962
6.0000	0.00071124
7.0000	0.00140583
8.0000	0.00273445
9.0000	0.00550866
10.0000	0.01274142
11.0000	0.05300109

TABLE 52

Theoretical reponses of box-section model in 3-dimensional boundary layer flow

REDUCED VELOCITY (V/fB)	FLEXURAL RESPONSES (z/b)
1.0000	0.00000153
2.0000	0.00001195
3.0000	0.00003877
4.0000	0.00009229
5.0000	0.00019152
6.0000	0.00037260
7.0000	0.00070661
8.0000	0.00134815
9.0000	0.00270278
10.0000	0.00627863
11.0000	0.02638330

Appendix C

TABLES OF FLOW MEASUREMENTS

TABLE 53

Flow Measurement of 2-dimensional Smooth Flow

Height (cm)	Velocity Ratio V/Vg	Turbulence Intensity (%)
2.5	0.67	17.7
5.1	0.78	11.4
7.6	0.86	8.6
10.2	0.89	6.5
12.7	0.90	5.5
15.2	0.92	5.0
17.8	0.95	4.1
20.3	0.99	3.4
22.9	1.00	2.5
25.4	1.00	2.3
27.9	1.00	2.2
30.5	1.00	2.2
33.0	1.00	2.4
35.6	0.99	2.2
38.1	0.99	2.1
40.6	1.00	2.5
43.2	0.99	2.4
45.7	0.97	2.6
48.3	0.97	2.6

TABLE 54

Flow Measurement of 2-dimensional Fine Grid Turbulent Flow

Height (cm)	Velocity Ratio V/Vg	Turbulence Intensity (%)
2.5	0.96	17.0
5.1	0.93	14.8
7.6	0.92	14.8
10.2	0.94	14.6
12.7	0.96	14.3
15.2	0.97	14.2
17.8	0.97	14.2
20.3	0.98	14.2
22.9	0.95	14.5
25.4	0.96	14.6
27.9	0.96	14.5
30.5	0.96	14.7
33.0	0.97	14.6
35.6	0.97	14.6
38.1	0.97	14.6
40.6	0.98	15.0
43.2	0.99	15.1
45.7	1.00	14.9
48.3	0.96	15.0

TABLE 55

Flow Measurement of 2-dimensional Coarse Grid Turbulent Flow

Height (cm)	Velocity Ratio V/Vg	Turbulence Intensity (%)
2.5	1.13	19.2
5.1	1.09	19.7
10.2	0.90	20.9
15.2	0.92	20.7
17.8	0.92	20.8
20.3	0.94	20.6
22.9	0.94	21.4
27.9	0.98	21.2
33.0	1.00	21.0
38.1	0.94	21.6
43.2	0.94	22.0
48.3	0.96	21.6

TABLE 56

Flow Measurement of 2-dimensional Boundary Layer Flow

Height (cm)	Velocity Ratio V/Vg	Turbulence Intensity (%)
2.5	0.16	61.6
5.1	0.31	36.4
7.6	0.41	26.4
10.2	0.51	19.5
12.7	0.58	17.9
15.2	0.63	16.3
17.8	0.71	14.5
20.3	0.77	11.9
22.9	0.80	10.7
25.4	0.87	9.3
27.9	0.90	8.2
30.5	0.96	6.0
33.0	0.97	5.3
35.6	0.98	4.0
38.1	0.99	3.3
40.6	1.00	2.6
43.2	1.00	2.5
45.7	1.00	2.4
48.3	1.00	2.4

TABLE 57

Flow Measurement of 3-dimensional Smooth Flow

Height (cm)	Velocity Ratio V/Vg	Turbulence Intensity (%)
2.5	0.56	19.8
5.1	0.76	12.7
7.6	0.86	9.2
10.2	0.88	8.0
12.7	0.92	6.1
15.2	0.93	4.9
17.8	0.94	4.4
20.3	0.95	4.1
22.9	0.95	4.1
25.4	0.95	4.0
27.9	0.95	4.0
30.5	0.95	3.9
33.0	0.97	3.7
35.6	0.99	3.3
38.1	1.00	2.6
40.6	0.99	1.9
43.2	0.99	2.1
45.7	0.99	2.0
48.3	0.99	2.1

TABLE 58

Flow Measurement of 3-dimensional Fine Grid Turbulent Flow

Height (cm)	Velocity Ratio V/Vg	Turbulence Intensity (%)
2.5	1.08	15.1
5.1	1.02	16.1
7.6	0.91	16.0
10.2	0.92	15.5
12.7	0.93	15.2
15.2	0.97	14.1
17.8	0.98	14.2
20.3	0.99	14.4
22.9	0.99	14.4
25.4	0.98	14.6
27.9	0.98	14.7
30.5	0.97	14.7
33.0	0.98	14.7
35.6	1.00	14.4
38.1	1.00	14.1
40.6	1.00	14.4
43.2	1.00	14.6
45.7	0.98	14.4
48.3	0.97	14.5

TABLE 59

Flow Measurement of 3-dimensional Coarse Grid Turbulent Flow

Height (cm)	Velocity Ratio V/Vg	Turbulence Intensity (%)
2.5	1.08	20.7
5.1	0.99	22.0
7.6	0.94	22.1
10.2	0.93	21.6
12.7	0.93	21.7
15.2	0.94	21.8
17.8	0.94	21.7
20.3	0.96	21.3
22.9	0.97	21.5
25.4	0.98	21.8
27.9	0.97	21.0
33.0	1.00	21.2
38.1	0.99	21.2
43.2	0.99	21.7
48.3	1.00	20.7

TABLE 60

Flow Measurement of 3-dimensional Boundary Layer Flow

Height (cm)	Velocity Ratio V/Vg	Turbulence Intensity (%)
2.5	0.10	53.2
5.1	0.16	54.4
7.6	0.25	47.9
10.2	0.37	33.0
12.7	0.46	24.1
15.2	0.53	19.3
17.8	0.58	16.6
20.3	0.63	14.8
22.9	0.69	13.6
25.4	0.77	12.3
27.9	0.85	10.4
30.5	0.90	8.6
33.0	0.93	8.1
35.6	0.95	5.8
38.1	0.97	3.7
40.6	0.99	2.9
43.2	0.99	2.4
45.7	0.99	2.3
48.3	1.00	2.3

Appendix D

VELOCITY SPECTRA

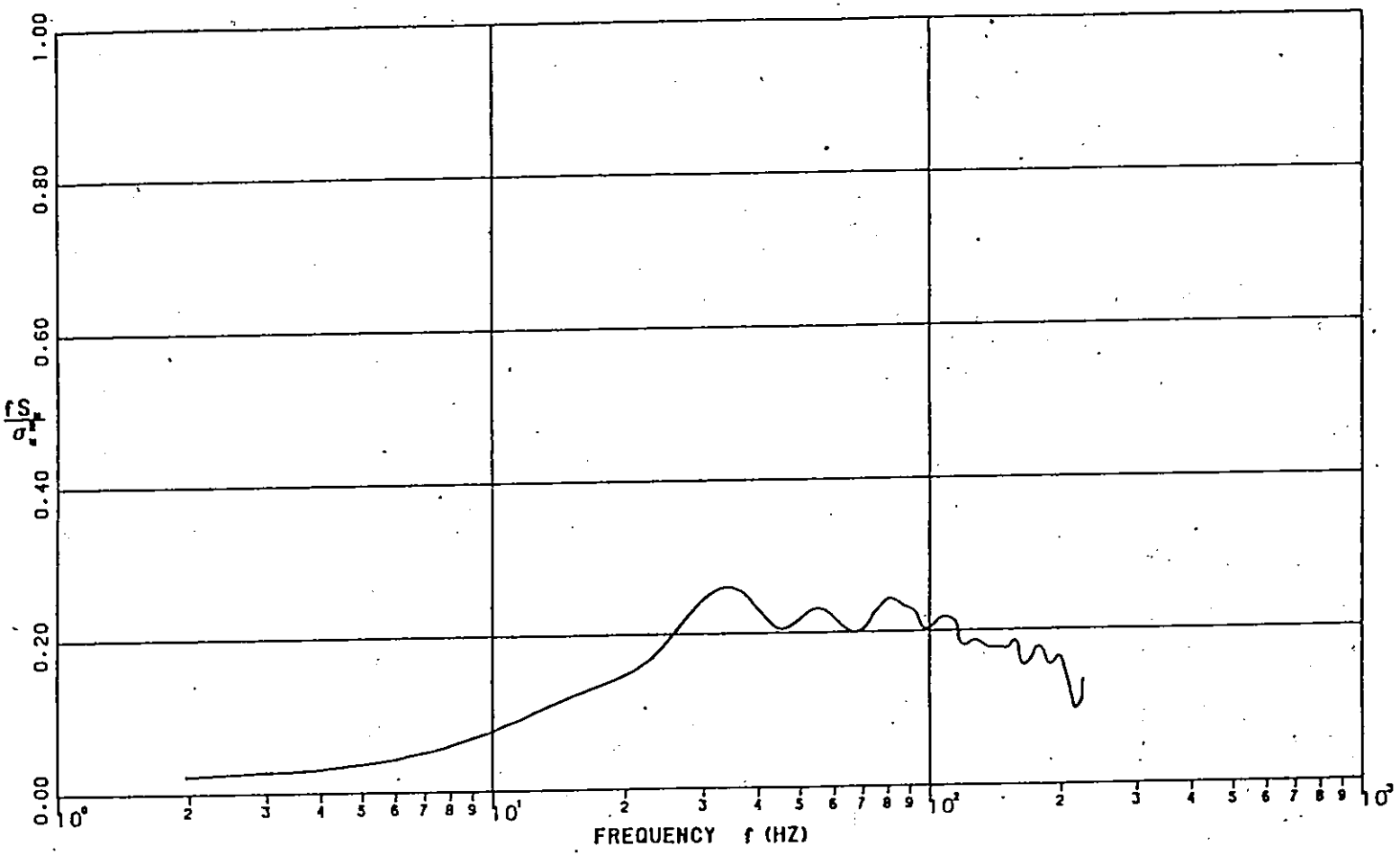

Figure 17: Normalized velocity spectrum of u-component in 2-dimensional smooth flow (V = 11.2 m/s)

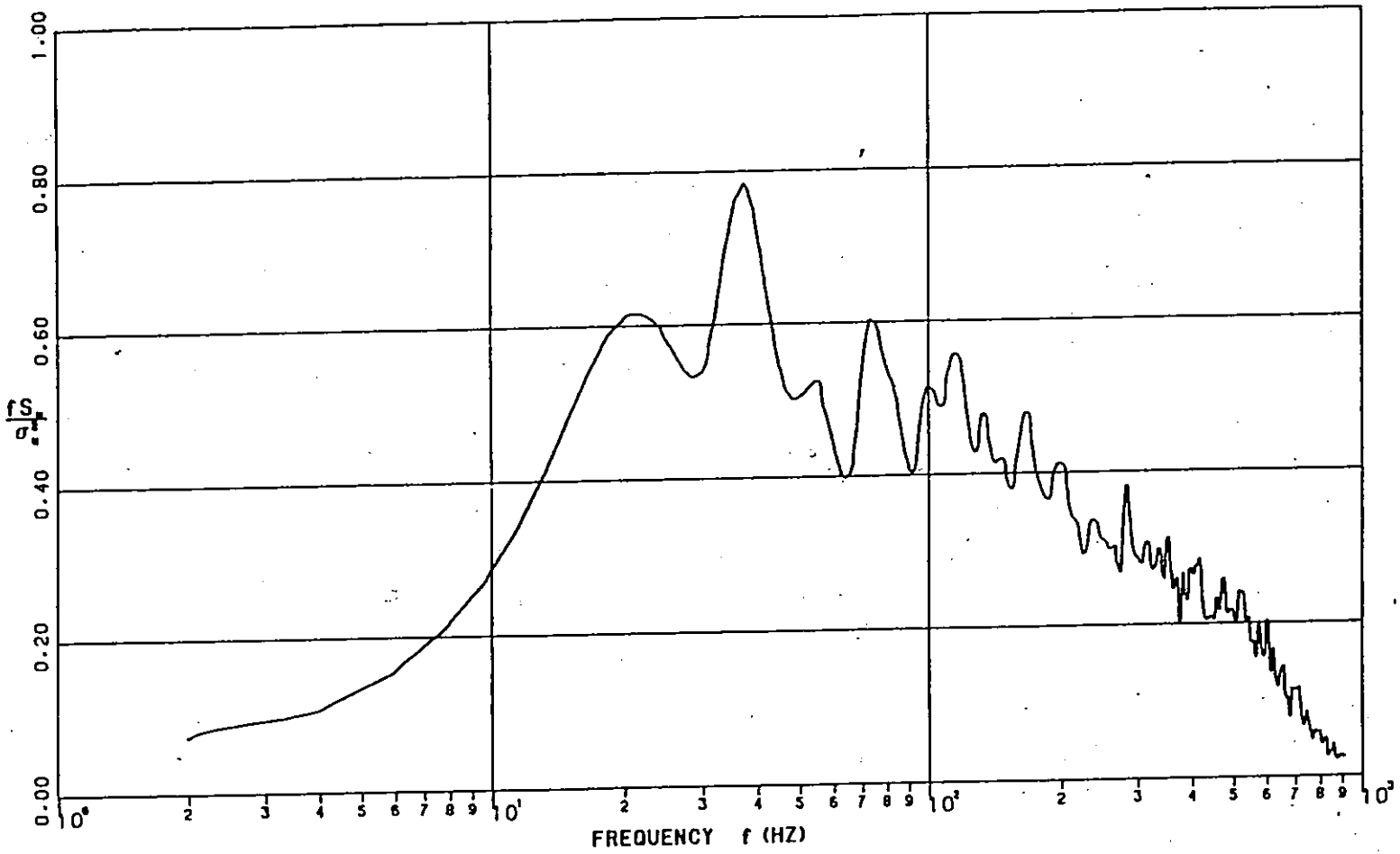

Figure 18: Normalized velocity spectrum of u-component in 2-dimensional fine grid turbulent flow (V_∞ = 7.3 m/s)

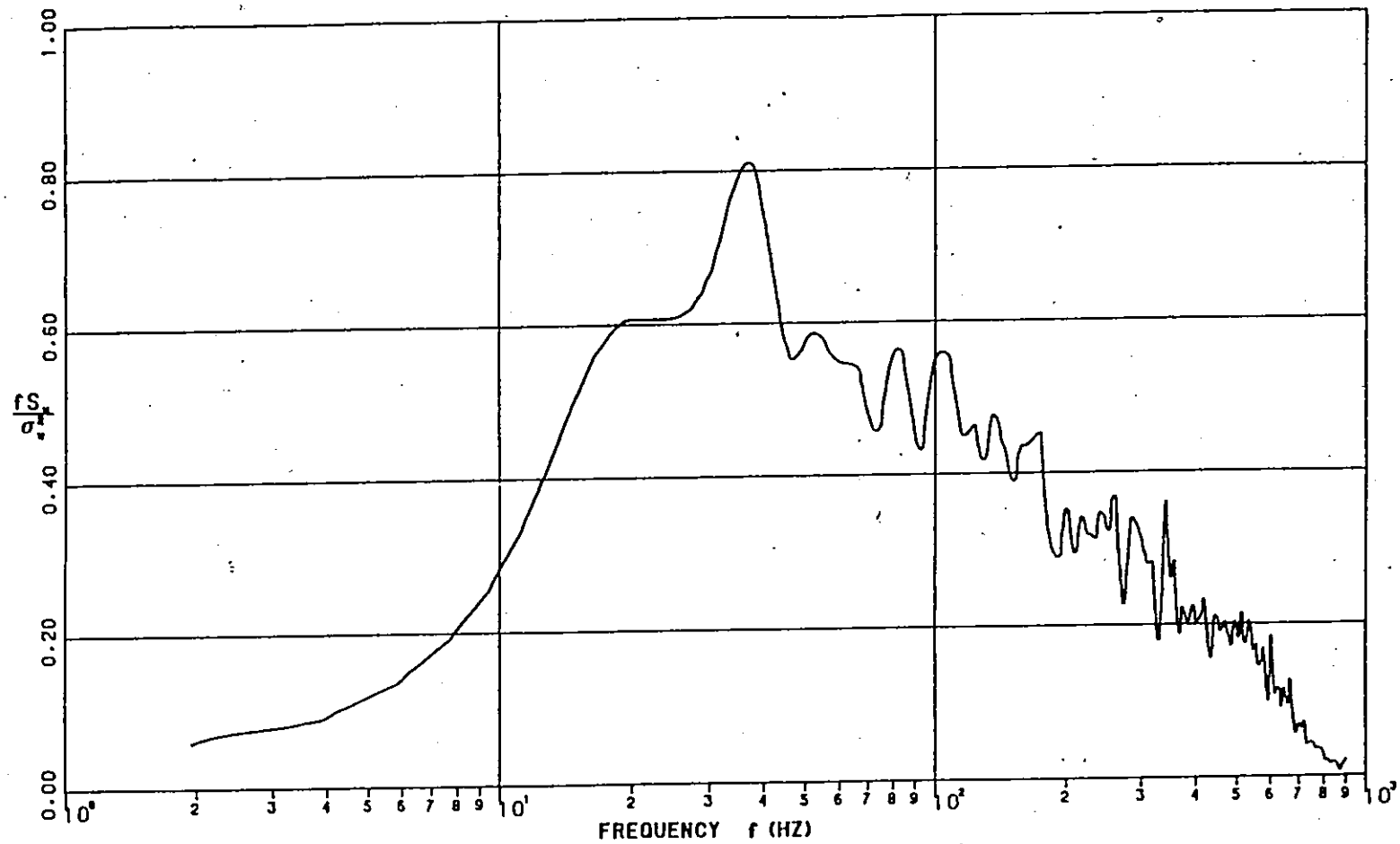

Figure 19: Normalized velocity spectrum of u-component in 2-dimensional coarse grid turbulent flow (V = 8.2 m/s)

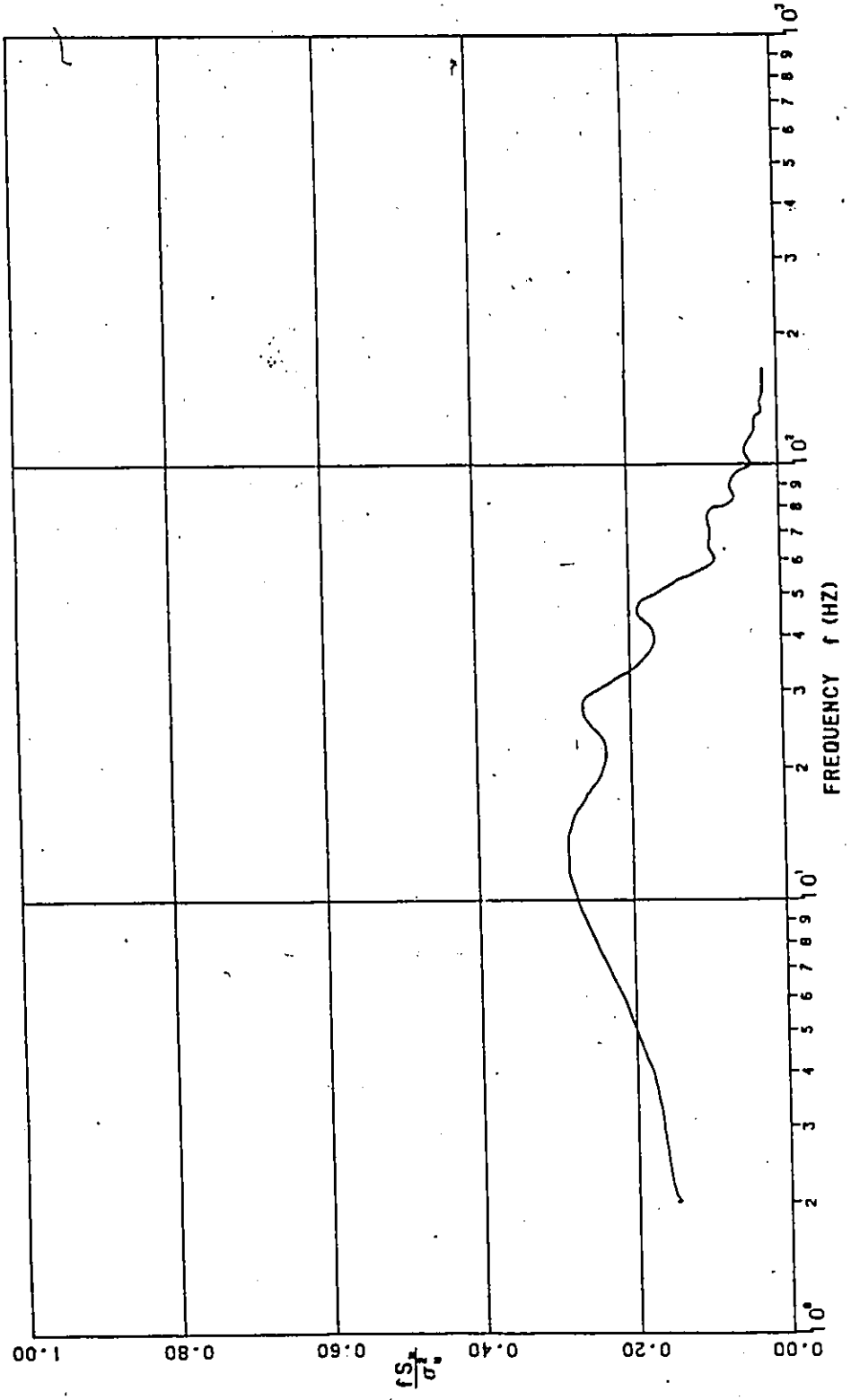

Figure 20: Normalized velocity spectrum of u-component in 2-dimensional boundary layer flow (V = 2.2 m/s)

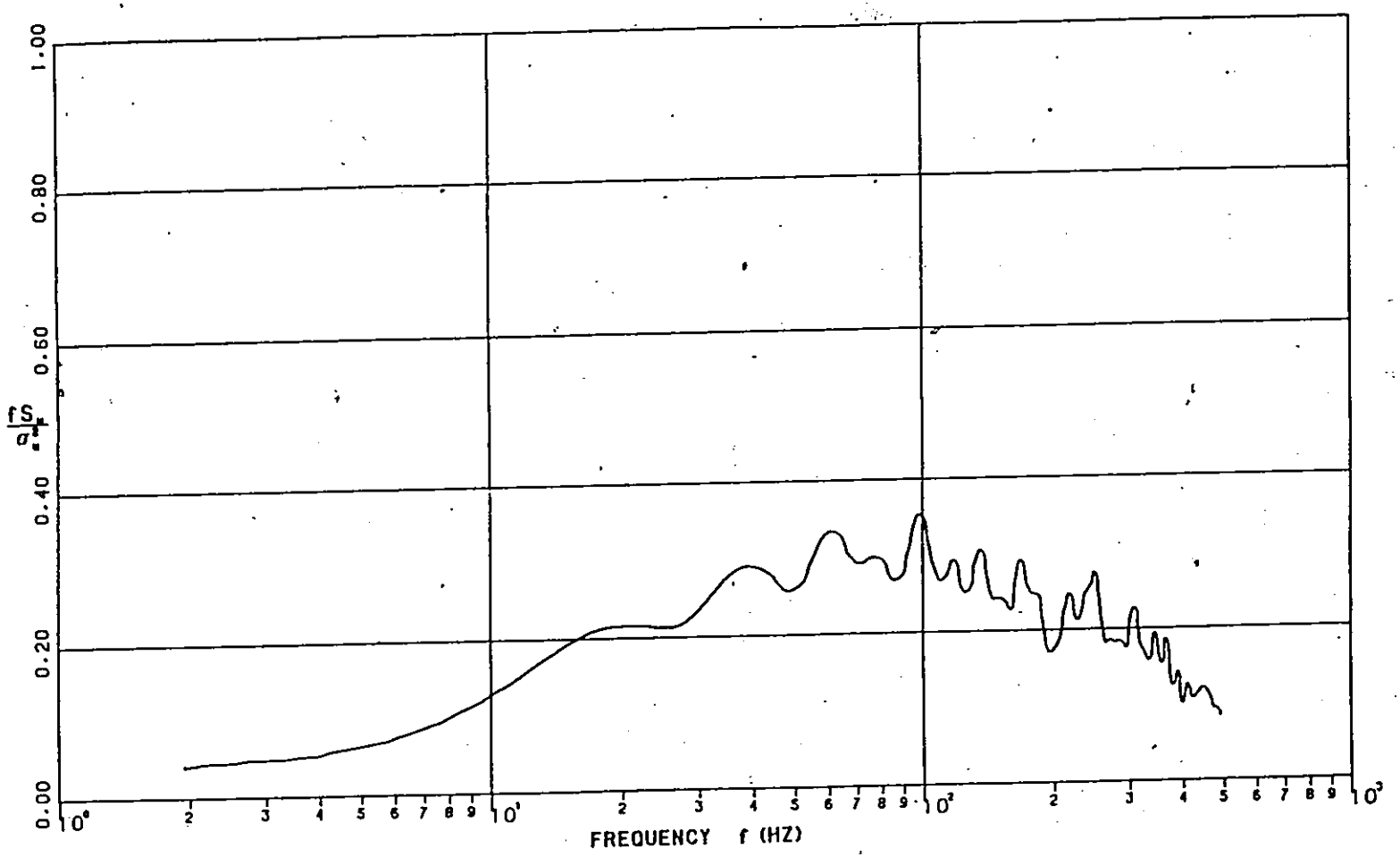

Figure 21: Normalized velocity spectrum of u-component in 3-dimensional smooth flow (V = 9.5 m/s)

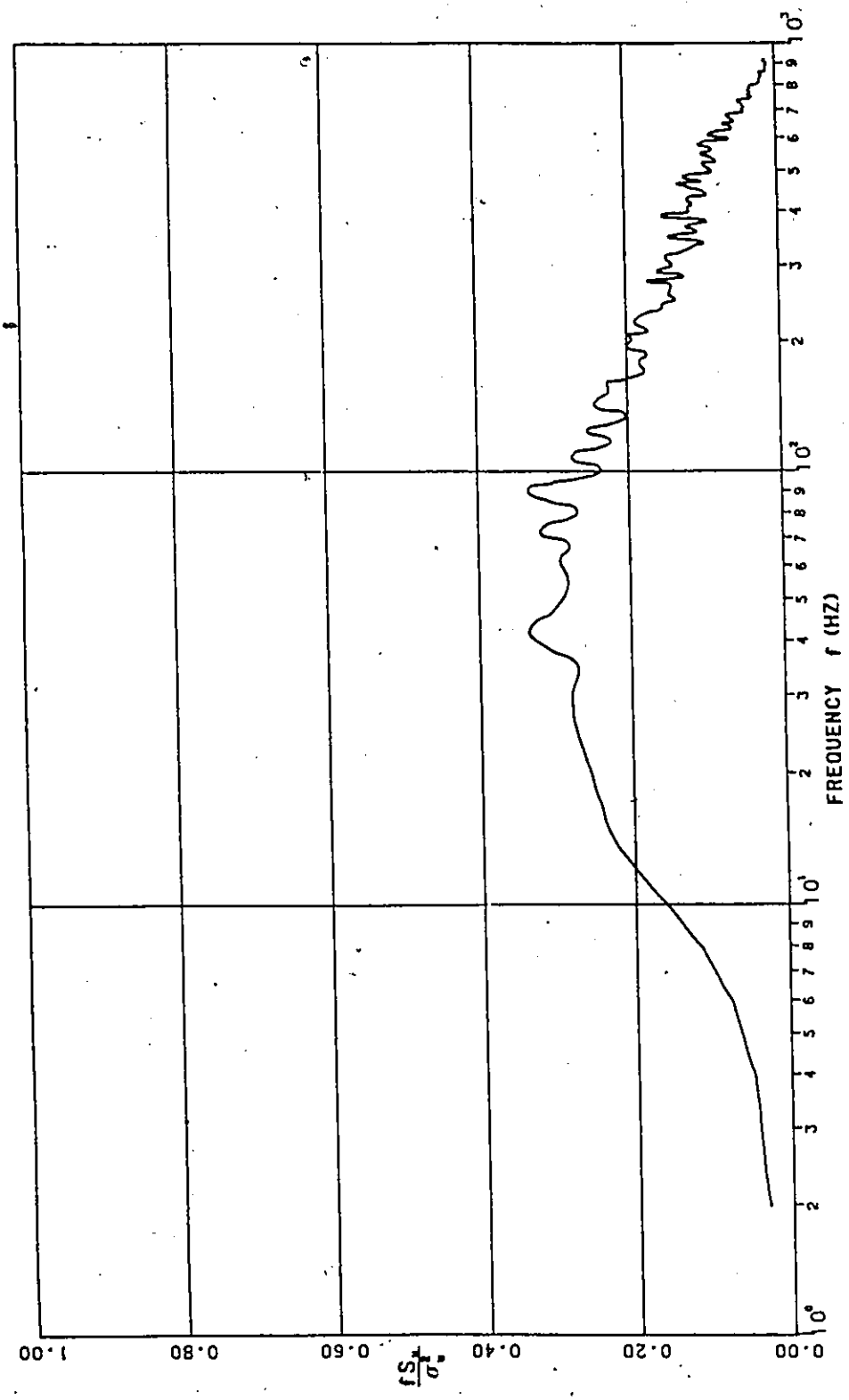

Figure 22: Normalized velocity spectrum of u-component in 3-dimensional fine grid turbulent flow (V = 8.2 m/s)

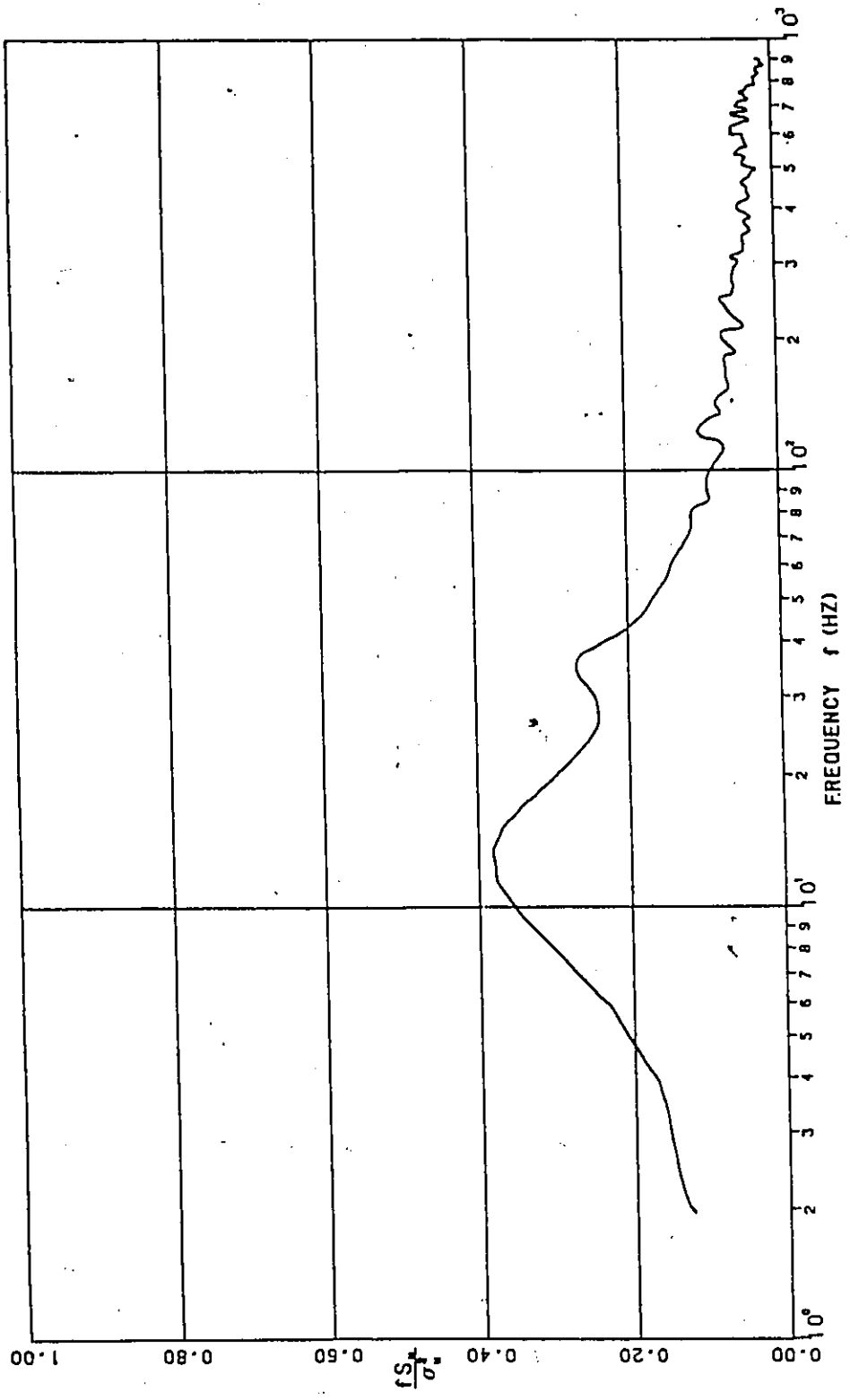

Figure 23: Normalized velocity spectrum of u-component in 3-dimensional coarse grid turbulent flow (V = 6.3 m/s)

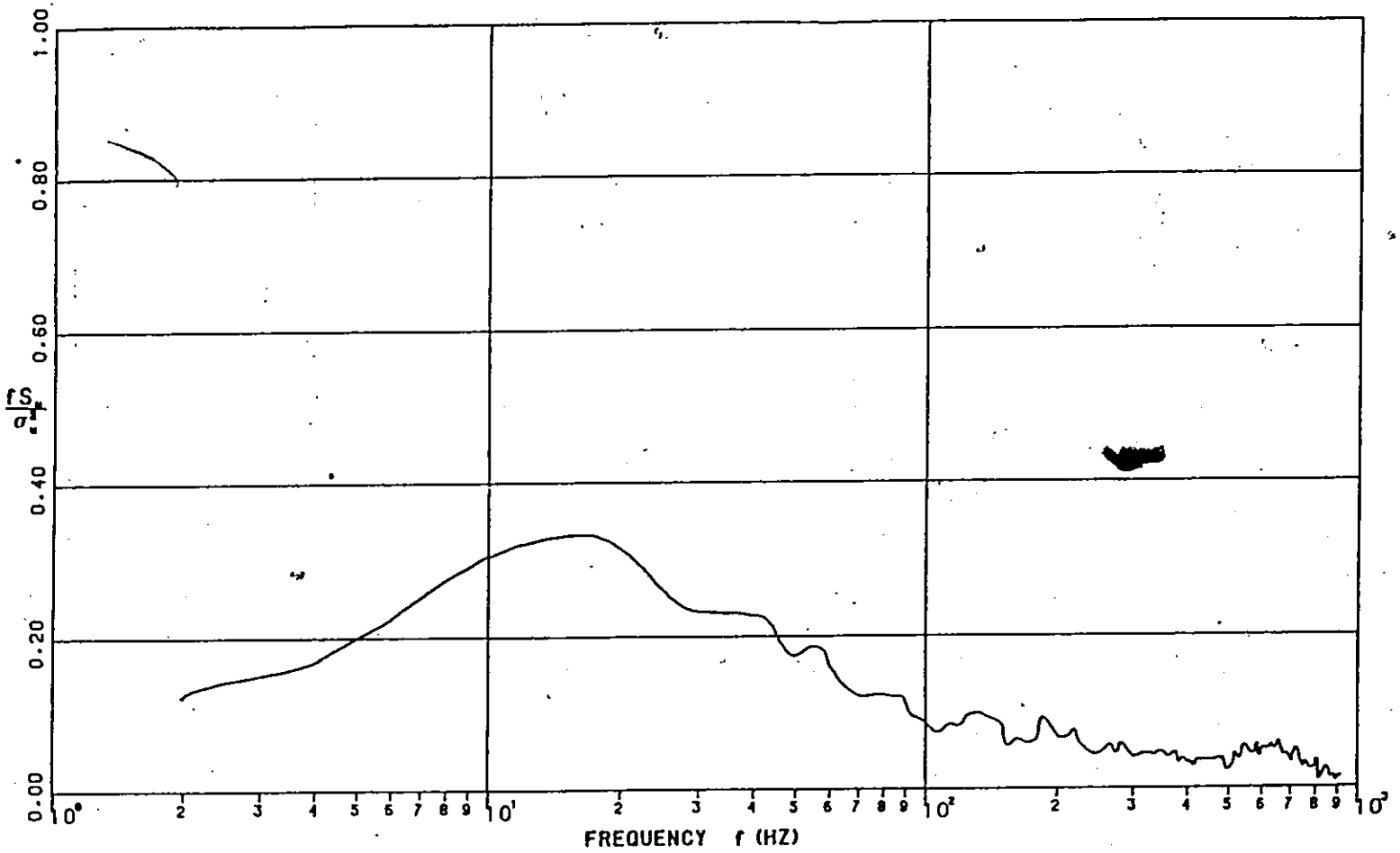

Figure 24: Normalized velocity spectrum of u-component in 3-dimensional boundary layer flow (V = 7.7 m/s)

Appendix E

CALIBRATION OF MODEL RESPONSES

Vertical and angular displacement of the model were calibrated to voltage signal from the gauge system. When vertical deflection was induced by a static load at the elastic axis, signal (A+B)/2 in voltage was recorded from the voltmeter and the deflection was measured by a micrometer. Thus the plot of the deflection against measured voltage gives calibration factor for vertical deflection.

In the calibration of torsional deflection, the centre of rotation was fixed by a pin-point support Angular rotation was plotted against the signal of (A-B)/2 to give calibrated value of angular deflection in terms of voltage.

Appendix F

COMPUTER PROGRAMS FOR THEORETICAL PREDICTIONS

PROGRAM I	Analysis of wind induced vibration of flat plate model
PROGRAM II	Analysis of wind induced vibration of torsional model
PROGRAM III	Analysis of buffeting response of galloping model
PROGRAM IV	Analysis of galloping response of galloping model

* These programs were copied from the other sources and modified for the present study by T.M.C. Kan. The original programs were available from H. Tanaka.

** PROGRAM I **

```
C  ***********************************************************
C  *                                                         *
C  *       PROGRAM TO FIND WIND INDUCED RESPONSE             *
C  *                OF FLAT PLATE MODEL                      *
C  *                                                         *
C  ***********************************************************
C
      DIMENSION Z(100),TOR(100),VELR(100),TI(8),ST(8),FP(8)
      COMPLEX*16 HO,H1,DEN,CC,ZL,AL,ZM,AM,BZ,BBA,AA1,AA2,
      COMPLEX*16 DAA3,AA4,EL,CC1,CC2,CC3,CC4,CC5,CC6
C
C
C     FZ    : FLEXURAL FREQUENCY OF THE MODEL
C     FA    : TORSIONAL FREQUENCY OF THE MODEL
C     ZZ    : LOGARITHMIC DAMPING IN FLEXURAL MODE
C     ZA    : LOGARITHMIC DAMPING IN TORSIONAL MODE
C     SL    : DERIVATIVE OF LIFT FORCE COEFFICIENT
C     SM    : DERIVATIVE OF PITCHING MOMENT COEFFICIENT
C     TI    : TURBULENCE INTENSITY
C     ST    : INTEGRAL LENGTH SCALE OF TURBULENCE
C     B     : WIDTH OF SECTION
C     HG    : DECK HEIGHT
C     GM    : MASS PER UNIT LENGTH
C     GI    : MASS MOMENT OF INERTIA PER UNIT LENGTH
C
C
C  INPUT DATA
C
      READ(5,1)FZ
1     FORMAT(/,30X,F13.5)
      READ(5,2)FA
2     FORMAT(30X,F13.5)
      READ(5,2)ZZ
      READ(5,2)ZA
      READ(5,2)B
      READ(5,2)SL
      READ(5,2)SM
        C=SM/SL
      READ(5,2)GM
      READ(5,2)GI
      READ(5,2)AD
      GMM=GM*2.0
      GII=GI*2.0
C
C
      WRITE(6,31)
31    FORMAT(1H1,///,20X,'THEORECTICAL RESPONSES OF FLAT
     *PLATE MODEL')
      WRITE(6,32)
```

```
32    FORMAT(20X,41('*'))
      WRITE(6,33)FZ
33    FORMAT(//,10X,'FLEXURAL FREQUENCY =',F13.6,'HZ')
      WRITE(6,34)FA
34    FORMAT(10X,'TORSIONAL FREQUENCY =',F13.6,'HZ')
      WRITE(6,35)ZZ
35    FORMAT(10X,'FLEXURAL DAMPING =',F13.6)
      WRITE(6,36)ZA
36    FORMAT(10X,'TORSIONAL DAMPING=',F13.6)
      WRITE(6,37)B
37    FORMAT(10X,'WIDTH OF SECTION =',F13.6,'MM')
      B=B/1000.0
      WRITE(6,38)SL
38    FORMAT(10X,'SLOPE OF DRAG COEFFICIENT =',F13.6)
      WRITE(6,39)SM
39    FORMAT(10X,'SLOPE OF MOMENT COEFFICIENT =',F13.6)
      WRITE(6,40)GM
40    FORMAT(10X,'MASS =',F13.6,'KG/M')
      WRITE(6,41)GI
41    FORMAT(10X,'MASS MOMENT OF INERTIA =',E13.4,'KGM')
      WRITE(6,42)AD
42    FORMAT(10X,'AIR DENSITY =',F13.6,'KG/M3')
      WRITE(6,43)C
43    FORMAT(10X,'ECCENTRICITY =',F13.6,'*B')
C
      WRITE(6,44 )TI(IU),ST(IU)
44    FORMAT(//,20X,'TURBULENCE INTENSITY =',
     *F13.6,'SCALE OF TURBULENCE =',F13.6)
      WRITE(6,45)
45    FORMAT(//,2X,'REDUCED VELOCITY',5X,'REDUCED TORSIONAL
     *RESPONSE',5X,'REDUCED FLEXURAL RESPONSE')
C
C  TO FIND CORRESPONDING RESPONSE FOR VARIOUS WIND SPEED
C     VR=REDUCED WIND SPEED
C
       DETM=100000.0
      IF(IU.LE.4)GO TO 911
      GM=GM*0.5
      GI=GI*0.5
      GO TO 912
911   GM=GMM
      GI=GII
912   CONTINUE
         DO 10 IV=1,72
           VR=FLOAT(IV)*0.5
C
C  FOR DIFFERENT FREQUENCIES
           SSZ=0.0
           SSA=0.0
C
           DO 11 IF=1,200
             XI=FLOAT(IF)*0.05
C
C  TO GENERATE  DIMENSIONLESS COEFFICIENTS
```

```
C
            BET=FA/FZ
            PI=4.0*ATAN(1.0)
            BB=B/2.0
            AMU=GM/(PI*AD*BB**2)
            ANU=GI/(PI*AD*BB**4)
C
C   TO GENERATE FREQUENCY RESPONSE FUNCTIONS
C
            XIS=XI**2
            PIC=PI**3
            PIS=PI**2
      AK=PI*XI/VR
      HO=CMPLX(1.0,-0.0455/AK)
      H1=CMPLX(1.0,-0.30/AK)
      CC=1.0-0.165/HO-0.335/H1
      CC1=CMPLX(0.0,1.0)
      ZL=-1.0-2.*CC/AK*CC1
      AL=-2.*CC/AK**2-CC1/AK*(1.+CC)
      ZM=CC1*CC/AK
      AM=-0.125+CC/AK**2-CC1*(1.-CC)/2./AK
      BZ=CMPLX(1.-XI*XI,2.*XI*ZZ)
      BBA=CMPLX(BET**2-XI**2,2.*BET*XI*ZA)
      AA1=AMU*BZ-ZL*XI**2
      AA2=-AL*XI**2
      AA3=-(ZM*XI**2)
      AA4=ANU*BBA-AM*XI**2
      DEL=AA1*AA4-AA2*AA3
      DET=CDABS(DEL)
      IF(DET.GE.DETM)GO TO 913
      DETM=DET
      VELM=VR
      FM=XI
913   R1=CDABS(AA4/DEL)
      R2=CDABS(AA2/DEL)
      R3=CDABS(AA3/DEL)
      R4=CDABS(AA1/DEL)
C
C   TO FIND SPECTRA OF RESPONSE
C
            A=(SL*VR**2/PIC)**2
C
C       TO FIND AERODYNAMIC ADMITTANCE FUNCTION
C
            BA=1./(1.+2.*PIS*XI/VR)
C
C       VELOCITY  SPECTRUM
C
C          VELOCITY SPECTRUM FOR SHEAR FLOW
C
            HG=0.1873
            C1=0.96*TI(IU)**2*HG/(B*VR)/(1+4.*HG*XI/B/VR)**2
C
C        VELOCITY SPECTRUM FOR HOMOGENOUS TURBULENCE FLOW
```

```
C
              TT=2.0*PI*ST(IU)*XI/B/VR
              C2=TT*(TI(IU)*0.51)**2/PI*(1.0+4.78*TT**2)
     &/(1.0+1.79*TT**2)**(11.0/6.0)
              IF(IU.EQ.1)C=C1
              IF(IU.EQ.2)C=C2
              IF(IU.EQ.3)C=C2
              IF(IU.EQ.4)C=C1
              IF(IU.EQ.5)C=C1
              IF(IU.EQ.6)C=C2
              IF(IU.EQ.7)C=C2
              IF(IU.EQ.8)C=C1
C
C  JOINT ACCEPTANCE FUNCTION
C
              IF(IU.GT.4) GO TO 23
C         FOR RIGID BODY
C
               SP=0.1524
              HX=8.0*SP*XI/B/VR
              IF(HX.GT.15)PP=0.0
              IF(HX.LE.15)PP=EXP(-HX)
              H=2.*(1.+(PP-1.)/HX)/HX
              GO TO 24
C         FOR SIMPLY SUPPORTED BODY
C
23             SP=0.6135
              HX=8.0*SP*XI/B/VR
              IF(HX.GT.15)PP=0.0
              IF(HX.LE.15)PP=EXP(-HX)
               HQ=HX**2+PI**2
               H=(HX/HQ)+2*PIS*(1.0+PP)/HQ**2
24            CONTINUE
C
C  INTEGRATION OF SPECTRA TO GET RESPONSE
               G=(2.*SM/SL)**2
              SZ=(R1**2+G*R2**2)*H*A*C*BA
              SA=(R3**2+G*R4**2)*H*A*C*BA
              SY=SZ/SA
              WRITE(6,237)SY
237           FORMAT(20X,E12.4)
              SSZ=SSZ+SZ*0.05
              SSA=SSA+SA*0.05
11            CONTINUE
            Z(IV)=SQRT(SSZ)/2.0
            TOR(IV)=SQRT(SSA)
            VELR(IV)=VR
            KOUNT=IV
       IF((Z(IV).GT.0.115).OR.(TOR(IV).GT.0.115))GO TO 14
10        CONTINUE
          GO TO 12
 14     KOUNT=KOUNT-1
 12        CONTINUE
      DO 991 I=2,KOUNT,2
```

```
991   WRITE(6,992)VELR(I),TOR(I),Z(I)
992   FORMAT(5X,F9.4,15X,F13.8,16X,F13.8)
           IF((IU.EQ.1).OR.(IU.EQ.5))KOUNT=VELM*2
C
C    TO PLOT RESPONSES
C
      VELR(KOUNT+1)=0.0
      TOR(KOUNT+1)=0.0
      Z(KOUNT+1)=0.0
      VELR(KOUNT+2)=XD
      TOR(KOUNT+2)=YDT
      Z(KOUNT+2)=YDB
       IP=IU
       IF(IU.GE.5)IP=IU-4
       CALL NEWPEN(IP)
      CALL FLINE(VELR,TOR,-KOUNT,1,0,1)
      CALL PLOT(30.0,0.0,-3)
      CALL FLINE(VELR,Z,-KOUNT,1,0,1)
      CALL PLOT(-30.0,0.0,-3)
C
C   TO FIND THE CRITICAL WIND SPEED OF THE FLAT PLATE
C
      IF((IU.NE.1).AND.(IU.NE.5))GO TO 1196
      ESP=0.000001
      NC=4
      VINT=0.5
      XINT=0.05
1130  VINT=VINT/(1.+FLOAT(NC))
      XINT=XINT/(1.+FLOAT(NC))
      IF((VINT.LT.0.000001).OR.(XINT.LT.0.000001))
     *GO TO 1192
      VRL=VELM+VINT/100.0
      CALL DELTA(VRL,FM,BET,AMU,ANU,ZA,ZZ,DETML)
      IF(DETML.LT.DETM)GO TO 1111
      VR1=VELM-VINT
      VR2=VELM
      GO TO 1112
1111  VR1=VELM
      VR2=VELM+VINT
1112  XIL=FM+XINT/100.0
      CALL DELTA(VELM,XIL,BET,AMU,ANU,ZA,ZZ,DETML)
      IF(DETML.LT.DETM)GO TO 1113
      XI1=FM-XINT
      XI2=FM
      GO TO 1114
1113  XI1=FM
      XI2=FM+XINT
1114  CONTINUE
C
C
      DO 1120 I=1,NC
      VR=VR1+VINT*FLOAT(I)
      DO 1120 J=1,NC
      XI=XI1+XINT*FLOAT(J)
```

```
      CALL DELTA(VR,XI,BET,AMU,ANU,ZA,ZZ,DET)
      IF(DET.GE.DETM)GO TO 1120
      DETM=DET
      VELM=VR
      FM=XI
1120  CONTINUE
1191  IF(DETM.GT.ESP)GO TO 1130
1192  WRITE(6,1199)VELM,FM
1199  FORMAT(///,'&&&&& CRITICAL WIND SPEED =',F10.5,6X,
     A'REDUCED FREQUENCY =',E 13.6)
      XC=VELM/2.0
       IF(IU.GE.5)XC=VELM
      CALL PLOT(XC,0.0,3)
      CALL PLOT(XC,23.0,2)
      CALL PLOT(0.0,0.0,3)
      CALL PLOT(30.0,0.0,-3)
      CALL PLOT(XC,0.0,3)
      CALL PLOT(XC,23.0,2)
      CALL PLOT(0.0,0.0,3)
      CALL PLOT(-30.0,0.0,-3)
1196  STOP
      END
C
C
C SUBROUTINE TO FIND THE DETERMINANT
C
      SUBROUTINE DELTA(VR,XI,BET,AMU,ANU,ZA,ZZ,DET)
      COMPLEX*16 HO,H1,CC,ZL,AL,ZM,AM,BZ,BBA,AA1,AA2,AA3,AA4,DEL,CC1
            XIS=XI**2
            PI=4.0*ATAN(1.0)
            PIC=PI**3
            PIS=PI**2
      AK=PI*XI/VR
      HO=CMPLX(1.0,-0.0455/AK)
      H1=CMPLX(1.0,-0.30/AK)
      CC=1.0-0.165/HO-0.335/H1
      CC1=CMPLX(0.0,1.0)
      ZL=-1.0-2.*CC/AK*CC1
      AL=-2.*CC/AK**2-CC1/AK*(1.+CC)
      ZM=CC1*CC/AK
      AM=-0.125+CC/AK**2-CC1*(1.-CC)/2./AK
      BZ=CMPLX(1.-XI*XI,2.*XI*ZZ)
      BBA=CMPLX(BET**2-XI**2,2.*BET*XI*ZA)
      AA1=AMU*BZ-ZL*XI**2
      AA2=-AL*XI**2
      AA3=-(ZM*XI**2)
      AA4=ANU*BBA-AM*XI**2
      DEL=AA1*AA4-AA2*AA3
      DET=CDABS(DEL)
      WRITE(6,808)VR,XI,DET
 808  FORMAT(3F20.9)
      RETURN
      END
```

** PROGRAM II **

```
C  ***********************************************************
C  *                                                         *
C  *        PROGRAM TO FIND WIND INDUCED RESPONSE            *
C  *              OF TORSIONAL MODEL                         *
C  *   QQQ                                                   *
C  ***********************************************************
C
      DIMENSION Z(100),TOR(100),VELR(100),TI(8),ST(8),FP(8)
      COMPLEX*16 HO,H1,DEN,CC,ZL,AL,ZM,AM,BZ,BBA,AA1,AA2,
      COMPLEX*16 DAA3,AA4,EL,CC1,CC2,CC3,CC4,CC5,CC6
C
C
C     FZ     : FLEXURAL FREQUENCY OF THE MODEL
C     FA     : TORSIONAL FREQUENCY OF THE MODEL
C     ZZ     : LOGARITHMIC DAMPING IN FLEXURAL MODE
C     ZA     : LOGARITHMIC DAMPING IN TORSIONAL MODE
C     SL     : DERIVATIVE OF LIFT FORCE COEFFICIENT
C     SM     : DERIVATIVE OF PITCHING MOMENT COEFFICIENT
C     TI     : TURBULENCE INTENSITY
C     ST     : INTEGRAL LENGTH SCALE OF TURBULENCE
C     B      : WIDTH OF SECTION
C     HG     : DECK HEIGHT    ,
C     GM     : MASS PER UNIT LENGTH
C     GI     : MASS MOMENT OF INERTIA PER UNIT LENGTH
C
C
C  INPUT DATA
C
      READ(5,1)FZ
1     FORMAT(/,30X,F13.5)
      READ(5,2)FA
2     FORMAT(30X,F13.5)
      READ(5,2)ZZ
      READ(5,2)ZA
      READ(5,2)B
      READ(5,2)SL
      READ(5,2)SM
        C=SM/SL
      READ(5,2)GM
      READ(5,2)GI
      READ(5,2)AD
      GMM=GM*2.0
      GII=GI*2.0
C
C
      WRITE(6,31)
31    FORMAT(1H1,///,20X,'THEORECTICAL RESPONSES OF FLAT
     *PLATE MODEL')
```

```
      WRITE(6,32)
32    FORMAT(20X,41('*'))
      WRITE(6,33)FZ
33    FORMAT(//,10X,'FLEXURAL FREQUENCY =',F13.6,'HZ')
      WRITE(6,34)FA
34    FORMAT(10X,'TORSIONAL FREQUENCY =',F13.6,'HZ')
      WRITE(6,35)ZZ
35    FORMAT(10X,'FLEXURAL DAMPING =',F13.6)
      WRITE(6,36)ZA
36    FORMAT(10X,'TORSIONAL DAMPING=',F13.6)
      WRITE(6,37)B
37    FORMAT(10X,'WIDTH OF SECTION =',F13.6,'MM')
      B=B/1000.0
      WRITE(6,38)SL
38    FORMAT(10X,'SLOPE OF DRAG COEFFICIENT =',F13.6)
      WRITE(6,39)SM
39    FORMAT(10X,'SLOPE OF MOMENT COEFFICIENT =',F13.6)
      WRITE(6,40)GM
40    FORMAT(10X,'MASS =',F13.6,'KG/M')
      WRITE(6,41)GI
41    FORMAT(10X,'MASS MOMENT OF INERTIA =',E13.4,'KGM')
      WRITE(6,42)AD
42    FORMAT(10X,'AIR DENSITY =',F13.6,'KG/M3')
      WRITE(6,43)C
43    FORMAT(10X,'ECCENTRICITY =',F13.6,'*B')
C
      WRITE(6,44 )TI(IU),ST(IU)
44    FORMAT(//,20X,'TURBULENCE INTENSITY =',
     *F13.6,'SCALE OF TURBULENCE =',F13.6)
      WRITE(6,45)
45    FORMAT(//,2X,'REDUCED VELOCITY',5X,'REDUCED TORSIONAL
     *RESPONSE',5X,'REDUCED FLEXURAL RESPONSE')
C
C  TO FIND CORRESPONDING RESPONSE FOR VARIOUS WIND SPEED
C     VR=REDUCED WIND SPEED
C
       DETM=100000.0
      IF(IU.LE.4)GO TO 911
      GM=GM*0.5
      GI=GI*0.5
      GO TO 912
911   GM=GMM
      GI=GII
912   CONTINUE
         DO 10 IV=1,72
           VR=FLOAT(IV)*0.5
C
C  FOR DIFFERENT FREQUENCIES
           SSZ=0.0
           SSA=0.0
C
           DO 11 IF=1,200
             XI=FLOAT(IF)*0.05
C
```

```
C  TO GENERATE  DIMENSIONLESS COEFFICIENTS
C
              BET=FA/FZ
              PI=4.0*ATAN(1.0)
              BB=B/2.0
              AMU=GM/(PI*AD*BB**2)
              ANU=GI/(PI*AD*BB**4)
C
C  TO GENERATE FREQUENCY RESPONSE FUNCTIONS
C
              XIS=XI**2
              PIC=PI**3
              PIS=PI**2
              A1=CMPLX(1-XIS,2.*XI*ZZ)
              A1=AMU*PIC*A1-PI*VR*SL*XI
              A2=CMPLX(-VR*VR*SL,-2*C*PI*XI*VR*SL )
              A3=CMPLX(0.0,-VR*PI*SM*XI*2.)
              A41=CMPLX(BET*BET-XI*XI,2.*ZA*BET*XI)
              A41=ANU*PIC*A41
              A42=CMPLX(2*VR*VR*SM,4*C*PI*VR*SM*XI)
              A4=A41-A42
              DEL=A1*A4-A2*A3
              R1=CDABS(A1/DEL)
              R2=CDABS(A2/DEL)
              R3=CDABS(A3/DEL)
              R4=CDABS(A4/DEL)
C
C  TO FIND SPECTRA OF RESPONSE
C
              A=(SL*VR**2/PIC)**2
C
C         TO FIND AERODYNAMIC ADMITTANCE FUNCTION
C
              BA=1./(1.+2.*PIS*XI/VR)
C
C         VELOCITY  SPECTRUM
C
C            VELOCITY SPECTRUM FOR SHEAR FLOW
C
              HG=0.1873
             C1=0.96*TI(IU)**2*HG/(B*VR)/(1+4.*HG*XI/B/VR)**2
C
C           VELOCITY SPECTRUM FOR HOMOGENOUS TURBULENCE FLOW.
C
              TT=2.0*PI*ST(IU)*XI/B/VR
              C2=TT*(TI(IU)*0.51)**2/PI*(1.0+4.78*TT**2)
     &/(1.0+1.79*TT**2)**(11.0/6.0)
              IF(IU.EQ.1)C=C1
              IF(IU.EQ.2)C=C2
              IF(IU.EQ.3)C=C2
              IF(IU.EQ.4)C=C1
              IF(IU.EQ.5)C=C1
              IF(IU.EQ.6)C=C2
              IF(IU.EQ.7)C=C2
```

```
            IF(IU.EQ.8)C=C1
C
C  JOINT ACCEPTANCE FUNCTION
C
            IF(IU.GT.4) GO TO 23
C        FOR RIGID BODY
C
             SP=0.1524
            HX=8.0*SP*XI/B/VR
            IF(HX.GT.15)PP=0.0
            IF(HX.LE.15)PP=EXP(-HX)
            H=2.*(1.+(PP-1.)/HX)/HX
            GO TO 24
C        FOR SIMPLY SUPPORTED BODY
C
23           SP=0.6135
            HX=8.0*SP*XI/B/VR
            IF(HX.GT.15)PP=0.0
            IF(HX.LE.15)PP=EXP(-HX)
             HQ=HX**2+PI**2
             H=(HX/HQ)+2*PIS*(1.0+PP)/HQ**2
24          CONTINUE
C
C  INTEGRATION OF SPECTRA TO GET RESPONSE
             G=(2.*SM/SL)**2
            SZ=(R1**2+G*R2**2)*H*A*C*BA
            SA=(R3**2+G*R4**2)*H*A*C*BA
            SY=SZ/SA
            WRITE(6,237)SY
237         FORMAT(20X,E12.4)
            SSZ=SSZ+SZ*0.05
            SSA=SSA+SA*0.05
11          CONTINUE
          Z(IV)=SQRT(SSZ)/2.0
          TOR(IV)=SQRT(SSA)
          VELR(IV)=VR
          KOUNT=IV
       IF((Z(IV).GT.0.115).OR.(TOR(IV).GT.0.115))GO TO 14
10       CONTINUE
         GO TO 12
 14     KOUNT=KOUNT-1
 12        CONTINUE
      DO 991 I=2,KOUNT,2
991   WRITE(6,992)VELR(I),TOR(I),Z(I)
992   FORMAT(5X,F9.4,15X,F13.8,16X,F13.8)
           IF((IU.EQ.1).OR.(IU.EQ.5))KOUNT=VELM*2
C
C   TO PLOT RESPONSES
C
      VELR(KOUNT+1)=0.0
      TOR(KOUNT+1)=0.0
      Z(KOUNT+1)=0.0
      VELR(KOUNT+2)=XD
      TOR(KOUNT+2)=YDT
```

```
      Z(KOUNT+2)=YDB
       IP=IU
       IF(IU.GE.5)IP=IU-4
       CALL NEWPEN(IP)
      CALL FLINE(VELR,TOR,-KOUNT,1,0,1)
      CALL PLOT(30.0,0.0,-3)
      CALL FLINE(VELR,Z,-KOUNT,1,0,1)
      CALL PLOT(-30.0,0.0,-3)
1196  STOP
      END
```

** PROGRAM III **

```
C  ***************************************************
C  *                                                 *
C  *       PROGRAM TO FIND WIND INDUCED RESPONSE     *
C  *                 OF GALLOPING MODEL              *
C  *                                                 *
C  ***************************************************
C
      DIMENSION Z(100),VELR(100),TI(8),ST(8),FP(8)
      COMPLEX*16 HO,H1,DEN,CC,ZL,AL,ZM,AM,BZ,BBA,AA1,AA2,AA3,AA4
      COMPLEX*16 DEL,CC1,CC2,CC3,CC4,CC5,CC6
C
C
C  INPUT DATA
C
      READ(5,1)FZ
1     FORMAT(/,30X,F13.5)
      READ(5,2)ZZ
2     FORMAT(30X,F13.5)
      READ(5,2)H
      READ(5,2)SL
      READ(5,2)GM
      READ(5,2)AD
      GMM=GM*2.0
C
C
      WRITE(6,31)
31    FORMAT(1H1,///,20X,'THEORECTICAL RESPONSES OF FLAT PLATE MODEL'
      WRITE(6,32)
32    FORMAT(20X,41('*'))
      WRITE(6,33)FZ
33    FORMAT(//,10X,'FLEXURAL FREQUENCY =',F13.6,'HZ')
      WRITE(6,35)ZZ
35    FORMAT(10X,'FLEXURAL DAMPING =',F13.6)
      WRITE(6,37)H
37    FORMAT(10X,'HEIGHT OF SECTION=',F13.6,'MM')
      H=H/1000.0
      WRITE(6,38)SL
38    FORMAT(10X,'SLOPE OF DRAG COEFFICIENT =',F13.6)
      WRITE(6,40)GM
40    FORMAT(10X,'MASS =',F13.6,'KG/M')
      WRITE(6,42)AD
42    FORMAT(10X,'AIR DENSITY =',F13.6,'KG/M3')
C
      WRITE(6,44 )TI(IU),ST(IU)
44    FORMAT(//,20X,'TURBULENCE INTENSITY =',
     *F13.6,'SCALE OF TURBULENCE =',F13.6)
      WRITE(6,45)
45    FORMAT(//,2X,'REDUCED VELOCITY',5X,'REDUCED TORSIONAL RESPONSE'
```

```
     *5X,'REDUCED FLEXURAL RESPONSE')
C
C   TO FIND CORRESPONDING RESPONSE FOR VARIOUS WIND SPEED
C      VR=REDUCED WIND SPEED
C
       IF(IU.LE.4)GO TO 911
       GM=GM*0.5
       GO TO 912
911    GM=GMM
912    CONTINUE
          DO 10 IV=1,72
            VR=FLOAT(IV)*0.5
C
C   FOR DIFFERENT FREQUENCIES
            SSZ=0.0
C
            DO 11 IF=1,200
              XI=FLOAT(IF)*0.05
C
C   TO GENERATE  DIMENSIONLESS COEFFICIENTS
C
              BET=FA/FZ
              PI=4.0*ATAN(1.0)
              AMU=GM/(PI*AD*H**2)
C
C   TO GENERATE FUNCTIONS
C
              XIS=XI**2
              PIC=PI**3
              PIS=PI**2
         AA1=CMPLX(1.-XI**2,2.*ZZ*XI)
         AA1=8.*PIC*AMU*AA1
         AA2=CMPLX(0.0,-2.*PI*XI*VR*SL)
         AA3=AA1+AA2
         R1=CDABS(1.0/AA3)
C
C   TO FIND SPECTRA
C
              A=(SL*VR**2)**2
C   TO FIND AERODYNAMIC ADMITTANCE FUNCTION
C
              BA=1./(1.+2.*PIS*XI/VR)
C
C         VELOCITY  SPECTRUM
C
C            VELOCITY SPECTRUM FOR SHEAR FLOW
C
              HG=0.1873
             C1=0.96*TI(IU)**2*HG/(B*VR)/(1+4..*HG*XI/B/VR)**2
C
C            VELOCITY SPECTRUM FOR HOMOGENOUS TURBULENCE FLOW
C
              TT=2.0*PI*ST(IU)*XI/B/VR
              C2=TT*(TI(IU)*0.51)**2/PI*(1.0+4.78*TT**2)
```

```
     &/(1.0+1.79*TT**2)**(11.0/6.0)
               IF(IU.EQ.1)C=C1
               IF(IU.EQ.2)C=C2
               IF(IU.EQ.3)C=C2
               IF(IU.EQ.4)C=C1
               IF(IU.EQ.5)C=C1
               IF(IU.EQ.6)C=C2
               IF(IU.EQ.7)C=C2
               IF(IU.EQ.8)C=C1
C
C  JOINT ACCEPTANCE FUNCTION
C
               IF(IU.GT.4) GO TO 23
                SP=0.1524
               HX=8.0*SP*XI/H/VR
               IF(HX.GT.15)PP=0.0
               IF(HX.LE.15)PP=EXP(-HX)
               HWW=2.*(1.+(PP-1.)/HX)/HX
               GO TO 24
23              SP=0.6135
               HX=8.0*SP*XI/H/VR
               IF(HX.GT.15)PP=0.0
               IF(HX.LE.15)PP=EXP(-HX)
                HQ=HX**2+PI**2
                HWW=(HX/HQ)+2*PIS*(1.0+PP)/HQ**2
24             CONTINUE
C
C  INTEGRATION OF SPECTRA TO GET RESPONSE
            SZ=R1**2*HWW*A*C*BA
            SSZ=SSZ+SZ*0.05
11            CONTINUE
            Z(IV)=SQRT(SSZ)
            VELR(IV)=VR
            KOUNT=IV
         IF(Z(IV).GT.0.105)GO TO 14
10          CONTINUE
            GO TO 12
 14       KOUNT=KOUNT-1
 12           CONTINUE
       DO 991 I=2,KOUNT,2
991    WRITE(6,992)VELR(I),Z(I)
992    FORMAT(5X,F9.4,16X,F13.8)
            IF((IU.EQ.1).OR.(IU.EQ.5))KOUNT=VELM*2
       VELR(KOUNT+1)=0.0
       Z(KOUNT+1)=0.0
       VELR(KOUNT+2)=XD
       Z(KOUNT+2)=YDB
        IP=IU
        IF(IU.GE.5)IP=IU-4
        CALL NEWPEN(IP)
       CALL FLINE(VELR,Z,-KOUNT,1,0,1)
1196   STOP
       END
```

** PROGRAM IV **

```
C     ***************************************************
C     *                                                 *
C     *      PROGRAM TO FIND GALLOPING RESPONSE         *
C     *                                                 *
C     ***************************************************
C
C
C DAMP=DAMPING RATIO
C AN=MASS PARAMTER
C AM=TOTAL MASS OF THE MODEL
C H=HEIGHT OF MODEL
      DIMENSION A(6),B(6),C(6),VEL2(200),VEL3(200),Y2(200)
      DIMENSION Y3(200)
      DAMP=0.009
      H=0.0125
      AIRDEN=1.205
      AM=0.03209
      ALENG=0.6096
      AN2=AIRDEN*H**2*ALENG/8.0/AM
      AN3=AN2*4.0
      F=15.7
C
C  GENERALIZED GALLOPING RESPONSE
C  UIN=1/U
C  AUIN=A/U
C  A=A/H*N/BETA
C  U=U*N/BETA
C
      DO 949 IQ=1,2
      READ(5,100)(A(I),B(I),C(I),I=1,6)
100   FORMAT(//,(E20.4,F20.4,F20.4))
      WRITE(6,101)
101   FORMAT(//,4X,'I',12X,'A',16X,'B',15X,'C'/)
      WRITE(6,102)(I,A(I),B(I),C(I),I=1,6)
102   FORMAT(I5,E20.6,2F15.6)
      WRITE(6,103)
103   FORMAT(//12X,'U',14X,'A'/)
      KOUNT=0
      AUIN=0.0
4     UIN=0.0
      DO 1 I=2,6
1     UIN=UIN+B(I)*C(I)*A(I)*AUIN**(I-1)
      UIN=C(1)*A(1)+UIN
      IF(UIN) 6,6,7
7     U=1./UIN
      ABAR=AUIN*U
      U=U+0.005
      IF(ABAR-0.30) 5,5,3
```

```
5       KOUNT=KOUNT+1
        IF(IQ.EQ.2)GO TO 888
        V2=(DAMP*U/AN2)*2*3.1416
        YY2=(ABAR*DAMP/AN2)/SQRT(2.0)
        IF(YY2.LT.1.7)KOUNT2=KOUNT
        VEL2(KOUNT)=V2
        Y2(KOUNT)=YY2
        GO TO 979
888     V3=(DAMP*U/AN3)*2*3.1416
        YY3=(ABAR*DAMP/AN3)/SQRT(2.0)
        IF(YY3.LT.1.7)KOUNT3=KOUNT
        VEL3(KOUNT)=V3
        Y3(KOUNT)=YY3
979     WRITE(6,105) KOUNT,U,ABAR
105     FORMAT(I6,2X,2E15.3)
6       AUIN=AUIN+0.002
        GO TO 4
3       CONTINUE
949     CONTINUE
        Y2(KOUNT2+1)=0.0
        Y3(KOUNT3+1)=0.0
        Y2(KOUNT2+2)=0.1
        Y3(KOUNT3+2)=0.1
        VEL2(KOUNT2+1)=0.0
        VEL3(KOUNT3+1)=0.0
        VEL2(KOUNT2+2)=5.0
        VEL3(KOUNT3+2)=5.0
        DO 921 I=1,KOUNT2
921     WRITE(6,234)VEL2(I),Y2(I)
234     FORMAT(2F16.6)
        DO 922 I=1,KOUNT3
922     WRITE(6,234)VEL3(I),Y3(I)
        CALL PLOTS(70.0,27.5)
        CALL PLOT(2.0,2.0,-3)
        CALL RECT(0.0,0.0,21.0,17.0,0.0,3)
        CALL AXIS(0.0,0.0,16HREDUCED VELOCITY,-16,17.0,0.0,
        0.0,5.0)
        CALL SYMBOL(11.4,-0.8,0.3,24,0.0,-1)
        CALL SYMBOL(11.7,-0.8,0.3,70,0.0,-1)
        CALL SYMBOL(12.0,-0.8,0.3,31,0.0,-1)
        CALL SYMBOL(12.3,-0.8,0.3,86,0.0,-1)
        CALL SYMBOL(12.6,-0.8,0.3,88,0.0,-1)
        CALL SYMBOL(12.9,-0.8,0.3,25,0.0,-1)
        CALL SYMBOL(-0.5,16.8,0.3,24,90.0,-1)
        CALL SYMBOL(-0.5,17.5,0.3,31,90.0,-1)
        CALL SYMBOL(-0.5,17.8,0.3,88,90.0,-1)
        CALL SYMBOL(-0.5,18.1,0.3,25,90.0,-1)
        CALL AXIS(0.0,0.0,23HR.M.S. REDUCED RESPONSE,23,21.0,
        90.0,0.0,0.1)
        CALL FLINE(VEL2,Y2,-KOUNT2,1,0,1)
        CALL NEWPEN(2)
        CALL FLINE(VEL3,Y3,-KOUNT3,1,0,1)
        CALL PLOT(0.0,0.0,999)
        END
```

UNIVERSITÉ D'OTTAWA
UNIVERSITY OF OTTAWA